Invited Speaker

581 Progress in STEM instrumentation: atomic-resolution SE imaging and meV-level energy resolution EELS
Dr. Ondrej Krivanek[1,2], Dr. Niklas Dellby[1], Dr. Michael Hotz[1], Dr. Joel Martis[1], Dr. Steven Quillin, Dr. Benjamin Plotkin-Swing[1], Dr. Tomas Radlicka[3], Dr. Gerardo Algara-Siller[4], Dr. Tracy Lovejoy[1]
[1]Bruker AXS Electron Microscopy Unit, Kirkland, USA, [2]Department of Physics, Arizona State University, Tempe, USA, [3]Institute of Scientific Instruments of CAS, Brno, Czech Republic, [4]Department of Physics & Center for the Science of Materials, Humboldt-Universität zu Berlin, Berlin, Germany
919 Continuous-flow LHe-cooling TEM sample holder with high stability at sub-10K and in situ biasing functionality
Penghan Lu[1], Denys Sutter[2], Dominik Biscette[2], András Kovács[1], Yan Lu[1], Joseph V. Vas[1], Michael Faley[1], Thibaud Denneulin[1], Damian Bucher[2], Amelia Estry[2], Johan Chang[2], Rafal E. Dunin-Borkowski[1]
[1]Ernst Ruska-Centre for Microscopy and Spectroscopy with Electrons, Forschungszentrum Jülich, Jülich, Germany, [2]condenZero, Zürich, Switzerland

Oral Presentation

17 Development state of the CEOS ground-potential monochromator
Felix Börrnert[1], Stephan Uhlemann[1], Heiko Müller[1], Volker Gerheim[1], Klaus Hessenauer[1], Holger Schulz[1], Maximilian Haider[1]
[1]CEOS GmbH, Heidelberg, Germany
95 Quantum Wavefront Shaping with a 48-element Programmable Phase Plate for Electrons
Francisco Vega[1,2], Dr. Chu-Ping Yu[1,2], Dr. Armand Béché[1,3], Prof. Dr. Jo Verbeeck[1,2]
[1]EMAT, University of Antwerp, Antwerp, Belgium, [2]NANOlab Center of Excellence, University of Antwerp, Antwerp, Belgium, [3]AdaptEM, Heverlee,, Belgium
101 High-throughput laboratory-based scattering X-ray Tensor Tomography
Azat Slyamov[1], Mr. Adriaan van Roosmalen[1], Mr. Kenneth Nielsen[1], Mr. Erik Lauridsen[1]
[1]Xnovo Technology ApS, Køge, Denmark
116 High-resolution STEM Image Acquisition Method for Tilted Specimen Using a New Type of Aberration Corrector
Wataru Koibuchi[1], Mr. Ryusuke Sagawa[1]
[1]JEOL, Akishima, JAPAN
117 Simultaneous Acquisition of 4D and EELS Data by Newly Developed Pixelated STEM Detector
Dr. Ryusuke Sagawa[1], Mr. Hiroki Hashiguchi[1], Mr. Akiho Nakamura[1], Ms. Shoko Shibagaki[1], Mr. Yutaka Kazama[1], Mr. Martin Huth[2], Mr. Yassine Imari[2], Mr. Valentin Kroner[2], Mr. Stefan Aschauer[2]
[1]JEOL Ltd., Akishima, Japan, [2]PNDetector GmbH, München, Germany
130 A new Ion Microscope for high-resolution imaging and SIMS nano-analytics
Dr. Alexander Ost[1], Torsten Richter[1], Olivier De Castro[2], Peter Gnauck[1], Jean-Nicolas Audinot[2], Tom Wirtz[2]
[1]Raith GmbH, Dortmund, Germany, [2]Luxembourg Institute of Science and Technology (LIST), Belvaux, Luxembourg
155 Atom Probe Tomography experiments performed in a (Scanning) Transmission Electron Microscope
Professor Williams Lefebvre[1], Gérald Da Costa[1], Castro Celia[1], Antoine Normand[1], Charly Vaudolon[1], Aidar Zakirov[1], Juan Macchi[1], Mohammed Ilhami[1], François Vurpillot[1]
[1]Univ Rouen Normandie, INSA Rouen Normandie, CNRS, Normandie Univ, GPM UMR 6634, Rouen, France

340 Low-voltage Secondary Electron Emission Spectromicroscopy using a Scanning Auger Microscope
Abbas Kosari Mehr[1], Mohammad Zaghloul[1], RitiK Tanwar[1], Wenzheng Cao[1], Silvia Maria Pietralunga[2], Anjam Khursheed[1], Alberto Tagliaferri[1]
[1]Polytechnic of Milan, Milan, Italy, [2]Consiglio Nazionale delle Ricerche of Italy (CNR), Milan, Italy
457 MÖNCH: A 25um hybrid pixel detector with sub-pixel resolution using deep learning
Xiangyu Xie[1], Luis Barba Flores[2], Benjamín Béjar Haro[2], Anna Bergamaschi[1], Erik Fröjdh[1], Elisabeth Müller[3], Kirsty Paton[1], Emiliya Poghosyan[3]
[1]PSD Detector Group, Paul Scherrer Institut, Villigen, Switzerland, [2]Swiss Data Science Center (SDSC Hub at PSI), Paul Scherrer Institut, Villigen, Switzerland, [3]Electron Microscopy and Diffraction Group, Paul Scherrer Institut, Villigen, Switzerland
501 Enhanced time resolution with a room-temperature energy dispersive X-ray PIN photodiode detector
Luca Serafini[1,2], Mr. Mylo Gijbels[1,2], Prof. Dr. Jo Verbeeck[1,2]
[1]EMAT, University of Antwerp, Antwerp, Belgium, [2]NANOlab Center of Excellence, University of Antwerp, Antwerp, Belgium
502 Development and application of In-situ atomic-scale straining&heating&biasing platform for TEM
Dr. Zhipeng Li[1,2], Dr. Jianfei Zhang[1], Dr. Haixin Li[1,2], Prof. Shengcheng Mao[1], Prof. Xiaodong Han[3], Prof. Ze Zhang[4]
[1]Beijing University of Technology, Beijing, China, [2]Bestron Science&Technology Co., Ltd., Beijing, China, [3]Southern University of Science and Technology of China, Shenzhen, China, [4]Zhejiang University, Hangzhou, China
611 Towards atomic-resolution electron energy loss spectroscopy in an uncorrected 30kV scanning electron microscope
Prof. Quentin Ramasse[1,2], Demie Kepaptsoglou[1,3], Takeshi Sunaoshi[4], Kazutoshi Kaji[4], Satoshi Okada[4], Yu Yamazawa[4], Tsutomu Saito[4], Michael Dixon[5], Sean Collins[1,2], Feridoon Azough[6], Robert Freer[6]
[1]SuperSTEM Laboratory, Daresbury, UK, [2]University of Leeds, Leeds, UK, [3]University of York, York, UK, [4]Hitachi High-Technologies Corp., Ibaraki, Japan, [5]Hitachi High-Tech Europe, Daresbury, UK, [6]University of Manchester, Manchester, UK

Poster Presentation

57 DQE measurement for TEM detectors: from the key parameter to an ambiguous estimate
Olivier Marcelot[1], Mme Cecile Marcelot[2]
[1]ISAE-SUPAERO, Toulouse, France, [2]CEMES-CNRS, Toulouse, France
91 A Novel Tool for Combined AFM, SEM, and Electrical Probing of Nanostructures
Chris Schwalb[1], Mr. Hajo Frerichs[1], Mr. Darshit Jangid[1], Mr. Sebastian Seibert[1], Mr. Lukas Stühn[1], Mrs. Marion Wolff[1], Mr. Andrew Jonathan Smith[2], Mr. Andreas Rummel[2]
[1]Quantum Design Microscopy GmbH, Pfungstadt, Germany, [2]Kleindiek Nanotechnik GmbH, Reutlingen, Germany
150 A retractable, compact Secondary Electron Energy Spectrometer attachment for Scanning Electron Microscopes
Wenzheng Cao[1], Prof. Anjam Khursheed[1]
[1]Politecnico di Milano, Milan, Italy
156 Opening the third dimension to your SEM with integrated fs-laser
Olena Vertsanova[1,2], Dr. Sabine Lenz[1], Martina Heller[1], Sebastian Krauss[1]
[1]Carl Zeiss Microscopy GmbH, Oberkochen, Germany, [2]National Technical University of Ukraine "KPI", Kyiv, Ukraine
180 Development of a pixelated STEM-in-SEM detector for microstructural features characterization
Julien Aubourg[1,2], Mr. Emmanuel Bouzy[2,3], Mr. Antoine Guitton[2,3], Mr. Jean-Jacques Fundenberger[2,3], Mrs. Yudong Zhang[2,3], Mr. Julien Guyon[2,3], Mr. Luc Morhain[2,3]

[1]JEOL (Europe) SAS, 1 All. de Giverny, 78290 Croissy, France, [2]Laboratoire d'Etude des Microstructures et de Mécanique des Matériaux (LEM3), Université de Lorraine, CNRS UMR 7239, Arts et Métiers, F-57070 Metz, France, [3]Laboratory of Excellence on Design of Alloy Metals for low-mAss Structures (DAMAS), University of Lorraine, 57073 Metz, France

182 A new EELS spectrometer, integrated with the microscope's optics

Dr. Peter Tiemeijer[1], Mr. Terry Dennemans[1], Mr. Sander Henstra[1], Mr. Dileep Krishnan[1], Mr. Sorin Lazar[1], Mr. Paolo Longo[1], Mrs. Maria Meledina[1], Mr. Sjaak Thomassen[1], Mr. Wouter Verhoeven[1]
[1]Thermo Fisher Scientific, Eindhoven, The Netherlands

211 Dose fractionation and alternative scanning strategies for beam damage mitigation in event-driven 4D-STEM

Arno Annys[1,2], Dr. Hoelen Robert[1,2], Mr. Matthias Quintelier[1,2], Prof. Joke Hadermann[1,2], Prof. Jo Verbeeck[1,2]
[1]EMAT, University of Antwerp, Antwerp, Belgium, [2]NANOlab Center of Excellence, University of Antwerp, Antwerp, Belgium

289 Multimodal OF2i-Raman – A novel high-throughput, single particle analysis method in liquids

Dr. Harald Fitzek[1,2], Christian Neuper[1], Dr. Christian Hill[3]
[1]Graz Centre for Electron Microscopy (ZFE), Graz, Austria, [2]Institute for Electron Microscopy and Nanoanalysis (FELMI), Graz, Austria, [3]Brave Analytics GmbH, Graz, Austria

325 4D STEM in SEM with a Fast Pixelated Direct Detector

Dr. Martin Huth[1], Dr. Björn Eckert[1], Dr. Petra Majewski[1], Dr. Stefan Aschauer[1], Prof. Lothar Strüder[2], Dr. Heike Soltau[1]
[1]PNDetector GmbH, Munich, Germany, [2]PNSensor GmbH, Munich, Germany

413 Optimizing Backscattered Electron Detection in SEM: Diode Layout and Collection Efficiency

Dr. Mozhdeh Abbasi[1], Dr. Maximilian Schmid[1], Dr. Alessia Mafodda[1], Dr. Stefan Aschauer[1]
[1]PNDetector GmbH, Munich, Germany

414 Empowering STEM in SEM: Integrative Approaches for Enhanced Detection

Dr. Maximilian Schmid[1], Mozhdeh Abbasi[1], Adam Meisel[1], Yassine Elamri[1], Dr. Alessia Mafodda, Dr. Stefan Aschauer[1]
[1]PNDetector GmbH, Munich, Germany

565 Multidimensional Electron Ptychography

Mr. Yu Lei[1], Biying Song[2], Zhiyuan Ding[2], Fucai Zhang[3], Xiaoqing Pan[4], Angus Kirkland[5], Dr Peng Wang[1]
[1]Department of Physics, University of Warwick, Coventry, United Kingdom, [2]College of Engineering and Applied Sciences, Nanjing University, Nanjing, China, [3]Department of Electrical and Electronic Engineering, Southern University of Science and Technology,, Shenzhen, China, [4]Department of Chemical Engineering and Materials Science, University of California, Irvine, United States of America, [5]The Rosalind Franklin Institute, Harwell Science and Innovation Campus, Didcot, United Kingdom

593 Atomic-scale microscopy of different materials by ultrashort THz-driven Atom Probe Tomography

Dr. Matteo De Tullio[1], Michella Karam[4], Simona Moldovan[4], Mr. Ivan Blum[1], Mr. Emmanuel Cadel[1], M.me Laurence Chevalier[1], Mr. Martin Andersson[3], Mr. Gustav Eriksson[3], Mr. Jonathan Houard[1], Mr. Marc Ropitaux[2], M.me Angela Vella[1]
[1]Univ Rouen Normandie, INSA Rouen Normandie, CNRS, Normandie Univ, GPM UMR 6634 , Rouen, France, [2]Univ Rouen Normandie, GLYCOMEV UR4358, SFR Normandie Végétal FED 4277, Innovation Chimie Carnot, IRIB, Rouen, France, [3]Department of Chemistry and Chemical Engineering, Chalmers University of Technology, Gothenburg, Sweden, [4]GPM Laboratory, CNRS UMR 6634, Rouen University, Normandy, France

613 Imaging Atomic Processes in Catalysts using a New High-Order Imaged-Corrected Environmental-TEM

Dr. Idan Biran[1], Mr. Ruben Bueno Villoro[1], Mr. Christian Kisielowski[2], Mr. Peter Christian Kjærgaard Vesborg[1,4], Mr. Maarten Wirix[3], Mr. Dennis Cats[3], Mr. Narasimha Shastri[3], Mr. Wessel Haasnoot[3], Mr. Jakob Kibsgaard[1,4], Mr. Thomas Bligaard[1,5], Mr. Christian Danvad Damsgaard[1,4,6], Mr. Joerg Jinschek[1,6], Mr. Stig Helveg[1]

[1]Center for Visualizing Catalytic Processes (VISION), Department of Physics, Technical University of Denmark, 2800 Kgs. Lyngby, Denmark, [2]The Molecular Foundry, Lawrence Berkeley National Laboratory, One Cyclotron Rd., Berkeley, USA, [3]Materials and Structural Analysis Division, Thermo Fisher Scientific, Eindhoven, Netherlands, [4]SURFCAT, Department of Physics, Technical University of Denmark, 2800 Kgs. Lyngby, Denmark, [5]Department of Energy Conversion and Storage, Technical University of Denmark, 2800 Kgs. Lyngby, Denmark, [6]National Centre for Nano Fabrication and Characterization (DTU Nanolab), Technical University of Denmark, 2800 Kgs. Lyngby, Denmark

687 Mitigation of beam damage on MoS2 using electrostatic beam blanking in TEM

Mr Joakim Kryger-baggesen[1], Mrs. Noopur Jain[2], Mr. Mark van Rijt[2], Mr. Ruud Krijnen[2], Mr. Marteen Wirix[2], Mr. Pritam Banerjee[3], Mr. Joachim Dahl Thomsen[5], Mr. Jakob Kibsgaard[1,4], Mr. Christian Damsgaard[1,3], Mr. Joerg Jinschek[1,3], Mr. Stig Helveg[1]
[1]Center for Visualizing Catalytic Processes (VISION), Department of Physics, Technical University of Denmark, Kgs. Lyngby, Denmark, [2]Thermo Fisher Scientific, Achtseweg Noord 5, 5651 GG Eindhoven, Eindhoven, The Netherlands, [3]National Center for Nano Fabrication and Characterization, Technical University of Denmark, Kgs. Lyngby, Denmark, [4]Surface Physics and Catalysis, Department of Physics, Technical University of Denmark, Kgs. Lyngby, Denmark, [5]Ernst Ruska-Centre for Microscopy and Spectroscopy with Electrons, Forshungszentrum Jülich, 52428 Jülich, Jülich, Germany

692 Recent developments and future trends in time-resolved cathodoluminescence: measuring dynamics at the nanoscale

Dr Herman Duim[1]
[1]Delmic, Delft, The Netherlands

720 Evaluation of SXES on different kind of materials : successes and failures

Jean-Louis Longuet[1]
[1]CEA Le Ripault, Monts, France

749 Microchannel Plate-based Detector with High Pressure Operation up to 1 Pa for Scanning Electron Microscopy

Mr Masahiro Hayashi[1], Mr. Yuya Washiyama[1], Dr. Matthias Sachsenhauser[2]
[1]Hamamatsu Photonics K.K., Hamamatsu , Japan, [2]Hamamatsu Photonics Deutschland GmbH, Herrsching, Germany

758 An analytical ion microscope for high-resolution imaging, nanoscale analytics and nanofabrication

Peter Gnauck[1], Torsten Richter[1], Alexander Ost[1]
[1]Raith GmbH, Dortmund, Germany

768 Crystalline analysis by W-SEM using a newly developed EBSD detector

Dr. Yohei Kojima[1], Yuta Matsumoto[1], Daniel Goran[2], John Gilbert[2], Naoki Kikuchi[1]
[1]JEOL, Ltd., 3-1-2, Musashino, Akishima, Japan, [2]Bruker Nano GmbH, Am Studio 2D, Germany

775 Novel, low-cost hardware for 'STEM in SEM' imaging

Mr Andrew Sturt[1], Dr Gareth Hughes[1], Dr Ian Griffiths[2], Dr Phani Karamched[1], Dr Neil Young[1]
[1]Department of Materials, University of Oxford, , United Kingdom, [2]JEOL (UK) Ltd, Welwyn Garden City, United Kingdom

831 3D calibration for SEM and optical microscopy - First results with next generation 3D standards

Dr.-Ing. Matthias Hemmleb[1], Celina Hellmich[2], Lena Heinrich[2], Sebastian Buetefisch[2]
[1]point electronic GmbH, Halle (Saale), Germany, [2]PTB Physikalisch-Technische Bundesanstalt, Braunschweig, Germany

910 Electron beam manipulation with auto-ponderomotive potentials for interaction-free measurements

Msc. Franz Schmidt-Kaler[1], Mr. Michael Seidling[1], Mr. Robert Zimmermann[1], Mr. Nils Bode[1], Mr. Fabian Bammes[1], Mr. Lars Radtke[1], Mr. Peter Hommelhoff[1]
[1]AG Laserphysik, Friedrich-Alexander Universität Erlangen-Nürnberg, Germany

954 New strategies of TEM sample preparation for the mitigation of carbon contamination

Dr. Julia Menten[1], Dr. Daniela Ramermann[1], Prof. Dr. Robert Schlögl[1,2], Dr. Walid Hetaba[1]

[1]Max Planck Institute for Chemical Energy Conversion, Mülheim an der Ruhr, Germany, [2]Fritz Haber Institute of the Max Planck Society, Berlin, Germany

983 Establishment of 30mm diameter milling and curtaining effect reduction by large area planar surface milling

Mr. Yuji Hasebe[1], Munehiro Kozuka[1], Takashi Sueyoshi[1], Akihiro Tanaka[1], Tatsuhito Kimura[1], Tamae Omoto[1], Yasuaki Yamamoto[1], Koji Todoroki[1], Hiroshi Onodera[1]
[1]JEOL Ltd, Akishima city/ Musahino3-1-2, Japan

992 Optimizing optical STEM detection for faster acquisition speeds in scanning electron microscopy

Arent J. Kievits[1], Monika Molnar[1], Jacob P. Hoogenboom[1]
[1]Department of Imaging Physics, Delft University of Technology, Delft, The Netherlands

1007 The importance of an open camera system demonstrated with wide-ranging applications of MerlinEM detector

Dr Matus Krajnak[1], Dr Gearoid Mangan[1]
[1]Quantum Detectors Ltd, Harwell Oxford, United Kingdom

1050 Fast mass spectrometry imaging for immunohistochemistry

Dr. Mariya Shamraeva[1], Dr. Edith Sandström[1], Kimberly G. Garcia[1], Distinguished Professor Ron M. A. Heeren[1], Dr. Ian G. M. Anthony[1], Dr. Sebastiaan van Nuffel[1]
[1]Maastricht MultiModal Molecular Imaging Institute (M4i), Maastricht, Netherlands

1086 Interference based optical instrument for high-throughput characterization of nanoparticles in complex biofluids

M.Sc.(Eng.) Carl Emil Schøier Kovsted[1], M.Sc. Yingchao Li[1], M.Sc.(Eng.) Lasse Pærgård Kristiansen[1], Ph.D. Jeppe Revall Frisvad[2], Ph.D. Jaco Botha[1], Ph.D. Emil Boye Kromann[1]
[1]Department of Health Technology, Technical University of Denmark, Kgs. Lyngby, Denmark, [2]Department of Applied Mathematics and Computer Science, Technical University of Denmark, Kgs. Lyngby, Denmark

1113 MEMS Monochromator

Martijn Adriaans[1], Dr. Jacob Hoogenboom[1], Dr. Ali Mohammadi-Gheidari[1]
[1]Delft University of Technology, Delft, The Netherlands

1161 Novel scan coil design for high spatiotemporal-resolution imaging in the scanning transmission electron microscope

Mr Adam Phipps[1,2], Dr. Lewys Jones[1,2], Dr. Jonathan Peters[1,2]
[1]Advanced Microscopy Laboratory, CRANN, Dublin, Ireland, [2]School of Physics, Trinity College Dublin, Dublin, Ireland

Late Poster Presentation

1182 Scanning patterns evaluations towards FIB-SEM/SIMS low-dose high-speed acquisition

Dr Andrés Miranda Martínez[1], Dr. Tom Wirtz[1], Dr. Santhana Eswara[1]
[1]Luxembourg Institute of Science and Technology (LIST), , Luxembourg

1320 In-Situ Microstructure-Mechanical Property Mapping of Multi-Component Materials Using PI 89 Auto SEM PicoIndenter

Sanjit Bhowmick[1], Kevin Schmalbach[1], Justin Cheng[2], Eric Hintsala[1], Douglas Stauffer[1], Nathan Mara[2]
[1]Bruker, Minneapolis, United States, [2]Department of Chemical Engineering and Materials Science, University of Minnesota, Minneapolis, United States

581

Progress in STEM instrumentation: atomic-resolution SE imaging and meV-level energy resolution EELS

Dr. Ondrej Krivanek[1,2], Dr. Niklas Dellby[1], Dr. Michael Hotz[1], Dr. Joel Martis[1], Dr. Steven Quillin, Dr. Benjamin Plotkin-Swing[1], Dr. Tomas Radlicka[3], Dr. Gerardo Algara-Siller[4], Dr. Tracy Lovejoy[1]
[1]Bruker AXS Electron Microscopy Unit, Kirkland, USA, [2]Department of Physics, Arizona State University, Tempe, USA, [3]Institute of Scientific Instruments of CAS, Brno, Czech Republic, [4]Department of Physics & Center for the Science of Materials, Humboldt-Universität zu Berlin, Berlin, Germany

IM-04 (1), Lecture Theater 1, august 27, 2024, 10:30 - 12:30

Background
Scanning transmission electron microscopy (STEM) has recently advanced in two major directions: atomic resolution imaging of surfaces using the Secondary Electron (SE) signal [1, 2], and ultra-high energy resolution electron energy loss spectroscopy (UHR-EELS) [3]. In this contribution, we review the progress at Bruker AXS (formerly Nion R&D) in these two fields.

Methods
A new SE detector for the Nion STEM has been developed, in the form of a compact Everhart-Thornley detector located within the objective lens polepiece, less than 20 mm from the sample. It uses an electrostatic deflector to direct slow electrons that came from the sample in an off-axis direction. The deflected electrons go through a wire mesh window and are accelerated towards a scintillator. Light produced by the scintillator is guided by a glass rod towards a fast and efficient photomultiplier tube (PMT). The design is UHV-compatible and bakeable. It avoids injecting any first or second-order aberrations, or significant instabilities into the primary beam traveling towards the sample, and the attainable spatial resolution of the STEM remains the same when the detector is turned on.

The generation of the SE signal is strongly affected by surface contamination on the sample, and we use a laser illumination system we have developed to clean samples in-situ. Samples cleaned in this way typically stay clean in the UHV sample chamber of our microscope. The microscope is normally equipped with an ultra-high energy resolution electron energy-loss spectroscopy (EELS) system, which can be used both for phonon studies and for general-purpose low loss and core-loss EELS, and elemental mapping. Combining SE imaging with EELS typically allows a more complete characterization of the sample than either technique on its own. Another advantage of our solution is that the Nion STEM is able to produce atom-sized electron probes at primary energies of 20-60 keV, for which the SE cross sections are larger, and the delocalization of the SE signal slightly smaller than for 100-300 keV operation.

Results
We have used SE imaging to examine several types of samples with many interesting results, which will be shown at the meeting. Monolayer and few-layer samples such as graphene, BN and MoS2 are especially interesting, as their thinness simplifies the modeling of how the incident fast electron beam interacts with the sample to produce SE signal.

As an example, in Figure 1 we show a medium-angle annular dark field image (MAADF), secondary electron image (SE) and an EELS map of the same area of monolayer graphene that contains single-atom substitutional impurities. All the images detect the single-atom substitutions, and provide further information. The MAADF image essentially “weighs” the atomic nuclei, the SE image allows atomic resolution to be reached on the surfaces of thick and even bulk samples, and the EELS map demonstrates that the chemical species of individual atoms can be readily identified by their energy loss signal.

On a parallel track, we continue to improve the energy resolution of our Ultra-High-Energy Resolution Monochromated EELS-STEM (U-HERMES) system. The best resolution we have attained so far is 2.6 meV (full width at half-maximum (FWHM) of the zero-loss peak (ZLP)), at 20 keV primary energy. These results and the challenges encountered when trying to push the resolution further will be presented at the meeting.

Figure caption:
a) MAADF image, b) SE image (Gaussian filtered), c) EELS elemental maps of the same area of monolayer graphene with B and N substitutions. Eo = 60 keV.

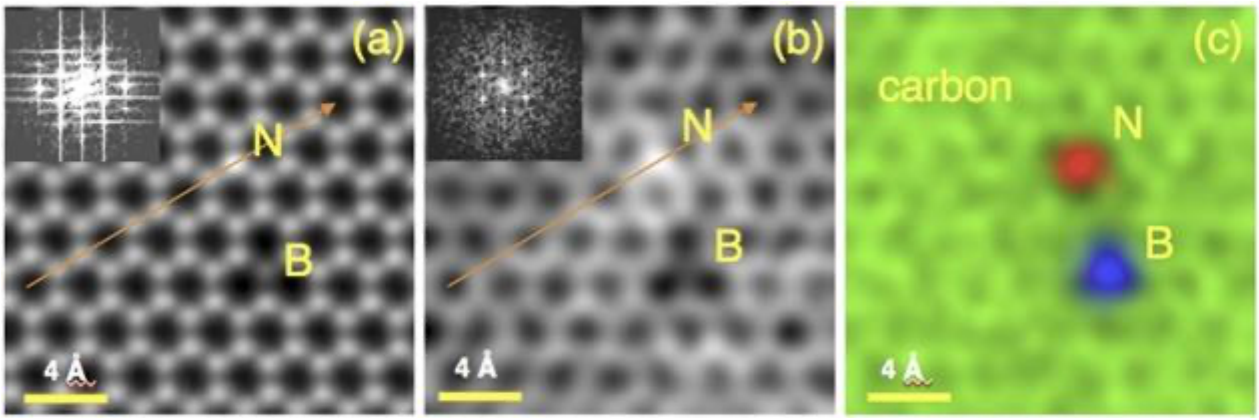

Keywords:

SE imaging, atomic resolution, meV-level-EELS

Reference:

[1] Y. Zhu et al., Nature Materials 8 (2009) 808-812.
[2] J. Martis et al., proceedings 20th IMC congress (Busan, Korea, 2023).
[3] T.C. Lovejoy et al., proceedings 20th IMC congress (Busan, Korea, 2023).

919

Continuous-flow LHe-cooling TEM sample holder with high stability at sub-10K and in situ biasing functionality

Penghan Lu[1], Denys Sutter[2], Dominik Biscette[2], András Kovács[1], Yan Lu[1], Joseph V. Vas[1], Michael Faley[1], Thibaud Denneulin[1], Damian Bucher[2], Amelia Estry[2], Johan Chang[2], Rafal E. Dunin-Borkowski[1]
[1]Ernst Ruska-Centre for Microscopy and Spectroscopy with Electrons, Forschungszentrum Jülich, Jülich, Germany, [2]condenZero, Zürich, Switzerland

IM-04 (2), Lecture Theater 1, august 27, 2024, 14:00 - 16:00

Background incl. aims
Cryogenic transmission electron microscopy (cryo-TEM) has been significantly advanced in the past decade for imaging macromolecular protein complexes and cellular structures with close-to-atomic resolution in three dimensions [1]. Beyond life sciences, cryo-TEM has also enabled observation of otherwise inaccessible information in weakly bonded and reactive materials that typically degrade under electron irradiation or environmental exposure [2]. Furthermore, many of the exotic properties in quantum materials, such as, superconductivity, charge density waves, quantum hall effect, and topological behaviours, only manifest at extremely low temperatures [3]. Historically, a few top-entry TEM stages were developed allowing specimen temperature cooled down to even 1.5 K [4]. Those designs were seldom followed up because of the preference towards more flexible and versatile side-entry specimen holders, especially to introduce different kinds of external stimuli for in situ and operando studies. On the other hand, currently existed liquid helium (LHe) cooling side-entry holders are usually very difficult, if not impossible, to reach and maintain a long-time stability of the ultimately low temperature (close to LHe temperature, 4.2 K). This is firstly limited by their considerable mechanical and thermal instability, and, in addition, their base temperature hold time is typically short because of the low latent heat of LHe and the limited cryogen capacity of the dewar attached to the back end of the holder.
Methods
In this context, a new miniaturized continuous-flow LHe cryostat was designed for in situ cryo-TEM applications. This was initially created for X-ray diffraction experiments in pulsed magnetic fields and later adapted to TEM side-entry holders by condenZero, a spin-off company from the University of Zurich, with further test and optimization in cooperation with the Ernst Ruska-Centre (ER-C) in Research Centre Juelich. The full setup is illustrated in the enclosed figure. A purpose-designed vibration damping stage, consisting of a few active and passive damping units, is of vital importance to this system. It suppresses significantly the external vibrations from the floor and environment as well as from the boiling of cryogen during transfer. The LHe transfer line is developed to maximise its flexibility and thermal efficiency, which further minimises the vibration as well as the cooling loss during transfer. A gas He outlet port is spared on the transfer line to support He recovery in order to save the consumption of the valuable He resource. The transfer line, at its end, is docked to the specimen holder with a bellow connected in between for the final stage vibration isolation. The holder can host either standard 3mm TEM grids or MEMS chips for in situ and operando cryogenic measurements. At least 10 electrical feedthrough is integrated to this holder, with 4 for the built-in Cernox temperature sensor and 6 for electrical biasing or heating. The tip of the holder, where the specimen sits, is fully surrounded (except two holes of 3 mm in the top and bottom for electron beam transmission) by a thermal shield cooled at the same temperature as the specimen to avoid contamination build-up when the sample is cooled but also to suppress the heat radiation from the objective pole piece and other components that are at room temperature. This system is currently installed on one of our image Cs-corrected microscopes, Titan HOLO, which is optimised for off-axis electron holography imaging (double biprisms with additional transfer lenses) as well as in situ and operando measurements (ultrawide pole piece gap). This microscope is recently upgraded with an

ultrafast beam chopper and an event-driven delay-line detector, which would eventually allow time-resolved cryogenic biasing measurements.

Results

A typical cool-down curve is shown in the enclosed figure. Starting from room temperature, a base temperature of 5.2 K, measured by the Cernox sensor very close to the specimen position, was reached within one minute and kept stable with temperature fluctuation of +/- 2.5 mK over hours. Because of the continuous flow design as well as the highly efficient cryogenics that currently consumes only 2-3 liter LHe per hour, the ultimately low temperature can easily last for more than 24 hours with the 100 liter LHe dewar. We have tested this system with a few applications, including magnetic solitons, superconductors, dielectrics and soft matters, by measuring their defocused Lorentz imaging, off-axis electron holography or electron diffraction. As an example, which is shown in the enclosed figure, the high stability of this system at ultimately low temperature allows us to quantitatively map the magnetic states of Bloch skyrmions in B20-FeGe at 5.2 K with 200 mT out-of-plane magnetic fields using off-axis electron holography. Furthermore, we also tested the in situ biasing and heating capabilities based on different MEMS chips on this holder. With four-probe measurements, we can measure the electrical resistivity drop of superconducting structure across its transition temperature and can also heat up very locally the specimen from cryogenic to elevated temperature (above room temperature).

Conclusion

We have developed a new continuous-flow LHe-cooling holder for in situ and operando cryogenic TEM applications. It is featured by very swift cool-down and ultra-long cryo-hold time at ultimately low temperature with minimal thermal fluctuation as well as in situ electrical biasing and local heating functions. Further optimisation on this system will also be discussed during the presentation.

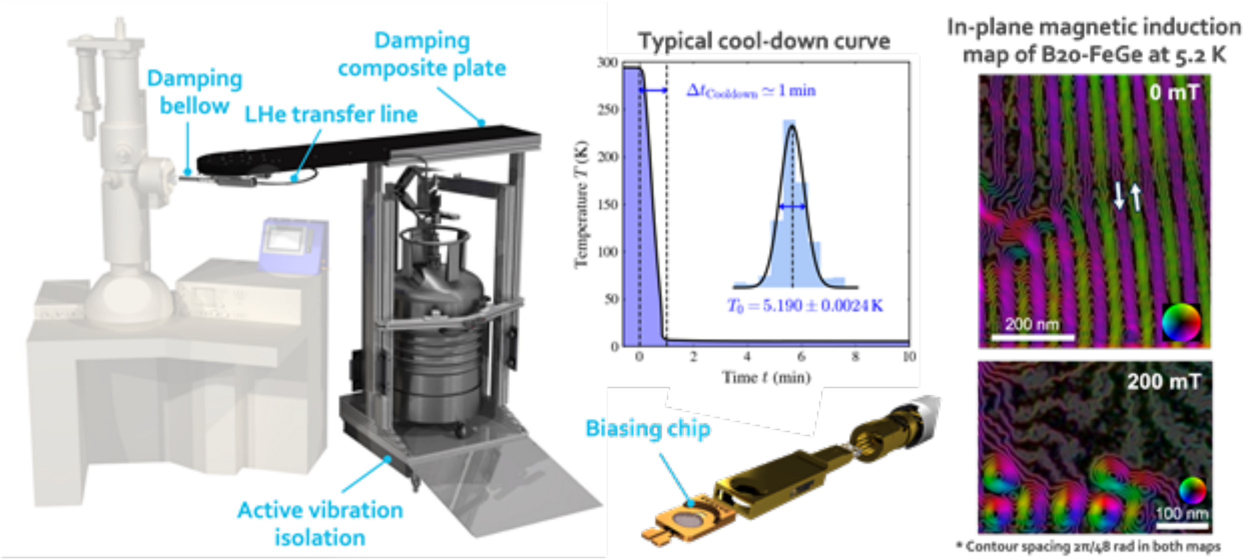

Keywords:

Liquid-helium, continuous-flow cryostat, cryo biasing

Reference:

[1] T. Nakane et al. Nature 587, 152 (2020).
[2] Y. Li et al. Science 358, 506 (2017).
[3] Y. Zhu, Acc. Chem. Res. 54, 3518 (2021).
[4] Y. Fujiyoshi et al. Ultramicroscopy 38, 241 (1991).
[5] F. Börrnert et al. Ultramicroscopy 203, 12 (2019).

17

Development state of the CEOS ground-potential monochromator

Felix Börrnert[1], Stephan Uhlemann[1], Heiko Müller[1], Volker Gerheim[1], Klaus Hessenauer[1], Holger Schulz[1], Maximilian Haider[1]
[1]CEOS GmbH, Heidelberg, Germany

IM-04 (1), Lecture Theater 1, august 27, 2024, 10:30 - 12:30

Electron energy loss spectroscopy (EELS) is a long established analytical method to investigate the chemistry as well as the electronic and optical properties of materials. There are several kinds of EELS, namely regards the energy of the primary electrons and if the geometry is in transmission or reflection. Each method provides distinct information about the sample. In particular, EELS often is integrated into an electron microscope adding spatial information to the spectroscopic signal with about the spatial resolution of the hosting microscope. In this respect, EELS in transmission at primary electron energies in the order of several 10 keV and above gained much popularity in the last decades due to the success of (scanning) transmission electron microscopy ((S)TEM). It evolved into a widespread characterisation method being able to deliver spectroscopic information at the atomic level.

The energy resolving power in modern instruments is often sufficient for just identifying the elemental composition of a material by absorption edge onset fingerprinting, and in many cases the respective bonding states can be investigated by looking at the edge fine structure. Nevertheless, a higher energy resolution would help to find very weak signals and make the fine structure less ambiguous. More importantly, a better energy resolution gives access to very small energy loss signals that otherwise would be shadowed by the fringe of the primary electron beam signal. There, most interesting information about the physical properties of the investigated specimen can be gained.

In spectroscopy using electrons, the energy distribution of the primary electron beam ΔE_0 is a major limiting factor for the energy resolving power of the spectrometer. Reducing ΔE_0 by means of a monochromator can enhance the energy resolving power of the system accordingly. Additionally, in (S)TEM, ΔE_0 in conjunction with the chromatic aberration of the imaging system is one of the limiting factors for the maximum spatial information transfer, especially at lower energies. Therefore, a monochromator can also help to enhance the spatial resolving power of (S)TEM instruments.

There are different types of electron monochromators; crossed electric and magnetic fields, called Wien filter or trochoidal monochromator, and electric or magnetic sector fields (prisms) combined in various geometries (α- or Ω-shaped, hemispheres, or using electron mirrors), leaving out more exotic schemes like radio frequency cavities for pulsed electron beams. To date, four different types of electron monochromators for (S)TEM instruments have been commercialised. First, the simple single-stage Wien filter and second, the more advanced double-stage Wien filter, both employing crossed electric and magnetic multipole fields and a straight optical axis. Third, the purely-electro-static Ω-monochromator using inhomogeneous sector fields bending the optical axis into an Ω-shape and fourth, the purely magneto-static ground-potential monochromator combining magnetic sector fields in such a way that the optical axis follows an α-shaped trajectory. For the first three cases the monochromator is added before the accelerator at low electron energies or at high potential. The fourth implementation is different in this respect. Here, the monochromator is added after the accelerator at high electron energies or at ground potential. The latter implementation ties in with earlier concepts from electron spectroscopy, where the energy-filtered source and the energy analyser are at the same potential. In that case, only the interaction with the specimen causes energy differences and disturbing effects from instabilities of the accelerator can be avoided. Moreover, having the monochromator, the spectrometer and the specimen at ground potential is very beneficial from a technological point of view since additional high-tension feed-through and energy transfer are not necessary. Recently, with a ground-potential monochromator implemented in a dedicated STEM, an unprecedented energy-resolution has been demonstrated and employed for phonon and aloof-beam plasmon spectroscopy. All four presently used monochromator implementations have in common, that the optical design are orthogonal systems with single-section symmetry, that is, the optical axis and the dispersive trajectories are all situated in one section. The optical axis can be curved in one section but not in two sections as long as a perfectly manufactured system without tolerances is considered.

In this contribution, we present the development state of our new design of a ground-potential monochromator based on magnetic prisms in a three-dimensional arrangement. This design abandons the energy selection at the central symmetry plane and the optical axis is not only curved in one section but in two sections. This allows for a highly symmetric and compact design with a variable energy window but no mechanically adjustable energy-filtering slits. Fixed blocking blades in combination with optical deflectors reside at distinct dispersive planes making the system robust and flexible. The practical design fits primary electron energies from 30 keV up to 300 keV and provides an energy resolving power of better than $2\cdot10-7$ with respect to the primary electron energy. Also, the resulting beam cross-over after the monochromator is free of residual spatial or angular dispersion. Very importantly, the new monochromator is designed to be potentially retro-fittable to existing microscopes, adding about 33 cm to the total height of the microscope column.

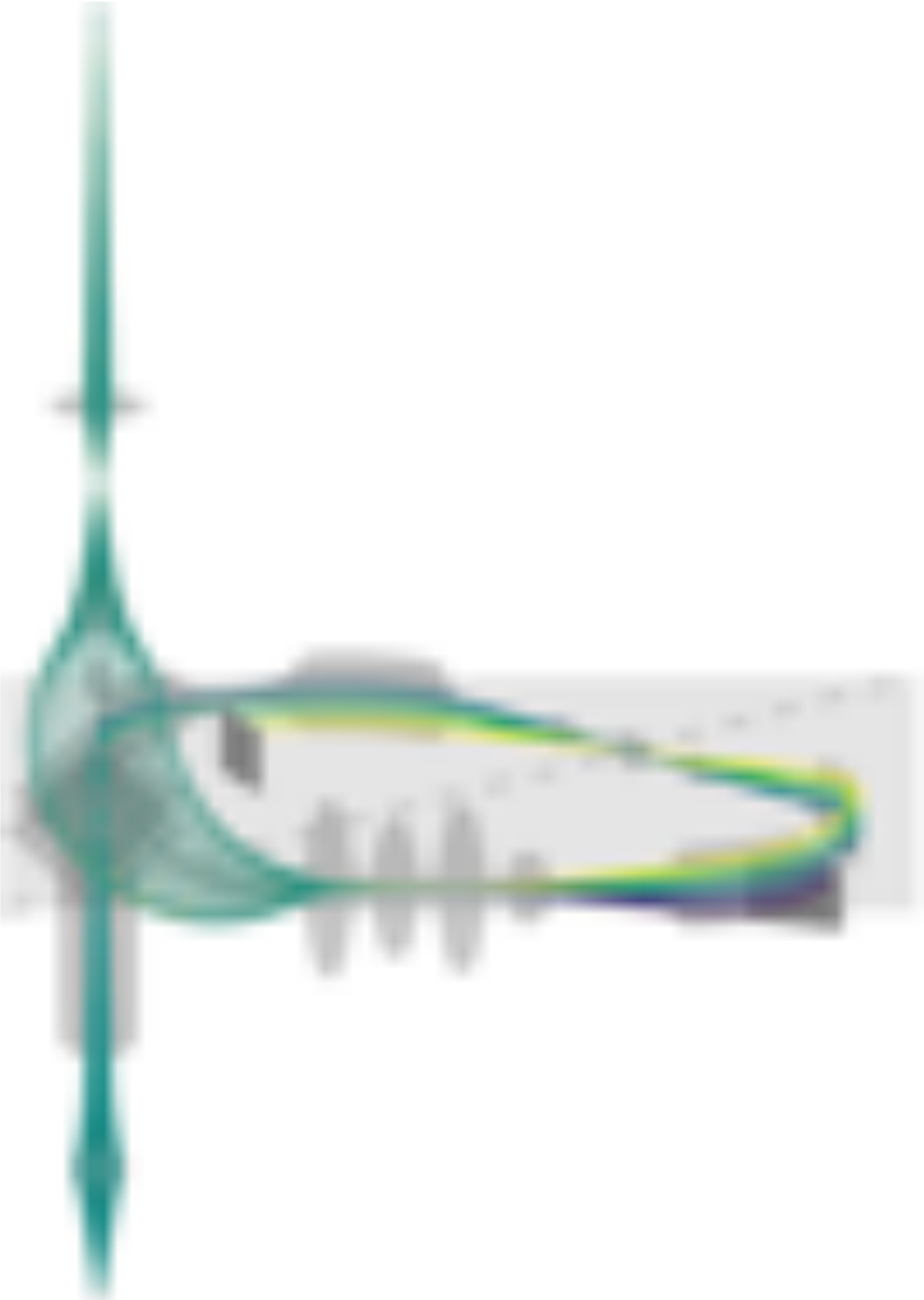

Keywords:

EELS, monochromator, TEM, STEM

95

Quantum Wavefront Shaping with a 48-element Programmable Phase Plate for Electrons

Francisco Vega[1,2], Dr. Chu-Ping Yu[1,2], Dr. Armand Béché[1,3], Prof. Dr. Jo Verbeeck[1,2]
[1]EMAT, University of Antwerp, Antwerp, Belgium, [2]NANOlab Center of Excellence, University of Antwerp, Antwerp, Belgium, [3]AdaptEM, Heverlee,, Belgium

IM-04 (1), Lecture Theater 1, august 27, 2024, 10:30 - 12:30

Similarly to Spatial Light Modulators (SLM) in optics, Electron Phase Plates (EPP) have emerged as a promising solution to several challenges in electron microscopy, such as in-focus phase contrast, adaptive tuning, and exotic beam preparation. Our proposed solution to a generalized EPP is based on an array of miniaturized Einzel lenses that can shift the electron wavefront locally. This electrostatic EPP can be positioned in the electron beam's path in a Transmission Electron Microscope (TEM). The supports and interconnections that make up the EPP will inevitably modulate the amplitude of the electron wavefront. However, the EPP also allows one to adjust the shape of the electron wavefront locally by applying a voltage to each phase pixel [1].
This work demonstrates a fully programmable electrostatic EPP of 48 phase-shifting elements mounted in a state-of-the-art TEM [2]. We prove the device's versatility by preparing a set of orthogonal probe shapes and reproducing the influence of specific geometric aberrations (e.g., defocus of a convergent electron probe). Furthermore, we show a fully automated Scanning TEM (S/TEM) routine in which the EPP corrects the aberration function without active user intervention. Finally, we discuss the device's potential for novel imaging techniques such as electron ptychography. Typically, this technique requires scanning a convergent electron probe over a small area of the sample, which may lead to a limited field of view [3]. Recent research has demonstrated the use of a quasi-parallel beam illumination with both amplitude and phase modulation of the electron wave. By successive shifts of the specimen stage and near-field intensity recording, reconstructions could be performed with a significant expansion of the field of view, with no resolution or electron dose sacrifice [4]. Here, we present reconstruction results obtained through a similar approach for far-field propagation, using different amplitude and phase modulation strategies, as permitted by our programmable EPP design, at different applied electron doses (total dose divided by the number of phase configurations).
The figure below illustrates the far-field ptychographic reconstruction results for three incident electron doses. The illumination on the sample is structured using an array representing the EPP. The columns, from left to right, depict the amplitude mask that is used to simulate the EPP, the phase and amplitude of the object ('Ground Truth'), the results obtained through an amplitude-only modulation ('Flat'), the outcomes of amplitude plus two random phase configurations ('Random'), and the results obtained using a reduced set of two Hadamard phase configurations ('Hadamard').
To summarize, we evaluate our electrostatic EPP in various S/TEM and TEM applications. Our findings indicate that an electrostatic EPP can be integrated into any electron microscopy setup, thereby broadening the device's scope of functions.

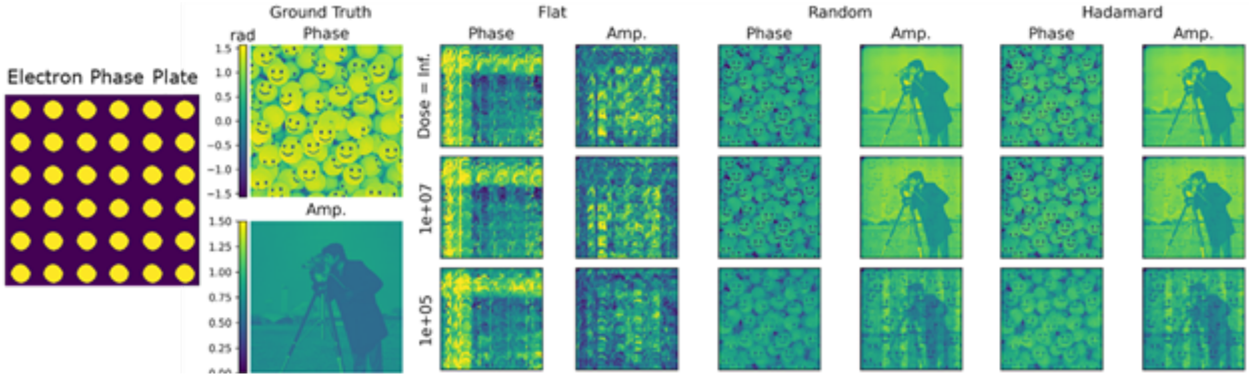

Keywords:

Phase Plate, Wavefront Shaping, Ptychography

Reference:

[1] Yu, C. P., et al. (2023). SciPost Physics, 15(6), 223
[2] Jiang, Y., et al. (2018). Nature, 559(7714), 343-349
[3] You, S., et al. (2023). Applied Physics Letters, 123(19)
[4] Financial support provided by the Research Foundation Flanders, project G042820N. The ERC funded the ADAPTEM project (grant nr: DLV-789598)

101

High-throughput laboratory-based scattering X-ray Tensor Tomography

Azat Slyamov[1], Mr. Adriaan van Roosmalen[1], Mr. Kenneth Nielsen[1], Mr. Erik Lauridsen[1]
[1]Xnovo Technology ApS, Køge, Denmark

IM-04 (1), Lecture Theater 1, august 27, 2024, 10:30 - 12:30

Background incl. aims

Scattering (or dark-field) contrast X-ray microscopy methods for orientation analysis have been gaining increased attention in recent years. The primary advantage of these methods is the ability to map anisotropic structures without directly resolving them, allowing for an extended field of view (FOV). Two different technologies, scanning small-angle scattering and full-field linear grating interferometry have been applied to a wide range of materials, such as fiber-reinforced composites and biological materials [1,2]. However, both methods have disadvantages with throughput: scanning methods have significant overhead in raster scanning the 2D FOV, while gratings require linear and rotational shifts to access 2D orientation sensitivity. A recently developed design of gratings comprised of circular unit cells grid allows single-shot mapping of orientations/scattering in 2D [3]. Each unit cell of the 2D grid provides information on local scattering, emulating raster scanning, while the circular design yields 2D orientation sensitivity, all in a single frame. This is particularly important when 3D scattering tensor information is of interest, achieved by what is known as X-ray tensor tomography (XTT) [4].

Here, we present the capabilities of the state-of-the-art XTT technology based on circular gratings, commercially available on the Exciscope Polaris imaging platform. Notably, we emphasize the simplicity and efficiency of the technology in the laboratory and validate the results against the synchrotron implementation of this technique.

Methods

The sample was prepared using a free-form carbon-fiber injection molding by Addifab, ApS (Fig. 1a). Laboratory and synchrotron measurements were performed on an Exciscope Polaris X-ray microscope and at the TOMCAT beamline, Swiss Light Source, Paul Scherrer Institute, respectively. Different grating design is implemented at two setups: phase-based at the synchrotron and absorption-based at the lab. This is due to the polychromaticity and divergence of the X-ray beam of the lab setup. The latter yields geometric magnification allowing for a detector with larger FOV and pixel size. In both setups, a total of 721 sample poses were collected. A series of 8 tile images at each sample pose was acquired with the phase-grating at the synchrotron setup due to the limited size of the X-ray beam.

Results

Stitching tile images from the Tomcat dataset as pre-processing generated one projection image per pose. Subsequently, both synchrotron and lab-setup datasets were reconstructed using identical algorithms and parameters (Fig. 1b). For validation, reconstructed 3D fiber orientation volumes were registered with affine transformation. The agreement between the two volumes was calculated as an inner product of fiber orientation vectors in each voxel, where values 0 and 1 describe an orthogonal and parallel alignment, respectively. A histogram of the per-voxel inner product (Fig. 1.c) reveals exceptional agreement of the results from two experiments with a mean value of 0.95.

Conclusion

Synchrotron facilities are at the forefront of the development and advancements of 3D X-ray imaging technologies. However, limited user access and a high level of complexity hinder the general use of such large-scale facilities. In this context, we present the capabilities of the state-of-the-art XTT technology with origins at synchrotron that has been successfully transferred into the laboratory environment. The transition of XTT with circular gratings to a commercial imaging platform is presented and validated against synchrotron measurements, revealing a high level of agreement.

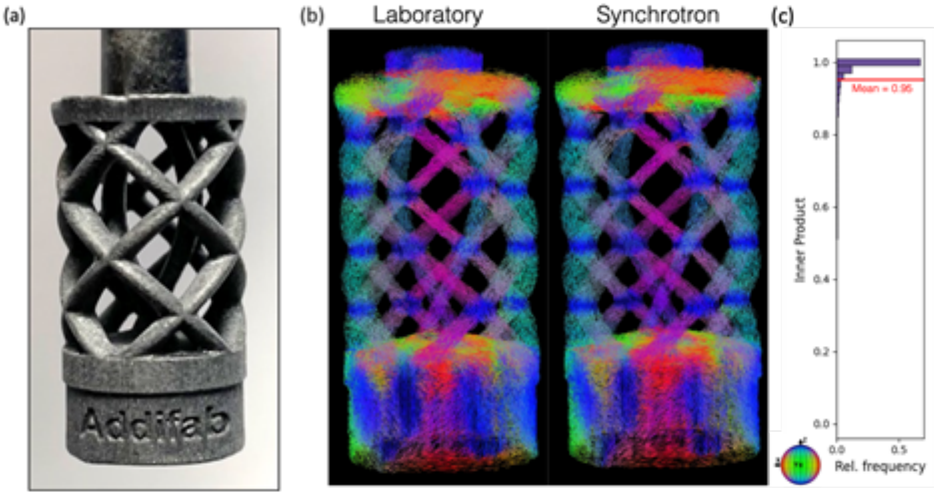

Figure 1. (a) A photograph of the FRP sample. (b) Reconstructed 3D fiber orientation from each dataset. The scale bar is 1 cm. c) Histogram of the inner product of fiber orientation vectors in each voxel.

Keywords:

Tensor-tomography, grating, small-angle scattering, fiber-orientation

Reference:

[1] Liebi, M., et al., Nature 527.7578 (2015):349-352.
[2] Jensen, T., et al., Phys. Rev. B 82.21 (2010):214103.
[3] Kagias, M., et al., Nat. Commun., 10 (1), (2019):1-9.
[4] Kim, J., et al., Appl. Phys. Lett., 116 (13) (2020):134102.
[5] Kim, J., et al., Composite Part B: Engineering, 109634 (2022).

116

High-resolution STEM Image Acquisition Method for Tilted Specimen Using a New Type of Aberration Corrector

Wataru Koibuchi[1], Mr. Ryusuke Sagawa[1]
[1]JEOL, Akishima, JAPAN

IM-04 (1), Lecture Theater 1, august 27, 2024, 10:30 - 12:30

When acquiring scanning transmission electron microscope (STEM) images, it is necessary to align the crystalline zone axis of a specimen tilt with a goniometer and a holder. Since the backlash and drift cannot be avoided in such operations, it is necessary to wait for the drift to settle after aligning crystalline zone axis for a high-quality image acquisition. Therefore, it is desirable to operate a goniometer or a holder mechanically as less as possible. Meanwhile, advances in aberration correction technology have been remarkable and three-hexapole type STEM corrector, Large Aperture STEM Corrector (LASCOR), was recently developed by CEOS GmbH [1, 2]. It is capable of correcting aberrations up to sixth-order three-lobe aberration which had been a limiting factor in the ASCOR corrector. With the LASCOR, the Ronchigram flat area has now been extended to 80 mrad in semi-angle at an acceleration voltage of 200 kV. Thanks to this large flat area, one can align crystalline zone axis using only optical elements (beam tilt and projector shift) of a microscope without any mechanical operation. In this study, we demonstrate a high-resolution STEM image acquisition using this technique.

The procedure is described here how to acquire STEM images of a specimen with a misaligned crystalline zone axis by the proposed method. Firstly, a condenser lens aperture is inserted at the center of the optical axis, and the electron beam is tilted by the beam tilt coils in Fig. 1. This beam tilt appears as the shift of a condenser lens aperture and it can be aligned to the crystal zone axis. The beam is detilted to the center of the detector plane by the projector alignment coils. In this setup, high-resolution STEM images are acquired.

Fig. 2(a) shows an experimentally recorded Ronchigram image with dashed circles indicating the amount of beam tilts used. As the flat area is as large as approximately 80 mrad in semi-angle, the electron beam can be tilted with little influence of geometrical aberrations. Fig. 2(b) ~ (e) show high-resolution STEM images of Si[110] single crystal obtained under different beam tilt conditions corresponding to the dashed circles in Fig. 2(a). It is demonstrated that even for a specimen tilt of over 60 mrad, atomic resolution imaging is achieved by aligning the zone axis using only the optical elements. However, under the tilted conditions, STEM images were blurred in the direction of the tilts, which can also be confirmed in each FFT image. It is assumed that the blurring is due to the effects of the combination of chromatic aberration and beam tilt. Further improvement of image quality can be expected by the use of a monochrometer or a chromatic aberration corrector. Although a specimen tilt causes defocus at the edges of an image and image shrinkage in the direction of the tilt, they can be corrected by changing the defocus during the scan and by a simple image processing, respectively. The correction parameters can be directly calculated by the azimuthal and tilt angles of the beam. The technique introduced here will facilitate an automated acquisition of STEM images and is expected to have applications in the field of semiconductor where it is particularly important to acquire a large number of STEM images quickly.

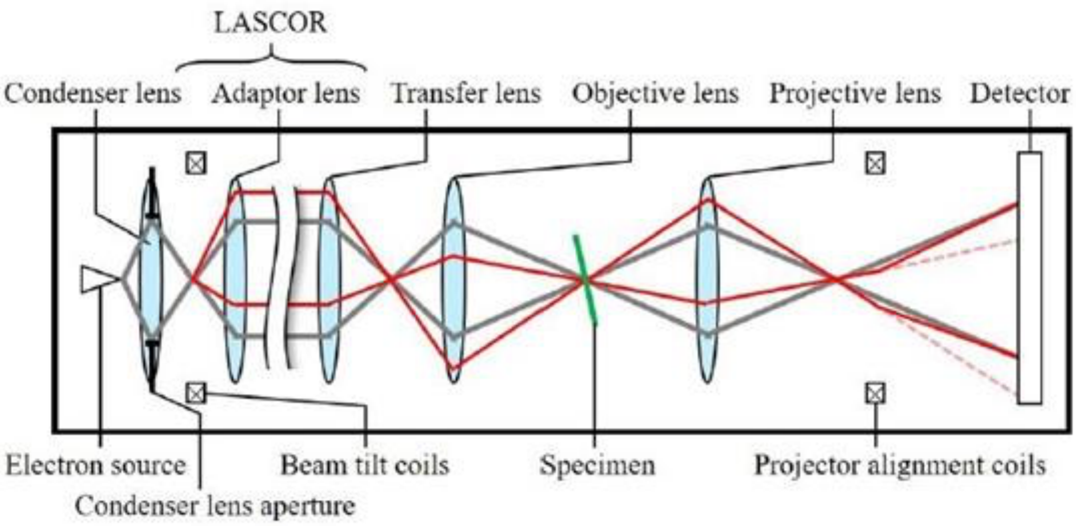

Fig. 1. Schematic ray path in a STEM for specimen with a misaligned crystalline zone axis. The normal ray path is shown in gray and the ray path for a tilted specimen is shown in red.

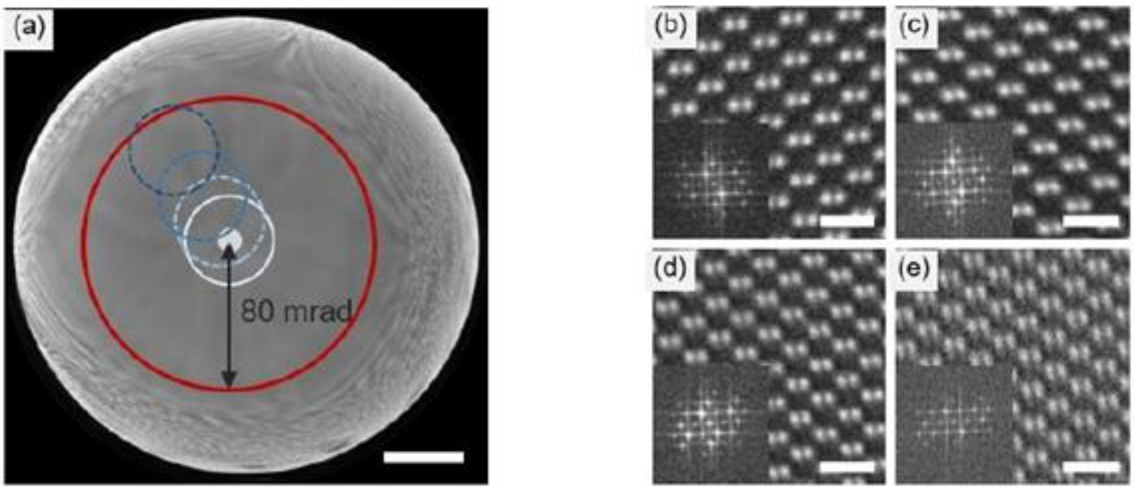

Fig. 2. (a) Ronchigram image with flat area extended to approximately 80 mrad acquired with the LASCOR. White dot indicates the optical axis and dashed circles represent the beam tilts used corresponding to (b), (c), (d), and (e). Scale bar = 50 mrad. (b, c, d and e) ADF-STEM and their FFT images of a Si[110] specimen recorded using a condenser lens aperture with convergence semi-angle of 26.1 mrad under 4 tilt conditions. (b) Without tilt and (c), (d) and (e) with 13.0, 32.0 and 65.2 mrad tilts, respectively. Scale bars = 0.5 nm.

Keywords:

STEM, Cs-corrector, Automation, Semiconductor, Zone-axis

Reference:

1. H Müller et al., Microscopy and Microanalysis, 12 (2006) p. 442.
2. S Uhlemann et al., Microscopy and Microanalysis, 28 (2022) p. 2630.

117

Simultaneous Acquisition of 4D and EELS Data by Newly Developed Pixelated STEM Detector

Dr. Ryusuke Sagawa[1], Mr. Hiroki Hashiguchi[1], Mr. Akiho Nakamura[1], Ms. Shoko Shibagaki[1], Mr. Yutaka Kazama[1], Mr. Martin Huth[2], Mr. Yassine Imari[2], Mr. Valentin Kroner[2], Mr. Stefan Aschauer[2]
[1]JEOL Ltd., Akishima, Japan, [2]PNDetector GmbH, München, Germany

IM-04 (1), Lecture Theater 1, august 27, 2024, 10:30 - 12:30

In scanning transmission electron microscopy (STEM), efforts to obtain specimen information as much as possible have long been made and variety types of detectors have been developed. Pixelated STEM detector is one of these instruments for utilizing diffraction information that was otherwise partly lost in the conventional single-channel STEM detectors. Various types of applications have been introduced using the 4-dimensional (4D) dataset which include synthetic STEM image reconstruction, field map visualization and phase image reconstruction by ptychography, etc. [1,2]. Meanwhile, electron energy loss spectroscopy (EELS) is also an important and popular means of obtaining information on the composition and even on the chemical bonding inside a sample. Considering the type of necessary electron signal for both 4D-STEM and EELS, they should go well with each other in many cases: the former needs a part of transmitted electron beam and scattered or diffracted beams and the latter needs a part of transmitted beam which is complementary to the former [3]. Although simultaneous analysis using both instruments has been anticipated, making a center hole in the middle of a pixelated detector to let electron beam pass through into an EELS spectrometer was a manufacturing challenge. PNDetector is a company manufacturing high-speed pnCCD camera which can be operated at 7,500 frames per second for the 4D-STEM application. It recently manufactured a prototype pnCCD sensor with a center hole while keeping other specs the same, realizing the simultaneous acquisition of 4D and EELS data [4].

The prototype pnCCD camera was installed on a JEM-F200 (JEOL Ltd.) electron microscope with a cold field emission gun (Fig. 1). Below the camera, CEFID (CEOS GmbH) EELS spectrometer was mounted. Scan was triggered by an ELA (DECTRIS AG) camera mounted on the CEFID as a post-filter detector. Then the microscope scanning system and the pnCCD camera readout were synchronized to it. In EELS application, scanning dwell time of more than several tens of milliseconds is usually required for a sufficiently high SN ratio of an EELS mapping data. In order to synchronize this somewhat slow scanning speed with the high-speed pnCCD camera, a multiple readout signals of the pnCCD camera was accumulated at each scanning position.

Fig. 2 shows the simultaneously obtained 4D-STEM and EELS data from a semiconductor sample. Fig. 2(a) shows a diffraction pattern image obtained at a certain position on the sample. Since the sensor has a hole, there is a circular area at the center of the image where no electron signal was generated. Camera length of the microscope was set so as to let the transmitted electron beam pass through the hole while keeping the diffracted signals inside the field of view of the camera. Fig. 2(b)~(d) are synthesized STEM images from each diffracted disk in Fig. 2(a). Because all the diffracted disks were recorded at every scanning position, different image contrasts were obtained from the same field of view, thus, the 4D-STEM data acquisition was demonstrated. Fig. 2(e)~(h) show simultaneously obtained EELS elemental mapping images of oxygen, nickel, silicon and titanium, respectively. Each image has a sufficiently high SN ratio and one can clearly tell the locations of each element inside the sample.

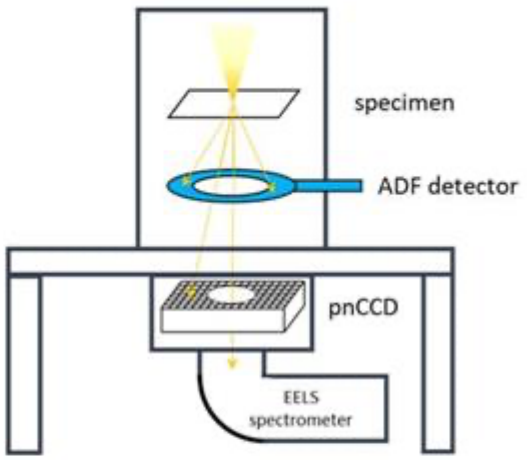

Fig. 1. Illustration of a simultaneous data acquisition of 4D-STEM and EELS with a pnCCD pixelated direct detector with a center hole in the middle.

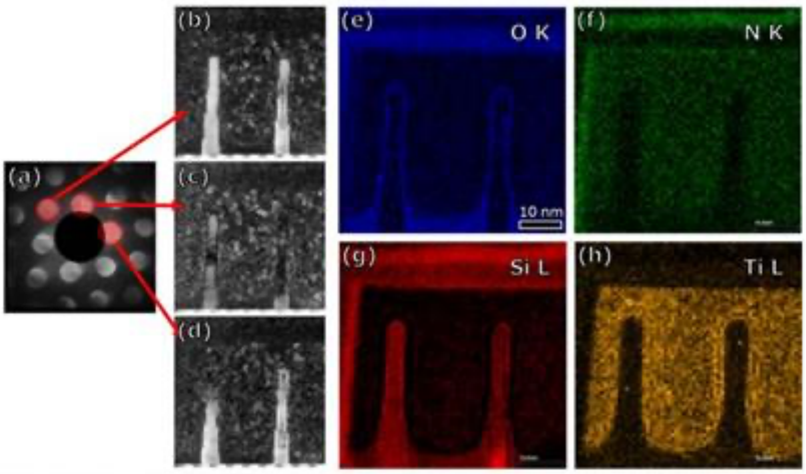

Fig. 2. Simultaneously recorded 4D and EELS data. (a) Diffraction pattern and (b~d) reconstructed STEM images from each diffraction disk in (a). (e~h) EELS elemental mapping images.

Keywords:

STEM, 4D, pixelated detector, EELS

Reference:

[1] TJ Pennycook et al., Ultramicroscopy, 151 (2015) p. 160.
[2] R Sagawa et al., Microsc. Microanal., 23 (2017) p. 52.
[3] B Song et al., Physical Review Letters, 121 (2018) p. 146106.
[4] M Huth et al., Microscopy and Microanalysis, 29 (2023) p. 401.

130

A new Ion Microscope for high-resolution imaging and SIMS nano-analytics

Dr. Alexander Ost[1], Torsten Richter[1], Olivier De Castro[2], Peter Gnauck[1], Jean-Nicolas Audinot[2], Tom Wirtz[2]
[1]Raith GmbH, Dortmund, Germany, [2]Luxembourg Institute of Science and Technology (LIST), Belvaux, Luxembourg

IM-04 (1), Lecture Theater 1, august 27, 2024, 10:30 - 12:30

Powerful material characterization techniques excelling in terms of lateral resolution and sensitivity are needed to study nanoscopic materials and their transformation processes in 3 dimensions at the relevant spatial scales. State-of-the-art Focused Ion Beam (FIB) technologies allow not only to visualize nanoscopic 3D structures, but also analytical surface measurements with Secondary Ion Mass Spectrometry (SIMS). SIMS is a powerful surface analysis technique which uses energetic primary ions to sputter the surface of a sample and to generate secondary ions separated by a mass analyzer to record chemical information. Advantages of SIMS are the high sensitivity, the high dynamic range, the ability to differentiate between isotopes and the access to the complete periodic table. Typical SIMS analysis modes are mass spectrum recording, depth profiling, 2D, and 3D imaging. In the past, the correlation of high-resolution ion microscopy with in-situ SIMS has allowed to acquire complementary topographic and chemical information for a deeper understanding of samples in various domains, including material sciences, geology, and biology [1].
The IONMASTER magSIMS is a novel system devoted to correlative high-resolution 2D/3D imaging and SIMS nano-analysis. The system is a unique combination of a Liquid Metal Alloy Ion Source (LMAIS) [2] and a dedicated magnetic sector SIMS unit. Within the LMAIS various ion species are emitted simultaneously from a single ion source (GaBiLi [3] and AuGeSi sources available) and are separated in a downstream Wien filter within the FIB column. This allows to choose the most suitable primary ion species depending on the application and also to toggle within a few seconds between the ion species. This has for instance the advantage to use heavy (e.g., Bi+ or Au+) primary ions to delayer the sample stepwise and to use lighter primary ions (e.g., Li+ or Si2+) to image the sample at high spatial resolution. These image planes can be stacked and used to create a 3D volumetric reconstruction of the sample [4]. The SIMS unit is equipped with an insertable/retractable extraction optics to transfer the generated secondary ions through the magnet based mass analyzer onto a focal plane detector. The latter allows parallel acquisition of full mass spectra for each scanned pixel within the chosen field of view [5] which gives the user a multitude of possibilities to post-process and correlate the SIMS image data.
Further key strengths of this FIB-SIMS platform are the possibility to use application specific primary ion beams, i.e. the ability to switch quickly between reactive primary ion species to maximize either positive (e.g., Au+ or Bi+ single primary ions and clusters) or negative ionization (e.g., Li+ primary ions) of the sputtered particles. The small beam diameter of the lightest primary ions (Li+ and Si2+) allows to perform high spatial resolution imaging in SIMS (< 20 nm) . The low penetration depth of heavy Bi+ and Au+ (and clusters) primary ions into the material enables excellent depth resolution. Moreover, the combination of a LMAIS FIB, a Laser Interferometer Stage with CAD based navigation, and a magnetic-sector SIMS offers a high potential for automatized workflows.
In this contribution, we will present the key features and the working principle of the IONMASTER magSIMS system equipped with a LMAIS. We will show results on correlative 2D and 3D imaging focused on applications including CIGS solar cells (Figure 1), geological and microelectronics samples investigated on the recently developed nano-analysis system. Thus, we will demonstrate that the new IONMASTER magSIMS paves the way for nano-analytics beyond the conventional methodology for sample analysis by combining the LMAIS technology with a stable stage and a SIMS unit for highest spatial resolution imaging.

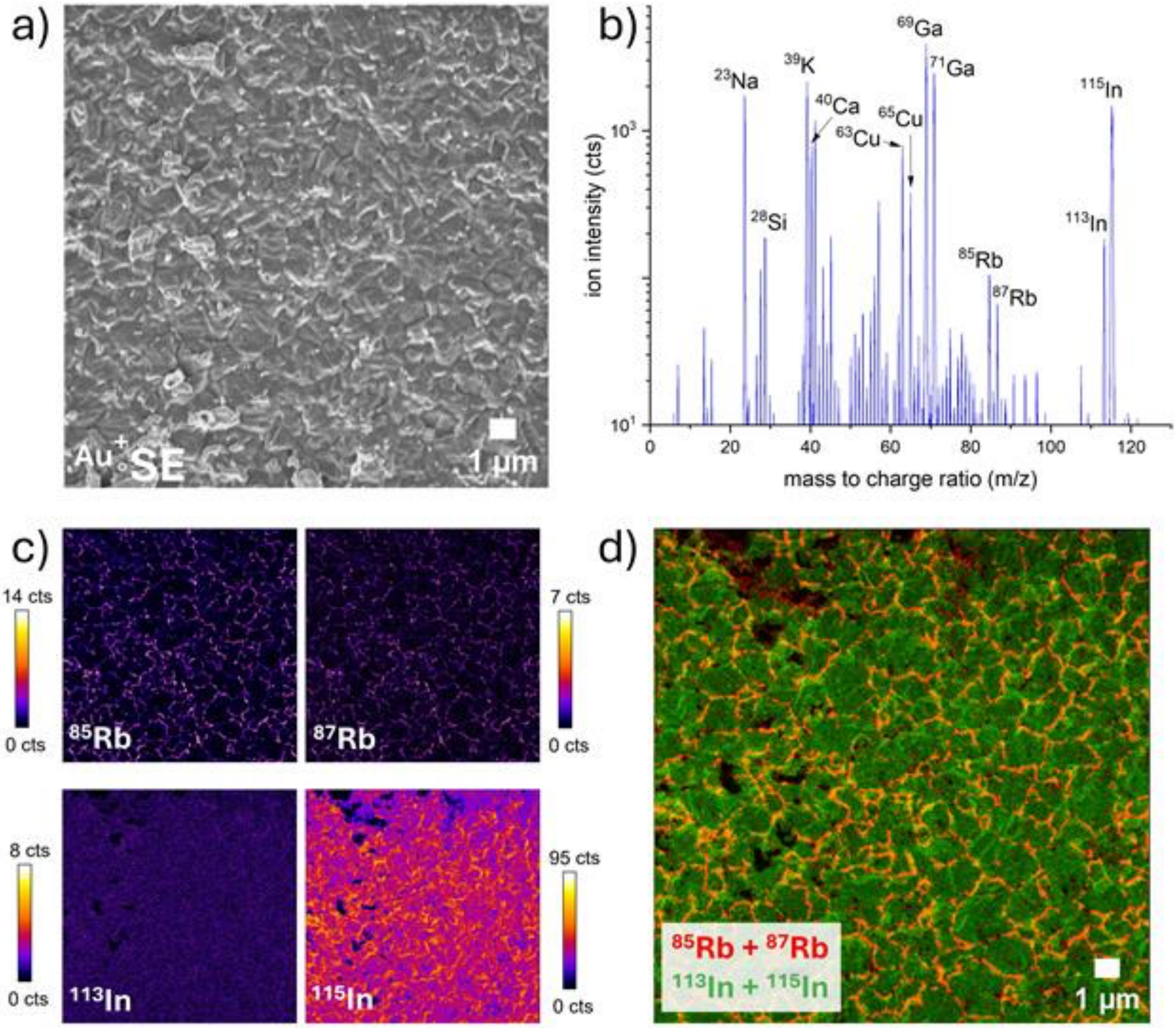

Figure 1: a) Secondary Electron (SE) image generated using a 35 keV Au^+ primary ion beam acquired on the IONMASTER magSIMS on a RbF-treated CIGS solar cell sample. b) Mass spectrum acquired in positive SIMS mode. c) SIMS image maps showing the distribution of ^{85}Rb, ^{87}Rb, ^{113}In, and ^{115}In of the same zone as a). d) Red-green map of the sum of the ^{85}Rb and ^{87}Rb (red) as well as ^{113}In and ^{115}In (green) isotopes showing that Rb segregated at the grain boundaries of the CIGS surface.

Keywords:

FIB, SIMS, Imaging, LMAIS, Applications

Reference:

1. J.-N. Audinot et al., ROPP 84 (2021), p. 105901.
2. L. Bischoff et al., Appl. Phys. Rev. 3 (2016), 021101.
3. L. Bischoff, S. Akhmadaliev, DE102007027097B4.
4. A. Nadzeyka et al., JVST B 41 (2023), 062802.
5. O. De Castro et al., Anal. Chem. 93 (2021), p. 14417–14424.

155

Atom Probe Tomography experiments performed in a (Scanning) Transmission Electron Microscope

Professor Williams Lefebvre[1], Gérald Da Costa[1], Castro Celia[1], Antoine Normand[1], Charly Vaudolon[1], Aidar Zakirov[1], Juan Macchi[1], Mohammed Ilhami[1], François Vurpillot[1]
[1]Univ Rouen Normandie, INSA Rouen Normandie, CNRS, Normandie Univ, GPM UMR 6634, Rouen, France

IM-04 (2), Lecture Theater 1, august 27, 2024, 14:00 - 16:00

Background
Atom Probe Tomography (APT) is intrinsically a 3D characterization technique that provides tomographic reconstructions of materials with a near atomic scale resolution. For APT, specimens must be prepared as sharp needles. This is most of the time realized using FIB SEM and before analysis in APT, specimens can easily be characterized in a TEM or STEM using specific holders or protocols. Hence, correlative analysis by (S)TEM and APT gives access to a wide range of information about the specimen. Unrivaled spatial resolution of (S)TEM, availability of 4D-STEM or diffraction with the combination of the 3D composition fields accessible by APT hence leads to a better description of materials by the correlation of structural, physical and chemical characterization.
To make correlative analysis by (S)TEM and APT more accessible, efforts have been foreseen and made to join both techniques in a single instrument [1-4]. This work presents the main achievement of an instrumentation project started at GPM in 2014, which is the implementation of an Atom Probe in a commercial JEOL F2 (Scanning) Transmission Electron Microscope.

Methods
Specifics TEM holders were designed first for a JEOL 2010 TEM, on which they were tested, and then transferred to a JEOL F2 installed at University of Rouen in 2022. These holders offer the possibility to perform APT experiments either at room temperature or cryo temperature (78K measured at the tip). They accept APT specimens which can be polarized with a positive voltage up to 8 kV. Electrostatic pulses are superimposed to trigger field evaporation with a pulse repetition rate of 20 kHz. The APT detector consists in an advanced-delay line setup, mounted on a port facing the goniometer of the microscope.

Results
The figure below shows the setup realized in the framework of this project. The ion sensitive and time resolved spatial detector is mounted behind the column (on the left in the image) and APT specimens are loaded classically in the goniometer, using home designed holders. All imaging conditions available with the microscope can be applied to characterize APT specimens. Here, an illustration is given with the automated crystal orientation mapping method. A nearly equiatomic Fe-Cr alloy with an ultrafine grain structure has been submitted to a heat treatment leading to spinodal decomposition. The visualization of grain boundaries in the APT specimen allows to localize unambiguously the location of APT analysis in the specimen.

Conclusion
This new instrument, combining APT with (S)TEM, opens up new prospects for unambiguously correlating the characterization of structural defects (such as grain boundaries, precipitates or dislocations) identified in TEM with the chemical characterization, atom by atom, accessible in tomographic atom probes.

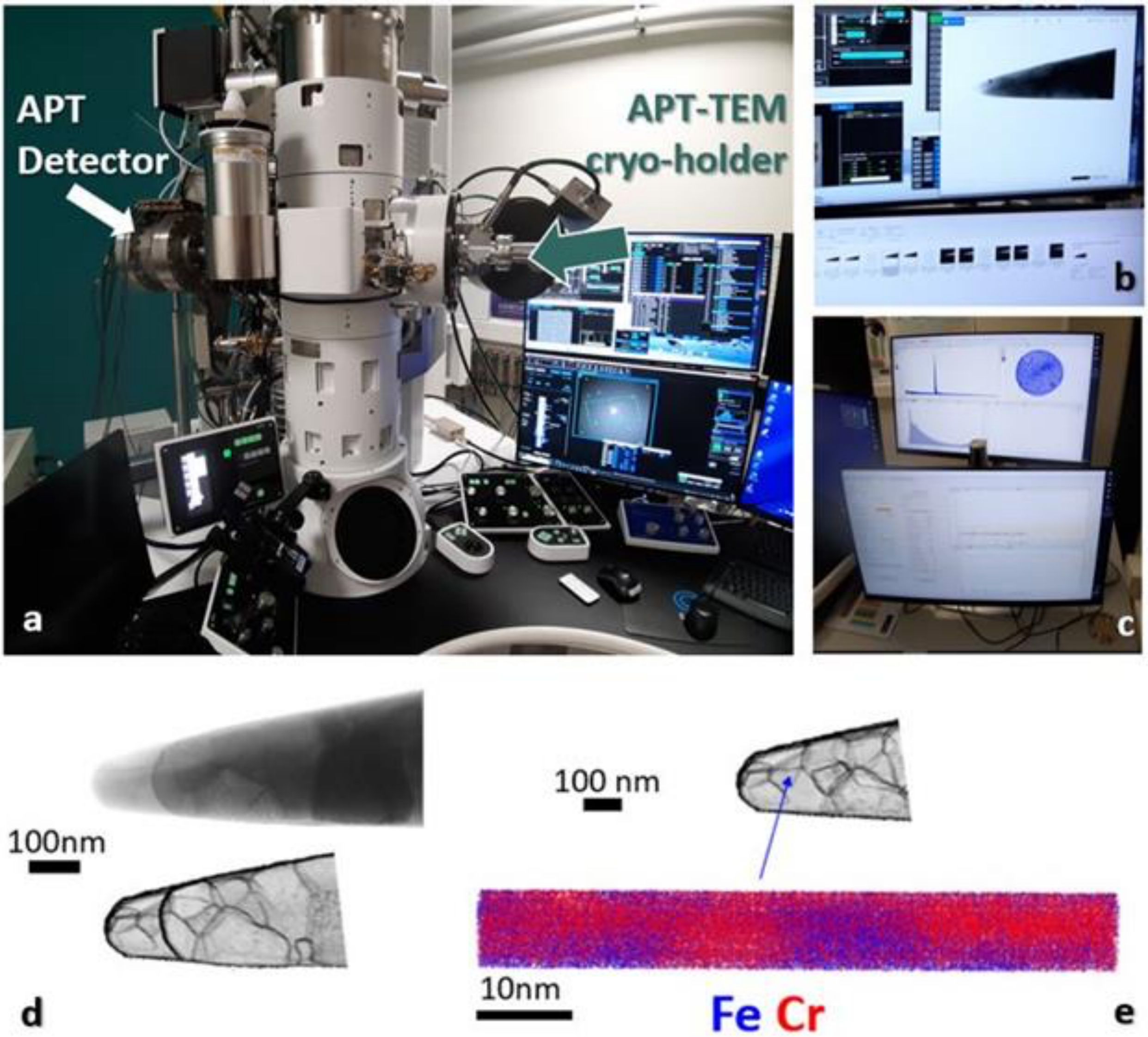

(a) JEOL F2 microscope equipped with an APT-TEM cryo-holder and APT detector both designed at GPM. (b) BF-STEM of a specimen and (c) sequence of acquisition of an Al-alloy. (d) Superimposition of images acquired before and after APT acquisition in JEOL F2. Top images are BF-STEM and images below show grain boundaries imaged with the ASTAR software of an ultrafine grain FeCr alloy. (e) APT reconstruction of the same alloy, showing the region of interest analyzed in APT.

Keywords:

Atom Probe Tomography, STEM, instrumentation

Reference:

[1] Kelly, T. F., et al., Microscopy and microanalysis 19, 652–664 (2013).
[2] W. Lefebvre, Workshop on Scientific Directions for Future Transmission Electron Microscopy, Forschungszentrum Jülich, Germany (Oct. 24-26, 2016)
[3] Atomic-Scale Analytical Tomography. (eds. Gorman, B. P., Ringer, S. P. & Kelly, T. F.) (Cambridge University Press, 2022).
[4] Kelly, T. et al. Microscopy and Microanalysis 26, 2618 (2020).

340

Low-voltage Secondary Electron Emission Spectromicroscopy using a Scanning Auger Microscope

Abbas Kosari Mehr[1], Mohammad Zaghloul[1], RitiK Tanwar[1], Wenzheng Cao[1], Silvia Maria Pietralunga[2], Anjam Khursheed[1], Alberto Tagliaferri[1]
[1]Polytechnic of Milan, Milan, Italy, [2]Consiglio Nazionale delle Ricerche of Italy (CNR), Milan, Italy

IM-04 (2), Lecture Theater 1, august 27, 2024, 14:00 - 16:00

Background
Having been utilized in scanning electron microscopes, secondary electron emission is considered a well-established nano-scale probe for mapping the surface morphology of materials. It has also been demonstrated that secondary electrons (SE) emitted from materials can provide additional information on the local work function, bulk density of state (DOS), surface potential, charging/discharging characteristics, and elemental/chemical properties of bulk materials. The nano-scale lateral resolution and surface sensitivity of low-voltage scanning microscopes give them a unique advantage for the investigation of surfaces. However, the surface contamination caused by exposure to electron beams has always been a limiting factor for this purpose. Since the yield of SE emission is higher than that of Auger emission, the secondary electron emission spectromicroscopy (SEES) performed in an ultra-high vacuum chamber using a scanning Auger microscope (SAM) can be a very powerful tool for surface characterization, especially in the case of ultra-thin materials. Moreover, the concurrent SEES and Auger spectromicroscopy can also provide useful information on the analysis of light elements and hold promise for enabling nanoscale hyperspectral electron spectromicroscopy studies of 2D materials.
Method
We adapt our scanning auger microscope (SAM), equipped with a cylindrical mirror analyzer (CMA) and operated in an ultra-high vacuum, to SEES by tilting the sample holder and applying a negative bias to the sample. We also measured DOS/SEES signals on different materials at low voltages of 500 and 1000 eV.
Results
The SEES results showed that the SAM can perform SEES on different materials when the sample is tilted and negatively biased. The experimental SEES results on metals are in agreement with the Chung and Everhart theory. Moreover, quantum-state contrast on different materials, including ultra-thin films, can be mapped using the SEES acquisition approach. However, the DOS information can be extracted partially, due to a degree of distortion in the signal.
Conclusion
From the results, one can conclude that the SAM can be a proper platform for SEES. However, a lens should be commissioned to pre-accelerate the SEs properly before the entrance to the CMA, mitigating the field distortion around the sample holder. Moreover, the technique can promise the quantum-state mapping of 2D materials due to the limited degree of beam-induced surface contamination.

Keywords:

Auger microscope, Secondary electron, spectroscopy

457

MÖNCH: A 25um hybrid pixel detector with sub-pixel resolution using deep learning

Xiangyu Xie[1], Luis Barba Flores[2], Benjamín Béjar Haro[2], Anna Bergamaschi[1], Erik Fröjdh[1], Elisabeth Müller[3], Kirsty Paton[1], Emiliya Poghosyan[3]
[1]PSD Detector Group, Paul Scherrer Institut, Villigen, Switzerland, [2]Swiss Data Science Center (SDSC Hub at PSI), Paul Scherrer Institut, Villigen, Switzerland, [3]Electron Microscopy and Diffraction Group, Paul Scherrer Institut, Villigen, Switzerland

IM-04 (2), Lecture Theater 1, august 27, 2024, 14:00 - 16:00

Background incl. aims
The adoption of direct electron detectors (DEDs) has led to the "resolution revolution" in cryogenic electron microscopy (cryo-EM) [1]. In Cryo-EM the state-of-the-art is back-thinned Monolithic Active Pixel Sensors (MAPS) due to their small pixel size (< 15 µm) and high-quality imaging capabilities. However, back-thinned MAPS have several drawbacks in terms of radiation hardness, frame rate, and non-optimal performance for low-energy electrons (≤ 120 keV), which are of increasing interest for better image contrast for a given electron dose and lower operational costs [2].
An alternative type of direct electron detector, Hybrid Pixel Detectors (HPDs), have been widely adopted for diffraction-based modalities in electron microscopy on the account of their high frame rates (> 1 kHz) and large dynamic range. However, currently available HPDs are limited in their suitability for imaging by their large pixels (≥ 55 µm) and multiple scattering of electrons in their thick (≥ 300 µm) sensors, such that the signal produced by incident electrons is recorded by many pixels, despite the large pixel pitch. MÖNCH [3] is a general-purpose, charge integrating HPD under development which is notable for its small, 25 µm pixels. Therefore, to fully realize the potential benefits of fast, radiation hard HPDs across the widest range of electron energies and experimental modalities of electron microscopy, we are developing deep learning methods to reconstruct the impact points of incident electrons from their complex track in the sensor with sub-pixel resolution.
Methods
We generated training samples including detector responses and impact points of individual incident electrons from both simulation and measurements. The simulation configuration closely mirrors the design parameters of the MÖNCH. Whereas previous studies [4] have been entirely based on simulations, we have, uniquely, prepared training samples with precise labels from experimental measurements by developing two novel data acquisition approaches, which will be presented in detail. For this purpose, as well as for the measurement of the detector's performance as quantified by its modulation transfer function (MTF) and detective quantum efficiency (DQE), a MÖNCH 03 prototype was mounted on a JEOL JEM-ARM200F NEOARM at the Paul Scherrer Institute for data collection.
Based on the simulated and experimental datasets, deep learning models were developed for impact point reconstruction. We will show details of the deep learning model design, training scheme, and evaluation results.
Results
Sub-pixel resolution was attained at all tested energy levels (200, 120, 80, 60 keV). For example, at energy levels of 200 keV and 60 keV, the resolutions were 1.8 pixels and 0.4 pixels for the conventional charge centroid method, while via the deep learning approaches the resolutions were 0.6 pixels and 0.3 pixels, respectively. Images of a test sample consisting of continuous carbon with gold nanoparticles at 200 keV are shown in Figure 1, processed using the conventional charge centroid method (left) and the deep learning approach (right). With the deep learning method, we were able to image the spacing of the {1 1 1} gold atomic planes, with a spacing of 2.35 Å. The MTF and DQE results at all energy levels, with and without the deep learning algorithms applied, will also

be presented as a benchmark of the system's capabilities. Lastly, the data processing pipeline for the MÖNCH detector for its use in electron microscopy will be discussed.

Conclusion

In this work, we have successfully developed deep learning approaches for localizing electron impacts on MÖNCH. Using measurement-based training enabled by the novel acquisition setup we have developed, sub-pixel spatial resolution was achieved across all electron energies tested. The improvement relative to the results obtained with the charge centroid method increased with electron energy. The spatial resolution obtained for 200 keV electrons (0.6 pixels) represents a threefold enhancement compared to the charge centroid method. Our results show that MÖNCH, with its spatial resolution enhanced using deep learning, is a highly promising detector for electron microscopy studies using electrons up to 200 keV.

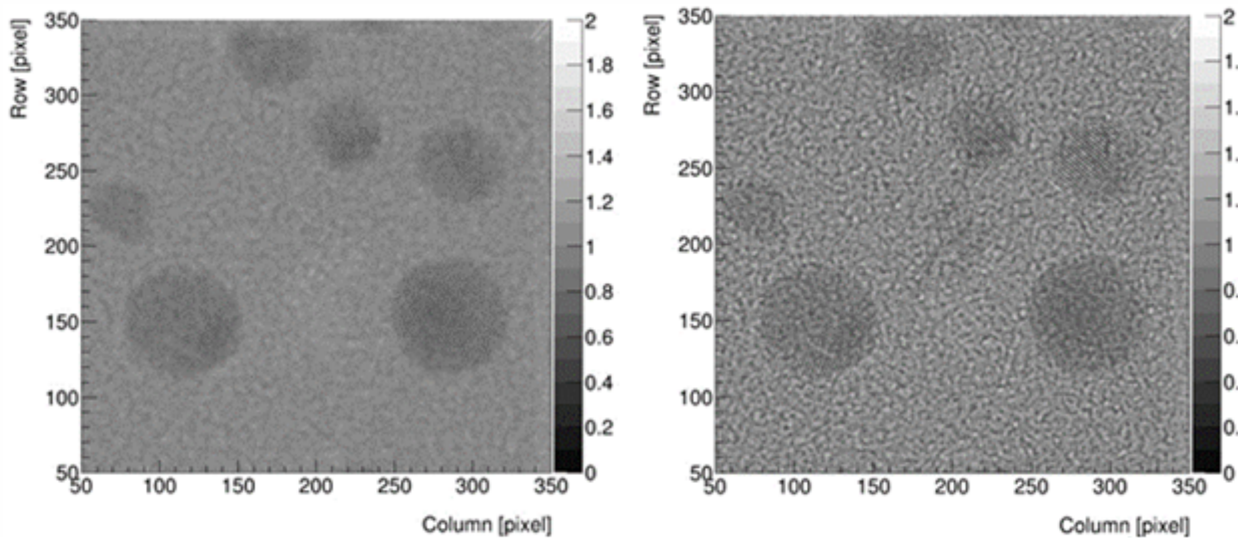

Keywords:

Hybrid Pixel Detector, Deep-Learning, Cryo-EM

Reference:

[1] W. Kühlbrandt, The Resolution Revolution, Science 343 (2014) pg. 1443-1444

[2] K. Naydenova et al, CryoEM at 100 keV: a demonstration and prospects, IUCrJ 6 (2019) pg. 1086-1098

[3] M. Ramilli et al, Measurements with MÖNCH, a 25 μm pixel pitch hybrid pixel detector, Journal of Instrumentation 12 (2017) pg. C01071, DOI 10.1088/1748-0221/12/01/C01071

[4] J. Paul van Schayck et al., Ultramicroscopy, 218 (2020), 113091

501

Enhanced time resolution with a room-temperature energy dispersive X-ray PIN photodiode detector

Luca Serafini[1,2], Mr. Mylo Gijbels[1,2], Prof. Dr. Jo Verbeeck[1,2]
[1]EMAT, University of Antwerp, Antwerp, Belgium, [2]NANOlab Center of Excellence, University of Antwerp, Antwerp, Belgium

IM-04 (2), Lecture Theater 1, august 27, 2024, 14:00 - 16:00

Energy dispersive X-ray spectroscopy (EDX) has demonstrated its utility across diverse fields, ranging from materials science to biology, serving as a user-friendly analytical technique in electron microscopy for elemental analysis and mapping of specimens. Detector technology has evolved from liquid nitrogen-cooled lithium-drifted silicon detectors (Si(Li)) to configurations featuring multiple large, tear-drop-shaped thermoelectric-cooled silicon drift detectors (SDDs). The former type allows for high count rates by having a large active area while keeping the anode capacitance low. Incident X-rays are absorbed in the bulk Si region and generate electron-hole pairs. The electrons then drift towards the anode under guidance of an electric field which is established and controlled by several increasingly reverse-biased ring electrodes covering one surface of the detector.
While this method is effective for elemental mapping and offers reasonable acquisition times, the precision of X-ray arrival time is limited by the relatively slow drift speeds and large active area size. X-rays absorbed near the anode are read out significantly faster than those absorbed farther away. This forms a major bottleneck for another promising electron microscopy application, namely EDX and energy electron loss (EELS) coincidence detection. Here the aim is to correlate transmitted electrons and X-rays in time. The coincidence information can greatly enhance the sensitivity for detecting trace elements in a matrix as compared to conventional EELS and EDX. Furthermore, the method allows the determination of the collection efficiencies without the use of a reference sample and can subtract the background signal for EELS and EDX without any prior knowledge of the background shape and without pre-edge fitting region. Another advantage is that the correlation data is revealed while preserving the full EELS and EDX signal without compromise in speed or acquisition time.
To tackle this issue, we are working on a proof-of-concept detector design consisting of a small reverse-biased Si PIN photodiode with a low-noise charge amplifier circuit. Si PIN photodiodes are reported to be suited for X-ray detection and are commercially available at low prices and in small sizes. What truly sets our approach apart is that contrary to the ongoing trend of ever-increasing size of active areas and number of detectors to increase solid collection angle and thus acquisition rates, we ensure sufficient collection by bringing our sensitive area and specimen very close together. The sensitive area can thus remain small, keeping the photodiode’s capacitance low enough to allow for high acquisition rates and low noise levels. Moreover, the small size minimizes the temporal broadening as initially aimed for. Regardless of where the X-ray is absorbed, the readout speed in a PIN photodiode will have little spread as the anode stretches over the entire back side of the PIN junction. Besides the fundamental improvement in time resolution, our concept offers numerous practical advantages. It provides a cost-effective method for integrating EDX capabilities into an electron microscope. Additionally, the use of a small PIN photodiode minimizes the necessity for cumbersome cooling, as the limited active area (and thus cross-section of the depletion layer) ensures that dark current (noise) remains limited even at room temperature.
So far several prototypes have been made and tested in a scanning electron microscope (SEM) as this allows for convenient piloting. Over the different iterations the leakage current, signal-to-noise ratio (SNR) and form factor have been improved. With Cu X-rays the current SNR of the single X-ray pulse signals we are measuring is above 5, with pulses exhibiting sub-50ns rise times (see left side of figure). The entire system consumes less then 750mW of power. We are on the brink of obtaining our

first energy spectrum and determining the energy resolution using the XG-lab digital DANTE pulse processor. Currently different photodiodes are being tested and compared as well as ways of preventing the X-rays from landing outside of the depletion layer of the photodiode where they lead to a slow and distorted signal.

In conclusion, we present the development of an in-house build room-temperature PIN photodiode X-ray detector to improve time resolution and allow for advancements in EDX and EELS coincidence experiments that so far have been hampered by the slow drift mechanism in SDD setups.

This work received funding from the Horizon 2020 research and innovation programme (European Union), under grant agreement No 101017720 (FET-Proactive EBEAM)

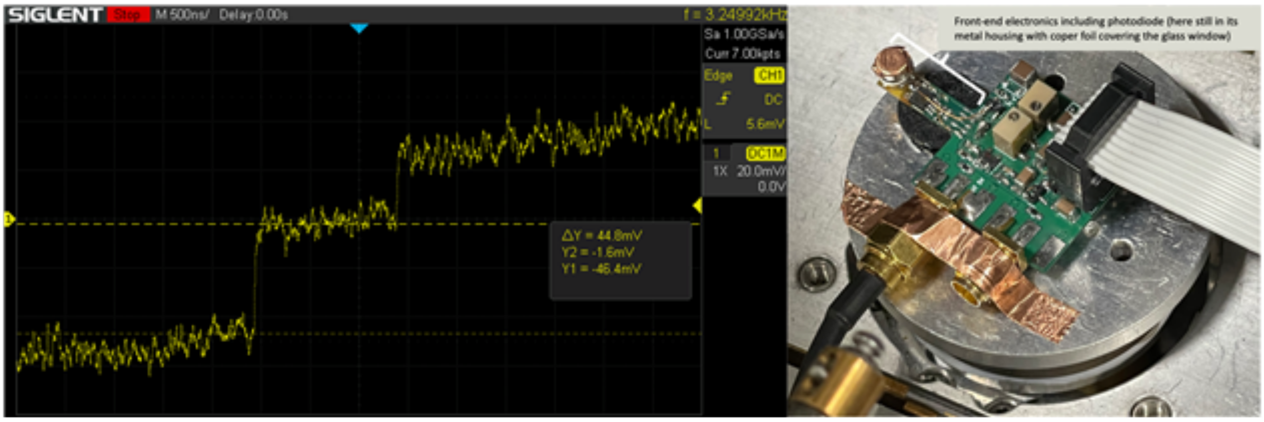

Keywords:

EDX, coincidence, PIN, charge-sensitive preamplifier

Reference:

[1] K. Thompson, Thermo Fischer Scientific, Tech.Note 52342 (2012)
[2] G. F. Knoll, Radiation Detection and Measurement, Wiley, 4th ed. (2010)
[3] D. Jannis et al. ; Appl. Sci. 11, 9058 (2021)
[4] F. J. Ramírez-Jiménez et al., AIP, 857, 395 (2006)
[5] M. Urban et al. ; Sensors, 23, 2201 (2023)

502

Development and application of In-situ atomic-scale straining&heating&biasing platform for TEM

Dr. Zhipeng Li[1,2], Dr. Jianfei Zhang[1], Dr. Haixin Li[1,2], Prof. Shengcheng Mao[1], Prof. Xiaodong Han[3], Prof. Ze Zhang[4]
[1]Beijing University of Technology, Beijing, China, [2]Bestron Science&Technology Co., Ltd., Beijing, China, [3]Southern University of Science and Technology of China, Shenzhen, China, [4]Zhejiang University, Hangzhou, China

IM-04 (2), Lecture Theater 1, august 27, 2024, 14:00 - 16:00

Background incl.aims
Due to increasing demands on better performance of materials of various fields working under harsh and complicated conditions and the constant minimization of devices, it is essential to reveal structure-composition-property correlation of materials from atomic-scale under working conditions in real-time. In-situ TEM technology is one of the most promising solutions to the above needs and has advancing rapidly in recent decades. However, it is greatly difficult to simulate working environment involving harsh thermal, mechanical, electrical stimuli, while performing real-time atomic-resolution observation and analysis of materials. For this reason, our group has dedicated to the development of an in-situ atomic-scale straining, heating and biasing system for TEM and has successfully applied the platform to study the atomic-scale response of various materials and revealing the mechanisms underneath.
methods
The multi-functional in situ TEM testing platform was developed mainly based on micro piezoelectric ceramic actuator and dedicated designs of MEMS chips with various heating and/or biasing functionalities. With a unique truss-like design, the heating chip can heat the sample from room temperature to 1200℃ with an accuracy of ±1℃ while allowing straining of the sample at any given temperature. The miniature straining actuator can apply a GPa-level stress, over 4 microns actuation displacement and an actuation resolution of 0.1 nm. The in-situ biasing chip can achieve precise application of electrical signals and pA and µV level measurement. The MEMS chips for heating and biasing and the miniature actuator for straining are fixated onto a rigid frame. A flexible printed circuit (FPC) connects the electrodes on the MEMS chips and the actuator to an outside control unit for the application and measurement of subtle signals. The rigid frame and the FPC comprises a functional cartridge, which can be conveniently connected to a specially designed double-tilt TEM holder.Various kinds of thermal/electrical/mechanical loading of samples can be carried out inside a TEM column. Throughout the entire loading process, the sample can be tilted freely around two orthogonal axes for ±15°. This capability is essential for achieving atomic-scale resolution, which requires precise alignment of the electron beam to a low-index zone axis of the sample during in-situ testing.
Results
With this in-situ platform, we carried out an in situ atomic-resolution study on the sliding-dominant deformation at general tilt grain boundary (GB) in platinum bicrystals. Both atomic-scale sliding along the GB and sliding with atom transfer across the boundary plane were observed directly in real-time.1 For the first time, we uncovered that tungsten fractures at 700℃ in a ductile manner via a strain-induced multi-step body-centered cubic (BCC)-to-face-centered cubic (FCC) transformation and dislocation activities within the strain-induced FCC phase.2 Using this technique, researchers has also revealed the atomic-scale process of GB dislocation climb in nanostructured Au during in situ straining.3
Conclusion

Based on highly integrated MEMS chips, miniaturized piezo actuator and unique double-tilt system, we have developed an in-situ TEM testing platform that allows real-time observation of micro-structure evolution at atomic scale under flexible coupling of mechanical, thermal and electrical fields. Researches on revealing the atomic scale mechanisms of GB plasticity and brittle-to-ductile transition of various metallic materials were carried out.

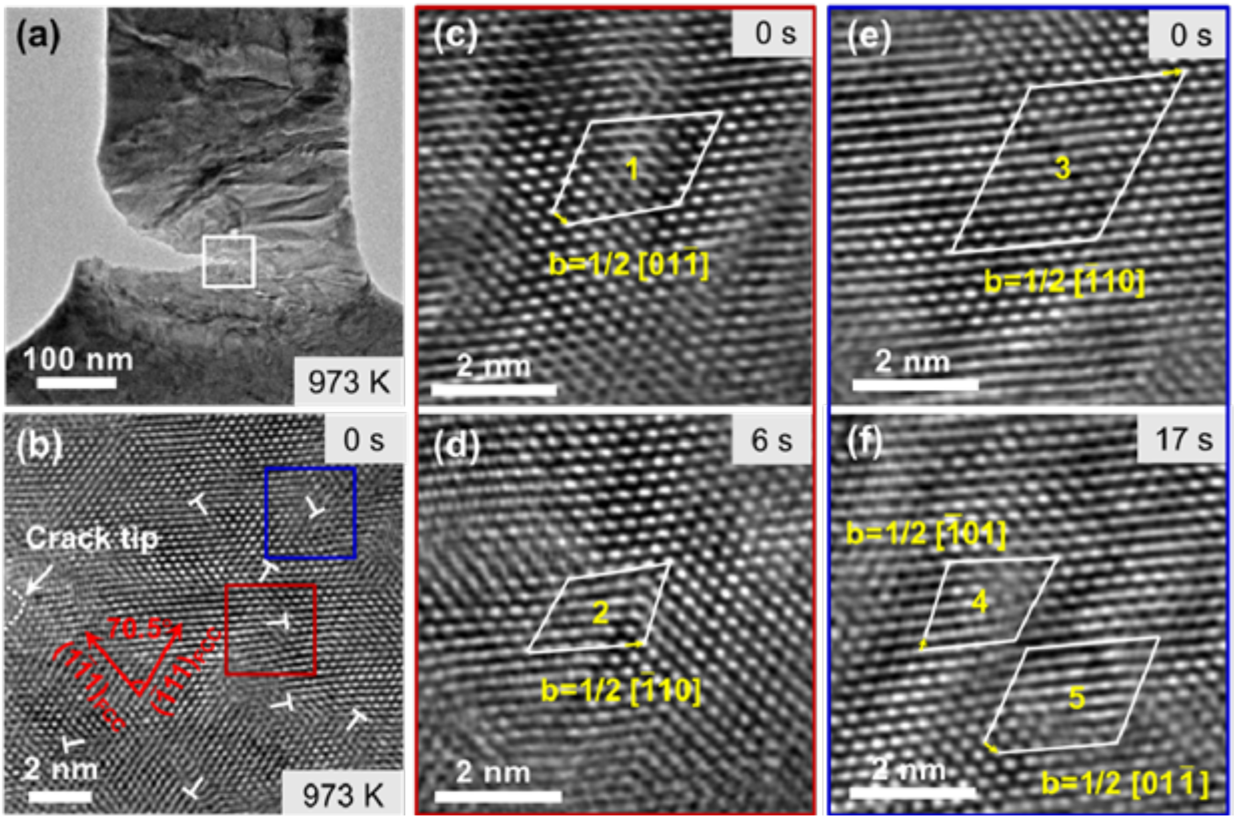

Keywords:

In-situ TEM; Atomic-scale; straining; Heating;

Reference:

1.Wang, Lihua, et al. "Tracking the sliding of grain boundaries at the atomic scale." Science 375.6586 (2022): 1261-1265.
2.Zhang, Jianfei, et al. "Timely and atomic-resolved high-temperature mechanical investigation of ductile fracture and atomistic mechanisms of tungsten." Nature Communications 12.1 (2021): 2218.
3.Chu, Shufen, et al. "In situ atomic-scale observation of dislocation climb and grain boundary evolution in nanostructured metal." Nature Communications 13.1 (2022): 4151.

611

Towards atomic-resolution electron energy loss spectroscopy in an uncorrected 30kV scanning electron microscope

Prof. Quentin Ramasse[1,2], Demie Kepaptsoglou[1,3], Takeshi Sunaoshi[4], Kazutoshi Kaji[4], Satoshi Okada[4], Yu Yamazawa[4], Tsutomu Saito[4], Michael Dixon[5], Sean Collins[1,2], Feridoon Azough[6], Robert Freer[6]
[1]SuperSTEM Laboratory, Daresbury, UK, [2]University of Leeds, Leeds, UK, [3]University of York, York, UK, [4]Hitachi High-Technologies Corp., Ibaraki, Japan, [5]Hitachi High-Tech Europe, Daresbury, UK, [6]University of Manchester, Manchester, UK

IM-04 (2), Lecture Theater 1, august 27, 2024, 14:00 - 16:00

Background incl. aims

As an era-defining technological advancement in the field of nanoscience and beyond, the effective implementation of aberration correction has allowed electron microscopy to routinely reach deep sub-angstrom-level spatial resolution. Recently, ultra-high-resolution monochromators relying on related electron-optical designs have further enabled electron energy loss spectroscopy (EELS) in the meV regime. Among many impactful consequences, these developments have seen the widespread adoption of low-voltage instruments, which can maintain very high spatial resolutions thanks to their aberration correctors, even down to 20kV, with 2-dimensional materials often providing the ideal sandbox and test objects, leading to the advent of practical ‘single-atom microscopy’ [1].

Beyond single-atom sensitivity, low-voltage operation is highly sought-after for reasons such as reduced knock-on damage to samples or increased inelastic cross-sections resulting in a high signal for spectroscopy. However, for a large number (perhaps even a majority) of practical materials science applications, the complexity and price of such instrumentation, especially when analytical capabilities are added, can be a drawback. In contrast, high-throughput capabilities with lower entry barriers in terms of cost and complexity, but which maintain a relatively high-resolution (but not always single-atom sensitivity), can often be preferable in order to address numerous scientific questions. These may in turn reveal further avenues for investigation that more complex instrumentation may then be used to explore.

Methods

One possible approach in recent years has led to the emergence of (low-voltage) scanning electron microscopes (SEMs) operated in a transmission geometry – or (T)SEMs [2]. When equipped with cold field emission sources, these instruments have been shown to reach 0.2nm information transfer in bright-field STEM imaging [3], and to provide remarkable flexibility for surface and spectroscopic investigations of functional materials [4].

Here, we show how the capabilities of such a high-resolution (T)SEM can be pushed even further towards near-atomic resolution. We use a Hitachi SU9000EA microscope, a low-kV (≤30kV) uncorrected (T)SEM equipped with a diffraction camera and a Hitachi electron energy-loss spectrometer developed for this instrument, which thanks to its cold-field emitter has a native energy resolution of ~0.3eV. In the optical configuration chosen for the experiments, the estimated probe size at 30kV acceleration voltage was below 0.4nm, sufficient to demonstrate atomic-resolution imaging and spectroscopy in carefully selected materials systems.

Results

Figure 1a shows a high-angle annular dark field (HAADF) image of a La1/3NbO3 ceramic (LNO) observed in [001] zone axis. The sample was prepared by crushing pellets of the sintered material into fine crystallites, and dispersing a chloroform suspension onto a lacey carbon support film, as described elsewhere [5]. The overall structure of this highly promising candidate thermoelectric material is that of a perovskite, but it exhibits two distinct alternating A-site planes: one fully occupied by La ions, while the alternate position is fully La-deficient: a model is overlaid on figure 1a. The Fourier transform of the image, inset, demonstrates information transfer down to 0.26nm in

HAADF (similar performance was also observed in bright field images, while atomic plane resolution was also observed in secondary images).

In this projection, the distance between non-deficient La cation planes is 0.8nm, making it an ideal test sample to use EELS to map with atomic-plane resolution the location of La in the structure. The observed oscillations, peaks and troughs, of the integrated intensity of the La M4,5 edge in an EELS linescan acquired along the indicated orange segment, figure 1b, follow exactly those of the simultaneously acquired HAADF signal – with the darker layers corresponding to La-deficient positions. The use of the La M4,5 edge, whose onset sits at the relatively high energy loss of 832eV, also serves to highlight the applicability of EELS in this uncorrected 30kV system, even at high energy losses.

Conclusion

These results demonstrate unambiguously atomic-plane resolution in EELS mapping in an uncorrected SEM, used in a transmission geometry. Together with high spatial resolution imaging capabilities across multiple signal channels (HAADF, BF, SE), this further demonstrates the versatility of these microscopes, whose advanced capabilities as (T)SEM-EELS instruments belie their relative operational simplicity and low cost.

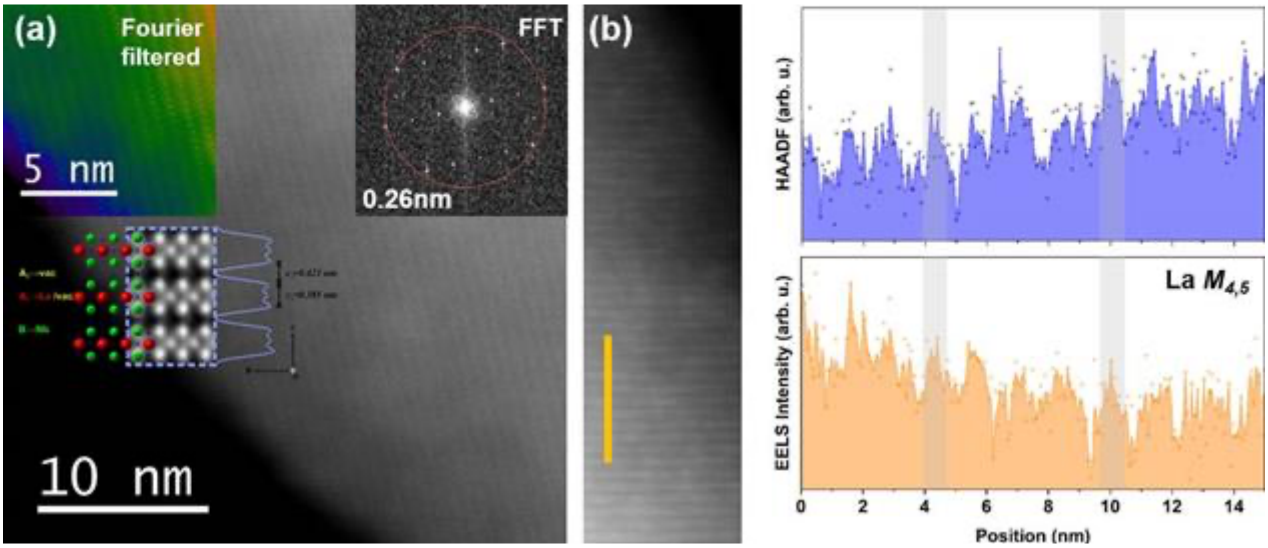

Keywords:

SEM, EELS, HAADF imaging, instrumentation

Reference:

[1] U. Kaiser et al., Ultramicroscopy 111 (2011), p. 1239.
[2] T. Sunaoshi et al., Microsc. Microanal. 22 (S3) (2016), p. 604.
[3] M. Konno et al., Ultramicroscopy 145 (2014), p. 28.
[4] N. Brodusch et al., Ultramicroscopy 203 (2019), p. 21.
[5] D. Kepaptsoglou et al., Inorg. Chem. 57 (2018), p. 45.

57

DQE measurement for TEM detectors: from the key parameter to an ambiguous estimate

Olivier Marcelot[1], Mme Cecile Marcelot[2]
[1]ISAE-SUPAERO, Toulouse, France, [2]CEMES-CNRS, Toulouse, France

Poster Group 1

Background incl. aims

Nowadays, the performance of CMOS electron detectors for transmission electron microscopes (TEM) are mainly compared by means of a unique parameter, the detective quantum efficiency (DQE). This parameter is largely promoted by camera providers, and is given as a unique number while it is known to strongly depend on the electron dose. In addition, the DQE calculation method may influence the result, as it will be presented in this study. Consequently, several DQE values can be found for one detector, and one should wonder if a unique DQE is the correct figure of merit for electron detectors.

One aim of this work is to demonstrate that the most commonly used method to calculate the DQE leads to strong uncertainties. To achieve this goal, measurements are conducted on an electron detector and a model is developed. Then, the second aim is to provide recommendations and trustable alternatives for detector comparisons.

Methods

The DQE depends on the spatial frequency w and is generally expressed as a component DQE(0) at the spatial frequency (0) times components depending on the spatial frequency, as in the following:

$DQE(w)=DQE(0)xMTF(w)^2/NTF(w)^2$

where MTF is the modulation transfer function and NTF the noise transfer function. MTF and NTF are well established so this work focuses on the DQE(0) calculation.

DQE(0) can be estimated by means of the full calculation of the various noise sources, including the shot noise, the gain variance "σg", the Fano noise "F", the dark current "DC" and the readout noise "NRO":

$DQE(0)=g^2/(g^2 (1+F)+\sigma g^2+(t\cdot DC+NRO^2)/n\_i)$

where "n_i" is the number of incident electrons, "g" is the detector gain, "t" the integration time

The gain is extracted thanks to a comparison between the integrated electrons and the beam current measured with a Faraday cap, and the gain variation is estimated from the spatial variance of a flat field picture. While these measurements are not too complex, it is much more difficult to measure the Fano noise. It can be estimated with the standard deviation of simulated deposited energy distributions. Then, the readout noise and the dark current are measured from several acquisitions performed in dark condition.

Since several years, a simplified method has been preferred for the DQE(0) estimation, and relies on the direct measurement of the detector output noise by means of the spatial variance of a flat field image. However, in this case, the large electron hole distribution generated by the beam is spread between pixels and the spatial variance is underestimated. To solve this issue, McMullan proposed in 2009 to extract the spatial variance on binned pixels, for which a saturation is achieved if the binning number is large enough. This method is referred as the McMullan method subsequently.

Results

A Gatan-Rio-16 camera mounted on a JEOL-2100 FEG microscope is used for this study. This detector being an indirect one, the Fano noise is due to the scintillator and is estimated at 0,25. The electron dose is chosen in order to achieve the half full well capacity of the detector. For n_i=107, DQE(0)_FullCalculation=0.79 and DQE(0)_McMullan=0.62.

These two results are quite different and it is supposed that the McMullan method over-estimates the output noise and therefore gives a lower DQE(0).
With the intention to demonstrate it, a simple model is built, based on the generation of a shot noise and a gain variation leading to a similar noise distribution acquired with the Gatan-Rio-16 camera. For this purpose, the standard deviation of the noise is adapted is order to get an extracted variance identical to the measured one. In addition, a Gaussian blur is added with the intention to simulate the electron spread over the pixels and is parametrized in a way to get the same saturation of the variance according the binning number. The resulting noise distribution does not match the measured one which is much more extended and show pixels with much higher noises.
Actually, the McMullan method requires to subtract two flat field pictures in order to remove dead and saturated pixels, and the fixed pattern noise which avoid a correct variance saturation. However, it is necessary to consider other defective pixels, such as the hot pixels with a higher gain. These defective pixels are not removed by the subtraction of two flat field images and may distort the variance extraction. To demonstrate it, the previous model is modified and one population of hot pixels is introduced. The hot pixels ratio and gain are adjusted in order to obtain a noise distribution similar to the one measured with the Gatan-Rio-16. A hot pixel density of 6×10^{-4} with a high gain of 30 lead to a noise distribution comparable with the experiment, and the spatial variance extracted with hot pixels is 50% higher compared to the one extracted without hot pixels (see the figure 1).
Therefore, it is demonstrated that the commonly used McMullan method leads to an underestimation of the DQE(0) because of hot pixels. Other limitations are found and discussed, based on the fact that the noise is distributed on a statistical population of hot pixel which may give different results at every DQE measurement.
Consequently, the DQE(0) should not be used as a unique number for the detector comparison because it depends on the electron dose, on the experimental condition and on the used method. In order to fairly compare detectors, it is therefore recommended to use other parameters clearly defined and measurable: the gain for an information on the sensibility, the MTF for the spatial resolution and the dark current for the radiation hardness.

Conclusion

The DQE(0) is measured on a commercial camera with two methods and it comes that the McMullan method, largely preferred by the camera providers, leads to large uncertainties. By means of a model, it is demonstrated that detector hot pixels induce an over-estimation of the output noise leading to the DQE under-estimation with the McMullan method.
The DQE suffering from large uncertainties it is recommend to use the gain, the MTF and the dark current for fair comparisons between detectors.

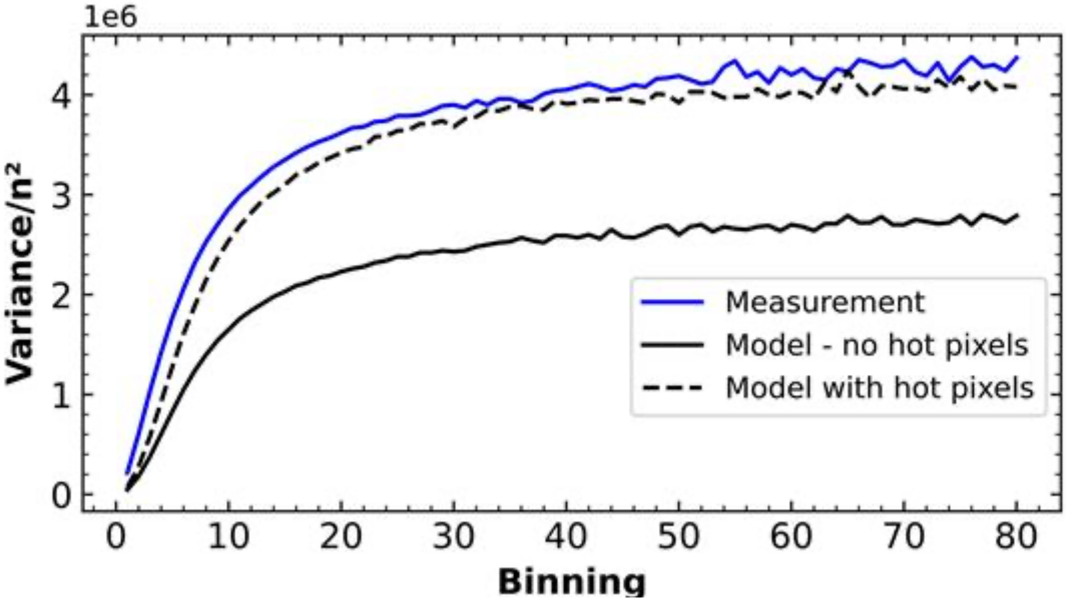

Keywords:

DQE; simulation; electron detector, TEM

Reference:

- G. McMullan, et Al., “Detective quantum efficiency of electron area detectors in electron microscopy,” Ultramicroscopy, vol. 109, no. 9, pp. 1126–1143, 2009.
- O. Marcelot, et Al., “Limitations and Drawbacks of DQE Estimation Methods Applied to Electron Detectors”, accepted for publication in Oxford Microscopy, 2024.

91

A Novel Tool for Combined AFM, SEM, and Electrical Probing of Nanostructures

Chris Schwalb[1], Mr. Hajo Frerichs[1], Mr. Darshit Jangid[1], Mr. Sebastian Seibert[1], Mr. Lukas Stühn[1], Mrs. Marion Wolff[1], Mr. Andrew Jonathan Smith[2], Mr. Andreas Rummel[2]
[1]Quantum Design Microscopy GmbH, Pfungstadt, Germany, [2]Kleindiek Nanotechnik GmbH, Reutlingen, Germany

Poster Group 1

Combining different complementary analytical methods into one instrument is a powerful technique for the contemporaneous acquisition of both structural and functional sample properties. Especially the combination of atomic force microscopy (AFM), scanning electron microscopy (SEM), and electrical nanoprobing can yield completely new insights for the study of various samples and nanostructures.
In this work, we introduce a highly integrated correlative microscopy platform, that seamlessly combines AFM and SEM within a unified coordinate system. In addition, a three-axis sample stage and a trunnion provide unique experimental capabilities such as profile view – an 80-degree tilt of the combined sample stage and AFM giving full SEM access to the cantilever tip region. This microscopy platform can easily be combined with a nanoprobing system that enables precise electrical characterization of nanoscale structures, offering insights into device functionality and performance. [1-2]
We present a variety of novel case studies to highlight the advantages of this new tool for interactive, correlative, in-situ nanoscale characterization of different materials and nanostructures. Initial results will focus on the analysis of mechanical and electrical properties of individual nanowires. The combination of SEM and nanoprobes enables easy manipulation and positioning of individual nanowires, whereas the in-situ AFM allows the characterization of topography, surface roughness, mechanical and electrical properties of the nanowire.[3-4] Using the SEM's high-resolution the AFM cantilever tip can be precisely positioned on an individual nanowire that is attached to the nanoprober and the topographical and mechanical properties can be determined (see Figure).
In addition, we will show results for electrical nanoprobing of semiconductor devices in combination with conductive AFM measurements. A semiconductor device can be electrically probed by simultaneous use of two nanoprobers while the AFM provides detailed information on the 2D conductance map of the device itself.
Based on the broad variety of applications regarding the inspection and process control of different materials and devices, we anticipate that this new inspection tool will be one of the driving characterization tools for correlative analysis on the nanoscale.

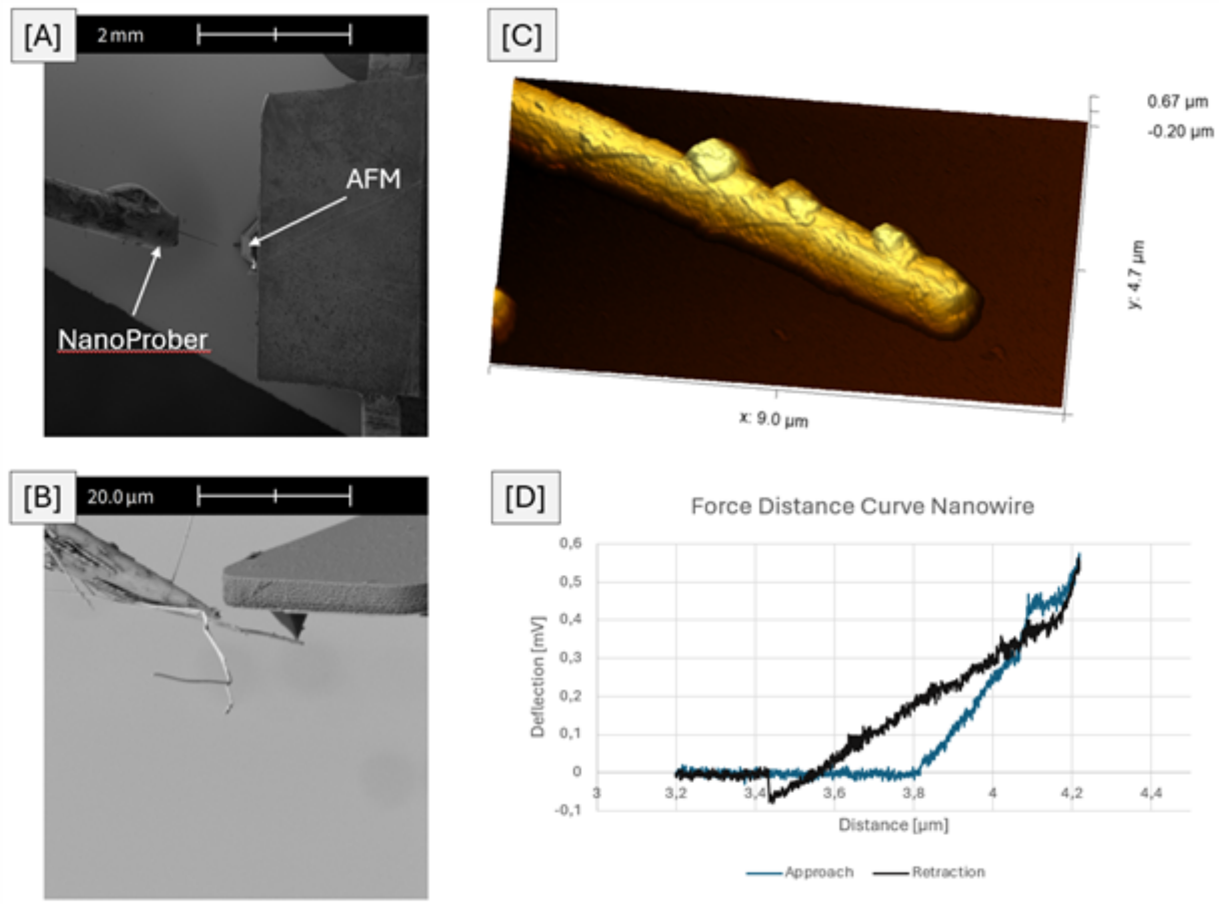

Keywords:

AFM, SEM, NanoProbing, Correlative Microscopy

Reference:

[1] M. Dukic, et al., Scientific Reports, 5 (1), 16393 (2015).
[2] J. M. Prohinig, et al., Scripta Materialia, 214, 114646 (2022).
[3] A. Alipour, et al., Microscopy Today 6, 17-22 (2023).
[4] Reisecker, et al., Adv. Funct. Mater. 2310110 (2023).

150

A retractable, compact Secondary Electron Energy Spectrometer attachment for Scanning Electron Microscopes

Wenzheng Cao[1], Prof. Anjam Khursheed[1]
[1]Politecnico di Milano, Milan, Italy

Poster Group 1

Background:
Energy spectrometers, such as the EDS (Energy Dispersive X-ray Spectroscopy) attachment in a Scanning Electron Microscope (SEM), have been widely used in material science for quantitative elemental analysis and contamination identification. However, EDS typically requires a minimum accelerating voltage of 6 kV and a high current primary beam to generate sufficient characteristic X-rays for accurate analysis. Unfortunately, these high voltages and currents can lead to charging effects in non-conductive materials like semiconductors and biological samples, hindering the analysis process. Additionally, EDS provides only microscale resolution due to X-rays being generated from a relatively large volume. As an alternative, Secondary Electron Energy Spectroscopy (SEES) has emerged as a promising method for achieving nanoscale quantitative material analysis using a low-voltage SEM (LVSEM) [1,2].
Methods:
A novel electric sector compact Secondary Electron Energy Spectrometer was designed and optimized using direct ray tracing of electrons through a Finite Element Method (FEM) field distribution. Based on the optimized design, a prototype was constructed and tested within a commercial SEM using a 1 to 2 KV low-energy primary beam. Various materials, including gold, copper, and silicon, were examined to assess the spectrometer’s elemental identification capabilities.
Results:
The simulation results predict that the spectrometer achieves a relative energy resolution of 1.54% for a polar entrance angular spread of 20°, azimuthal angular spread of 150°, and a working distance of less than 10 mm. Experimental results confirm that different elements can be easily distinguished based on their secondary electron energy spectra FWHM and peak position, as shown in the graphic, in which test experimental SE energy spectra of gold and copper samples are presented.
Furthermore, due to its compact size, the spectrometer can be conveniently installed or removed.
Conclusions:
A compact/retractable electric sector secondary electron energy spectrometer attachment for SEMs has been designed, and is predicted to have high energy resolution and high collection efficiency. This new attachment can be seamlessly integrated into the SEM chamber, greatly enhancing the capabilities of the SEM system with its quantitative elemental analysis and material science ability.
Furthermore, 2D mapping and dopant profiling are also expected in the near future.

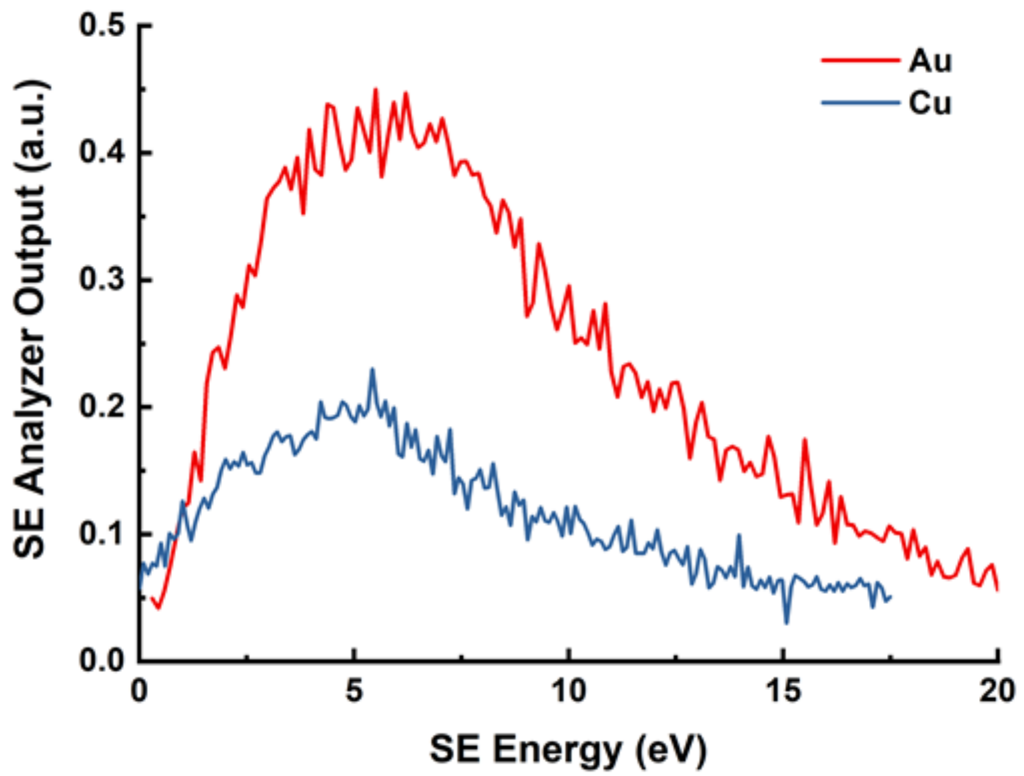

Keywords:

SEM, Energy spectrometer, elemental analysis

Reference:

[1] Hoang H Q, Osterberg M, Khursheed A. A high signal-to-noise ratio toroidal electron spectrometer for the SEM[J]. Ultramicroscopy. 2011, 111(8):1093-100.
[2] Han W, Zheng M, Banerjee A, et al. Quantitative material analysis using secondary electron energy spectromicroscopy[J]. Scientific Reports. 2020, 10(1):22144.

156

Opening the third dimension to your SEM with integrated fs-laser

Olena Vertsanova[1,2], Dr. Sabine Lenz[1], Martina Heller[1], Sebastian Krauss[1]
[1]Carl Zeiss Microscopy GmbH, Oberkochen, Germany, [2]National Technical University of Ukraine "KPI", Kyiv, Ukraine

Poster Group 1

Background
Scientists and engineers in materials research laboratories performing sample preparation using focused ion beam (FIB) or plasma focused ion beam (PFIB) instruments face challenges in accessing deeply buried structural features and preparing large cross-sections and trenches at micro- and mesoscale sizes. Such preparation by FIB or PFIB is time-consuming and ineffective, as it occupies an expensive microscope that could be used for more efficient processes: high-quality imaging, high-precision analysis, and sample preparation for atomic-resolution imaging. There is a need for an effective solution for the rapid preparation of site-specific micro- and mesoscale samples.
Methods
In response to these challenges, the authors present a laser scanning electron microscope (LaserSEM) as a new Zeiss solution for fast and cost-efficient high-quality site-specific sample preparation. The Zeiss LaserSEM is a field-emission scanning electron microscope (FE-SEM) with an integrated fs-laser for large 3D volume sample fabrication. This solution enables to achieve a fast site-specific preparation from the meso- to the microscale. The Zeiss LaserSEM accelerates workflows such as 3D tomography on huge sections, preparation of arrays of pillars for micromechanical testing, or even multi-modal workflows e.g. correlative experiments between X-ray microscope (XRM) and scanning electron microscope (SEM).
Results
The examples of rapid access to undersurface features by fs-laser and Cut2ROI Workflow with the ability to identify, access, prepare, and analyze deeply buried sites with precise navigational guidance using the correlation between X-ray and electron microscopes from ZEISS are presented. The fs-laser processing recipes for different materials and their application for a large cross-sectioning with further energy dispersive spectroscopy (EDS) and electron back scatter diffraction (EBSD) analysis, as well as pillar preparation for nanoindentation, compression tests, and nanoCT, are presented.
Conclusion
Integration of fs-laser into SEM allows rapid access to deeply buried structures and fast large-volume material removal and achieves high resolution and contrast imaging with the benefits of Zeiss Gemini optics. ZEISS LaserSEM is a site-specific cross-section and micro/mesoscale fabrication solution that rapidly prepares samples by accurately removing millimeter volumes of material using integrated FE-SEM imaging to achieve accuracy.

Keywords:

LaserSEM, sample preparation, SEM

Development of a pixelated STEM-in-SEM detector for microstructural features characterization

Julien Aubourg[1,2], Mr. Emmanuel Bouzy[2,3], Mr. Antoine Guitton[2,3], Mr. Jean-Jacques Fundenberger[2,3], Mrs. Yudong Zhang[2,3], Mr. Julien Guyon[2,3], Mr. Luc Morhain[2,3]
[1]JEOL (Europe) SAS, 1 All. de Giverny, 78290 Croissy, France, [2]Laboratoire d'Etude des Microstructures et de Mécanique des Matériaux (LEM3), Université de Lorraine, CNRS UMR 7239, Arts et Métiers, F-57070 Metz, France, [3]Laboratory of Excellence on Design of Alloy Metals for low-mAss Structures (DAMAS), University of Lorraine, 57073 Metz, France

Poster Group 1

Background incl. aims:
Microstructural investigations provide engineers with information to computationally predict the performance of components and electron microscopy is a well-versed technique for analyzing micro/nanostructural features. Two types of electron microscopes are commonly used and provide complementary information: Transmission Electron Microscope (TEM) at the micro/nanoscale and Scanning Electron Microscope (SEM) at the macro/mesoscale. Historically, Scanning Transmission Electron Microscopy in Scanning Electron Microscope (STEM-in-SEM) techniques were predominantly used by biologists due to their user-friendly nature and their ability to analyze specimens at low accelerating voltages (30 kV or below). This made STEM-in-SEM techniques complementary to conventional TEM ones as the latter generally use high accelerating voltages (~200 kV). Recent advances in electron guns and electromagnetic lenses have sparked growing interest in STEM-in-SEM techniques across various scientific disciplines. However, researchers often face challenges in establishing the precise imaging conditions required to obtain comprehensive micrographs, thus limiting their interpretation and analysis.
Methods:
In this study, we propose a novel STEM-in-SEM approach, which aims to overcome the practical limitations of traditional techniques for microstructural characterization in thin foils. The technique leverages an advanced detector designed to replicate TEM-like characterizations while minimizing the presence of artifacts that commonly hinder comprehensive analyses. In addition, this STEM-in-SEM technique benefits from On-Axis Transmission Kikuchi Diffraction (On-Axis TKD), thus allowing diffraction pattern acquisition with a high signal-to-noise ratio.
Results:
First results already show the possibility to acquire diffraction patterns and to image dislocations under modulable bright-field and dark-field conditions.
Conclusion:
By implementing this pixelated STEM-in-SEM technique, we anticipate significant advancements in the field of microstructural characterization by obtaining TEM-like and TEM-complementary information. Ultimately, the developed technique should facilitate studies to obtain detailed information about thin foil specimens, thereby contributing to a broader range of scientific applications.

Keywords:

Electron microscopy, STEM-in-SEM, On-Axis TKD, Microstructures characterization

Reference:

Brodu, E., Bouzy, E., Fundenberger, J.-J., Guyon, J., Guitton, A., & Zhang, Y. (2017). On-axis TKD for orientation mapping of nanocrystalline materials in SEM. Materials Characterization, 130, 92-96. https://doi.org/10.1016/j.matchar.2017.05.036

182

A new EELS spectrometer, integrated with the microscope’s optics

Dr. Peter Tiemeijer[1], Mr. Terry Dennemans[1], Mr. Sander Henstra[1], Mr. Dileep Krishnan[1], Mr. Sorin Lazar[1], Mr. Paolo Longo[1], Mrs. Maria Meledina[1], Mr. Sjaak Thomassen[1], Mr. Wouter Verhoeven[1]
[1]Thermo Fisher Scientific, Eindhoven, The Netherlands

Poster Group 1

The Selectris energy filter was introduced in 2020 [1]. This filter comprises a large tapered prism and ten multipoles most of which are implemented as dodecapoles. These enable stable and superior correction of non-isochromaticy and image distortions. Now, we are developing an EELS spectrometer based on the technology of this filter.
Compared to energy filtered imaging, the optics of EELS has the additional challenge that a broad range of electron energies (up to several thousands of eV wide) must be simultaneously transferred through the microscope and through the spectrometer, from specimen to detector, without introducing chromatic blur or chromatic distortions. This is a non-trivial task, especially when we desire that such transfer is maintained across different microscope settings (different camera lengths) and across different spectrometer settings (different dispersions and different spectrum offsets). Maintaining this can only be ensured by closely integrating the optics of the microscope and of the spectrometer, to keep the chromatic defocus in the microscope matched with the focus of the spectrum. Otherwise, the superior performance offered by the tapered prism and ten multipoles could only be fully enjoyed at (one or) a few specific experimental settings, and would be lost when switching to other camera lengths or other dispersions or other energy offsets.
Compared to the Selectris energy filter, our EELS spectrometer has the following additional functionalities: (i) above mentioned integration between the optics of the TEM and the spectrometer, (ii) a dedicated detector optimized for fast read-out, low-noise, and radiation hardness, (iii) fast electrostatic elements (shutter, bias tube, deflector) for near-simultaneous acquisition of multiple (dual, triple, ...) regions of the EELS spectrum, and (iv) fully automated EELS tuning routines.
Figure 1 illustrates the optical performance of our spectrometer. It shows triple-EELS for $DyScO_3$ taken at 60kV, monochromated, 30mrad semi-convergence angle, 5mm spectrometer entrance aperture, and at five different camera lengths. The top panel shows data acquired without correction for the chromatic effects: clearly, the chromatic blur leads to resolution loss at the higher energy losses and at the smaller camera lengths. Bottom panel shows data acquired with on-the-fly correction of the chromatic effects: resolution is ensured across all settings, even for the challenging case of ΔE=1300eV at 60kV, and semi-collection angle of 49mrad (CL=25mm).
The stability of the Selectris, the full automation of the EELS tuning, and the integrated correction for chromatic effects greatly improve the ease-of-use and productivity of the new spectrometer.

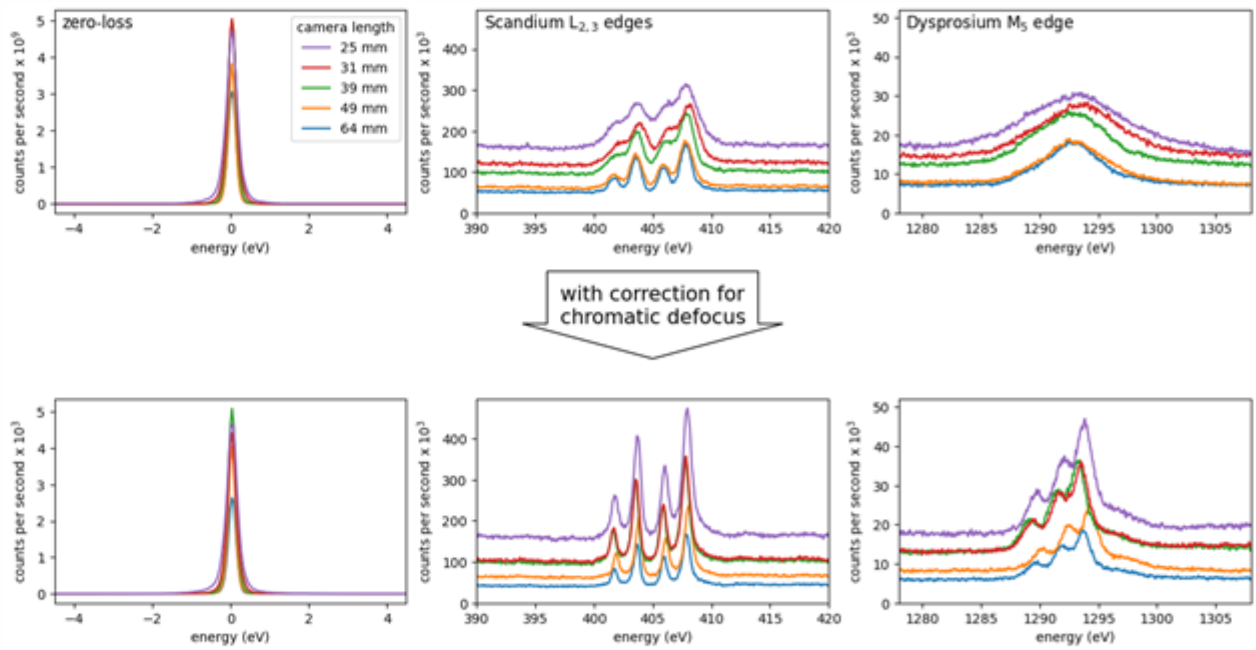

Keywords:

EELS spectrometer optics automation

Reference:

1] T. Nakane et al., Nature 587 (2020) 152, Single-particle cryo-EM at atomic resolution.

211

Dose fractionation and alternative scanning strategies for beam damage mitigation in event-driven 4D-STEM

Arno Annys[1,2], Dr. Hoelen Robert[1,2], Mr. Matthias Quintelier[1,2], Prof. Joke Hadermann[1,2], Prof. Jo Verbeeck[1,2]
[1]EMAT, University of Antwerp, Antwerp, Belgium, [2]NANOlab Center of Excellence, University of Antwerp, Antwerp, Belgium

Poster Group 1

The introduction of event-driven direct electron detectors, e.g. those based on the Timepix3 chip (Amsterdam Scientific Instruments CheeTah T3, Advacam AdvaPIX TPX3), has removed a major constraint in scanning transmission electron microscopy (STEM), making it possible to achieve momentum-resolution by recording the far-field intensity at each scan position with no dwell time or dose penalty. In contrast, most of the popular frame-based detectors still impose a minimum acquisition time of a few tens of microseconds. Such recording times are at least an order of magnitude larger than what can typically be achieved by the microscope's scanning system. Additionally, frame-based representations are inefficient regarding data size and processing speed, especially when using large or repeated scans. Consequently, event-driven detection has significant advantages for fast 4D-STEM data acquisition, including electron ptychography.

The development of user-programmable scan engines allows another layer of optimization, particularly with the introduction of alternative scan patterns, which have been shown to permit mitigation of the overall specimen deterioration during an experiment. This mitigation can be related to the accumulation of damage sites (e.g. charge carriers induced by radiolysis or atomic defects created by knock-on displacement) when the electron incidence is strongly localized, and the naturally occurring diffusion of those defects. The more the total electron dose is homogenized in time and space, the better the damage distribution spreads out, and the less likely local accumulations of damage sites become, thus preventing irremediable destruction of the specimen structure. When combining an optimized scan strategy with an event-driven detector, one can obtain the information richness of 4D-STEM, combined with favorable beam damage behavior, as often praised in conventional TEM.

Here, an experimental set-up that routinely allows fast dose-fractioned event-driven 4D-STEM with custom scan strategies is described. A software toolkit controls and synchronizes the scan engine and detector, performing in-line processing of the event data stream for live visualization. Initial experimental results will be presented, demonstrating the interest of dose fractionation in microprobe investigations of beam-sensitive metal-organic frameworks and high-resolution imaging. Additionally, a more fundamental and theoretical analysis of electron-induced damage diffusion statistics is performed by using a simple split operator approach, thus modeling the damage distribution function in space and time, within a given STEM recording. The cases where a fractionation of the scan window is performed or when an overfocused or time-dependent probe is employed are investigated, and conclusions are drawn regarding their potential to lower beam damage while keeping the dose constant.

Keywords:

Event-driven detection, 4D-STEM, Beam damage

Reference:

[1] D. Jannis et al. ; Ultram. 233, 113423 (2022)
[2] A. Velazco et al. ; Ultram. 232, 113398 (2022)
This work received funding from the Horizon Europe framework under grant agreement n. 101094299 (IMPRESS) and the EU's Horizon 2020 framework under grant agreement n. 101017720 (FET-Proactive EBEAM). JV and JH acknowledge an SBO FWO national project n. S000121N (AutomatED).

289

Multimodal OF2i-Raman – A novel high-throughput, single particle analysis method in liquids

Dr. Harald Fitzek[1,2], Christian Neuper[1], Dr. Christian Hill[3]
[1]Graz Centre for Electron Microscopy (ZFE), Graz, Austria, [2]Institute for Electron Microscopy and Nanoanalysis (FELMI), Graz, Austria, [3]Brave Analytics GmbH, Graz, Austria

Poster Group 1

Background incl. aims
The efficient detection and analysis of micro- and nano-particles is a topic of increasing importance, both due to their wide spread use in industrial process and the increasing issue of environmental pollution, especially with micro- and nanoplastics [1]. We specifically focus on the analysis of micro- and nano-particles in liquids, most commonly water. Here we aim to combined the advantages of microscopy based methods, which typically measure on the "single-particle" level, but require sample preparation and can be cumbersome to use for the measurement of a larger number of particles, with the low sample preparation requirements and high-throughput of ensemble based methods [2]. To this end, we combine OptoFluidic Force Induction (OF2i®) with a Raman microscopy based setup. OF2i® uses a laser beam to trap particles inside a flow cell and determines both particle sizes and concentration by observing the scattered light and acceleration of single particles through the measurement cell with an ultramicroscope setup. Raman microscopy can determine the composition of both organic and inorganic particles (but not metals), by observing the inelastically scattered light of a laser focused onto a particle. A multimodal OF2i®-Raman setup can therefore provide the best of both worlds, allowing for high-throughput "flow-through" measurements with little to know sample preparations, whilst providing analytical information on the single particle level.

Methods
The multimodal OF2i-Raman setup is based on a conventional OF2i instrument (BRAVE B-Curious). The conventional OF2i consists of a 2D optical trap in a microfluidic flow channel and an ultramicroscope observing the elastically scattered light perpendicular to the laser propagation direction [3]. The ultramicroscope is modified into two beam paths (elastic and inelastic scattering), with the elastic path functioning as a regular OF2i and the inelastic path is coupled to a Raman spectrometer. The Raman spectrometer is operating in a mode similar to "line-illumination" imaging mode in Raman microscopy, thus allowing for the simulations Raman measurement of particle spectra along the particle flow direction. For the optical trap a linearly polarized laser (wavelength: 532nm/power up to 2W) is used either as a Gaussian beam or a doughnut shaped Laguerre-Gaussian.

Results
We have consturcted a OF2i-Raman setup prototyp and have achieved a prove of principle of the setup for the detection of both organic (polystyrene, see graphic) and inorganic (TiO2) particles. In order to achieve the highest possible sensitivity in the Raman measurements we had to modified the standard OF2i-approach, which uses a laser beam propagating in the flow direction to accelerated the trapped particles, to one where the laser beam is propagating against the flow direction, thus slowing down the particles and allowing for longer accquisition times in the Raman. For challaning particles (small particles, small Raman crosssection) this approach also allows us to fully trap specific particles, in the focus of the Raman-setup. Furthermore, the modified OF2i-Raman-approach has been used for hyphenation with ICP-MS [4].

Conclusion
With our novel approach combining OF2i and Raman microscopy, spectroscopic analysis of micro- and nanoparticles, on the single particle level, is possible with high-throughput, directly in water (or other liquids) and minimal sample preparation. We are thus convinced that this approach can contribute to the growing research into environmental pollution with microplastics as well as other fields of research on the topic of micro- and nano-particles. In addition, the potential of our new approach for further hypenation with complementary analytic techniques has already been demonstrated [4] and we are convinced that combing different analytical techniques in a seamless way is the way forward towards a universal analytical tool box for nanoparticles.

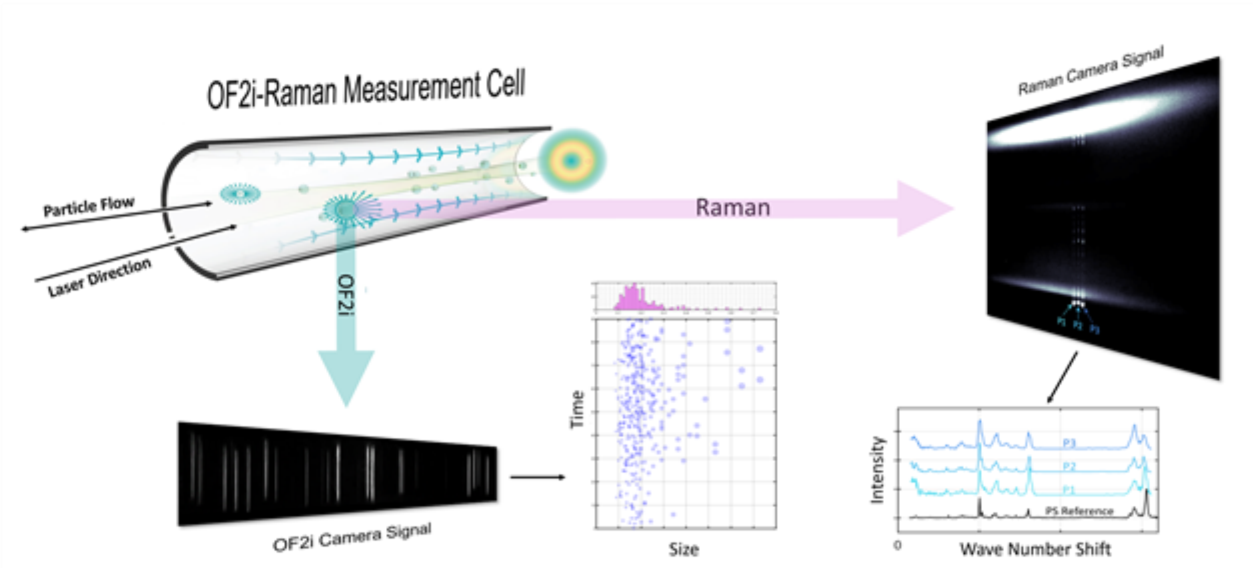

Keywords:

Multimodal, Raman, Particle analysis, Microplastic

Reference:

[1] Mitrano, D. M., Wick, P., & Nowack, B. (2021). Placing nanoplastics in the context of global plastic pollution. Nature Nanotechnology, 16(5), 491-500.
[2] Cai, H., Xu, E. G., Du, F., Li, R., Liu, J., & Shi, H. (2021). Analysis of environmental nanoplastics: Progress and challenges. Chemical Engineering Journal, 410, 128208.
[3] M. Šimić et al. Real-Time Nanoparticle Characterization Through Optofluidic Force Induction, Physical Review Applied 18, no. 2 (2022): 024056
[4] Neuper C., Šimić M., Lockwood T., Gonzalez de Vega R., Hohenester U., Fitzek H., et al. Optofluidic Force Induction meets Raman Spectroscopy and Inductively Coupled Plasma – Mass Spectrometry: A new hyphenated technique for comprehensive and complementary characterisations of single particles. Manuscript submitted.
[5] The authors are deeply grateful to project FFG Bridge 895429 Nano-VISION for funding.

325

4D STEM in SEM with a Fast Pixelated Direct Detector

Dr. Martin Huth[1], Dr. Björn Eckert[1], Dr. Petra Majewski[1], Dr. Stefan Aschauer[1], Prof. Lothar Strüder[2], Dr. Heike Soltau[1]
[1]PNDetector GmbH, Munich, Germany, [2]PNSensor GmbH, Munich, Germany

Poster Group 1

In the TEM community, four-dimensional scanning transmission electron microscopy (4D STEM) imaging is meanwhile a commonly used technique for a wide range of materials. In a scanning electron microscope (SEM), usually the backscattered and emitted electrons from the sample surface are recorded by the available detectors. The used electron energy is typically at 30keV or lower. If a thin sample is to be measured in transmission, single cell or multi-channel STEM diodes are used to collect STEM images at a fixed distance below the sample, as there is no optical lens between the sample and the detector. This allows for basic bright field (BF) or differential phase contrast (DPC) signatures to be measured.

To open the use of SEM instrumentation to a broader range of applications and more complex investigations, we used our pixelated pnCCD (S)TEM camera [1] with 264x264 pixels to perform first 4D STEM measurements in a SEM. The camera can record up to 7500 frames per second, which corresponds to a dwell time of 133 microseconds. We modified the camera design such that a compact detector module is placed below the sample position along the optical axis of the microscope, while the camera electronics is mounted outside the vacuum chamber.

In this contribution, we present first measurements with the pnCCD (S)TEM camera operated at room temperature (see Fig. 1) in a Tescan Mira3 SEM, taken at different electron energies from 9keV to 30keV.

Keywords:

4D-STEM STEM SEM

413

Optimizing Backscattered Electron Detection in SEM: Diode Layout and Collection Efficiency

Dr. Mozhdeh Abbasi[1], Dr. Maximilian Schmid[1], Dr. Alessia Mafodda[1], Dr. Stefan Aschauer[1]
[1]PNDetector GmbH, Munich, Germany

Poster Group 1

Scanning electron microscopes (SEMs) with their variety of attachments designed for surface observation and analysis stand as a key instrument in research institutes and quality testing facilities worldwide. The essence of the SEM is to induce the emission of various electron products from the specimen, among which backscattered electrons (BSEs) play a pivotal role. These BSEs emerging from the specimen carry information of composition and structure and play an important role in material and life science. Therefore, while most SEMs are equipped with a standard BSE detector, optimizing the measurement process of BSEs becomes crucial when considering the wide range of measurements into account and pushing the limits for aiming the maximum performance. In addition to the detection efficiency of the detector, the geometry of the set-up also plays a decisive role. We therefore address the question of how the layout of the detector affects the specific geometries present in SEM setups [1].

In SEM in general, ensuring clear visualization of specimen features relies on several factors, including beam current, pixel dwell time, working distance, and detector efficiency. Below a certain minimum contrast threshold, specimen details may become indistinguishable. However, for certain specimens or setups it may not always be feasible to increase beam currents, adjust beam energy, or change the working distance to enhance contrast. In such cases, maximizing the collection of electrons (here BSEs), becomes essential for obtaining satisfactory results. Achieving this involves optimizing the diode layout, thus emphasizing the importance of selecting suitable detectors aligned with specific measurement requirements for effectively optimizing SEM imaging parameters [2]. But despite the important role of BSE collection efficiency across scientific and industrial domains, the literature addressing this aspect remains relatively sparse, posing a significant challenge for comprehensive research in this field.

We conduct experiments measuring the backscattered electron collection at various working distances to determine the optimal conditions for each type of diode. To provide a quantitative assessment, we introduce the Geometric Collection Efficiency (GCE), defined as the ratio of BSE impinging on the active area of the diode to the total number of BSE leaving the sample. We present GCE values for different diode layouts across varying working distances. These results are supported by simulations of GCE based on the cosine distribution of BSE and the setup geometry.

Our study aims to illuminate a crucial aspect influencing the performance and accuracy of Back-scattered electron Detector (BSD). We seek to quantitatively understand the collection efficiency of backscattered electrons across a diverse range of BSD. Employing BSD with varying active areas ranging from 40 to 420 mm² and hole diameters ranging from 1 to 5.6 mm. Moreover, these findings enable the identification of the most suitable diode layout for specific measuring geometries.

Typically, the diode aperture should be sufficiently small to minimize backscattered electron (BSE) loss at shorter working distances, while the outer diameter of the diode must be large enough to capture a greater proportion of BSE at larger working distances. However, this general approach must be adapted to fit within an existing setup, where the hole size additionally impacts the field of view, and the outer diameter may obscure or interfere with other detectors within the SEM. Therefore, it is imperative to determine the optimal diode layout considering both geometric collection efficiency and mechanical constraints of the setup. Subsequently, we will showcase images from various applications, spanning from low working distance (WD) and low keV scenarios to high-current applications accompanied by parallel energy-dispersive X-ray spectroscopy (EDX) measurements at higher WDs.

In conclusion, our investigation utilizes various BSD with distinct geometries to assess their suitability for diverse applications in SEM. Through systematic evaluation of detector performance under varying experimental parameters, we aim to offer insights into selecting the most appropriate detector for specific imaging tasks or analytical objectives.

Fig. 1. Comparing simulated and experimental Geometric Collection Efficiency (GCE) values for diverse Backscattered Electron (BSE) chips with different geometrical configurations. The analysis reveals a close agreement, providing insights into the performance and accuracy of each chip.

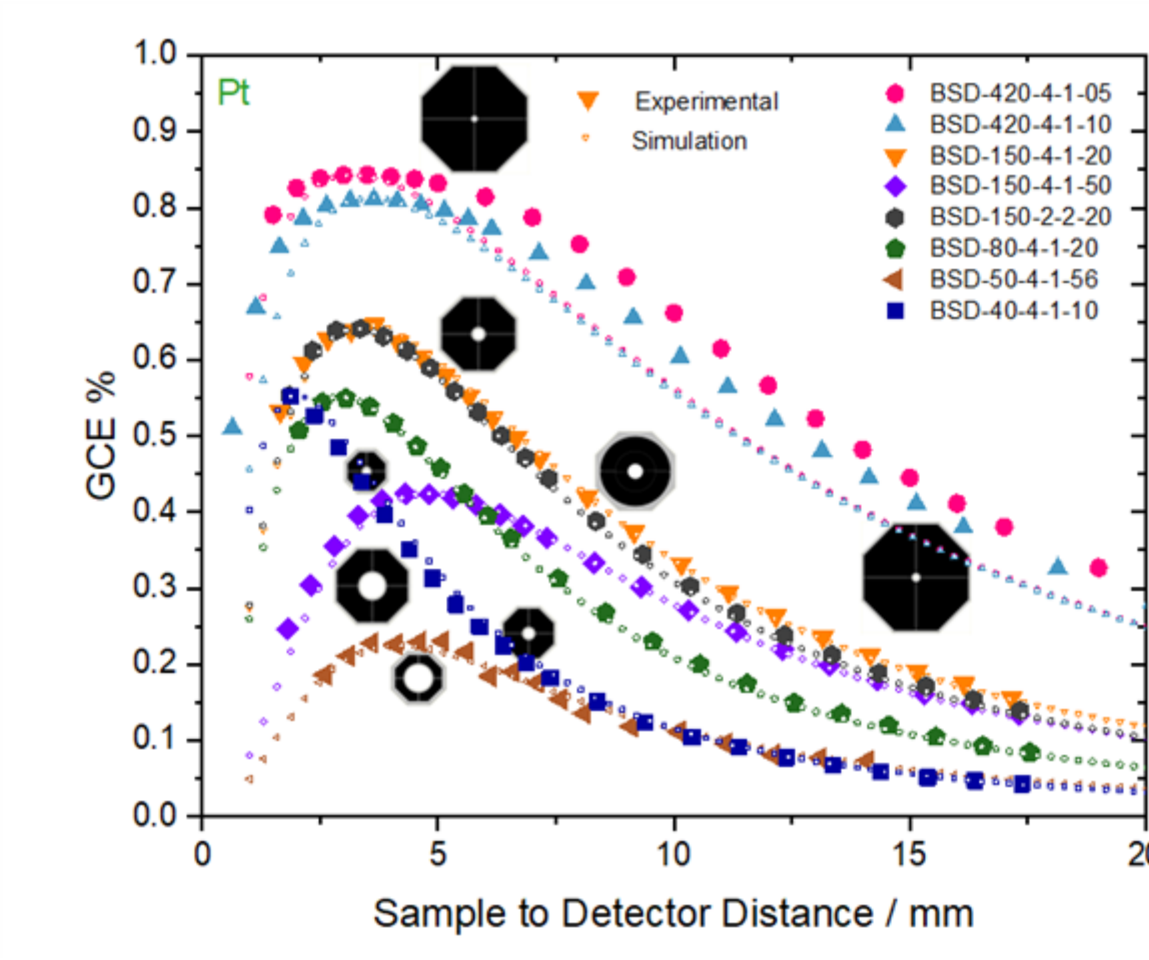

Keywords:

Scanning Electron Microscope,Backscattered Electrons,Detector Efficiency

Reference:

1. J. I. Goldstein, et. al, Scanning electron microscopy and X-ray microanalysis, 4th ed, Springer New York, NY (2017), https://doi.org/10.1007/978-1-4613-3273-2.
2. L. Reimer, Scanning Electron Microscopy, Physics of Image Formation and Microanalysis, 2nd ed Springer Berlin, Heidelberg (1987), https://doi.org/10.1007/978-3-540-38967-5.

414

Empowering STEM in SEM: Integrative Approaches for Enhanced Detection

Dr. Maximilian Schmid[1], Mozhdeh Abbasi[1], Adam Meisel[1], Yassine Elamri[1], Dr. Alessia Mafodda, Dr. Stefan Aschauer[1]
[1]PNDetector GmbH, Munich, Germany

Poster Group 1

In parallel to finding new records in resolution in high energy Transmission Electron Microscopes (TEM) applications - somehow a little behind the scenes - the Scanning Electron Microscopes (SEMs) and TEM machines reach out for each other. Scanning Transmission Electron Microscopy (STEM) in SEM becomes a more and more versatile tool for economical STEM examinations. This may be as a pre-study for further STEM measurements in high end machines or as the final inspection tool. Even though this is an ongoing trend, there is still a gap between the detection capabilities of transmitted electrons in SEM and TEM machines. In SEM, STEM detectors mostly range from passive detection - via generated secondary electrons - to diode arrays and simple segmented diodes. In contrast, in TEM machines the varieties span from single cell detectors over multi segmented ring diodes to fully pixelated electron cameras. Nevertheless, there is a strong demand of expanding the detection possibilities in the SEM closer to TEM machines in order to increase the overlap in detection variability. Here, we introduce a versatile multi-channel STEM setup which can be used in SEM as well as TEM sharing the same platform but addressing the specialties of both worlds.

To perform STEM in SEM with the versatility of the TEM system one needs to address the differences in SEM in relation to TEM :

1. In SEMs the electron energies with <30keV are vastly lower than in TEMs. Therefore, the detector diodes are optimized to support electron energies from below 2 keV to 300keV.
2. SEMs in general offer higher scanning rates than TEM machines. Therefore, the pixel dwell times of down to few tens ns are supported.
3. While all diodes can be used in TEM and SEM, new diode geometries are added to address the different setup geometry in SEM. As seen in figure 1. the range starts with 4 channel segmented diodes and goes up to multi-segmented ring structures with and without BF cell.
4. Two mechanical concepts are chosen to fit most microscope chambers as well as addressing the radiation safety in SEM and TEM. Figure 2(a) shows the manual insertion mechanism for SEM systems. It is optimized for x-y-z positioning in SEM chambers. Figure 2(b) shows the pneumatic insertion mechanism mainly for TEM systems with y-z positioning. While the SEM mechanics cannot be adapted to TEM systems, the pneumatic mechanics can also be used for SEM and is therefore mentioned here.

Besides these differences the system shares the same platform. This includes the amplification chain, the acquisition system, and the ability to support up to 13 individual channels. The platform is divided into two configurations. For the use of the image acquisition system of the microscope there is the possibility to use a 4-channel amplification system. This outputs a user specified combination of the 4 signals (4 to 1) to be digitized by an auxiliary input of the SEM. This system also offers minimal pixel dwell times of few tens of ns but is limited in displaying information in parallel.
To utilize the capability of acquiring up to 13 channels in parallel the second configuration comes with a separate imaging acquisition system. Each of the signals is amplified and digitized separately and the signals can then be digitally combined if needed. Here the minimum pixel dwell time is below 200 ns and there is no limitation in parallel acquisition, displaying or mixing of the individual signals.

In our contribution we will show the results of both configurations with different diode layouts. These examples show how these systems enlarge the STEM in SEM capabilities by sharing more information from the specimen and thus help to close the gap between transmitted electron detection in SEM and TEM.

Fig. 1. Examples of diode layouts for STEM application in SEM and TEM

Fig. 2. Mechanical insertion mechanism for positioning the detectors in the microscope. (a) Manual mechanism for use in SEM. (b) Pneumatic mechanism for use in SEM and TEM

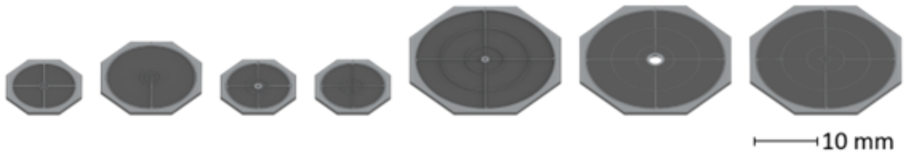

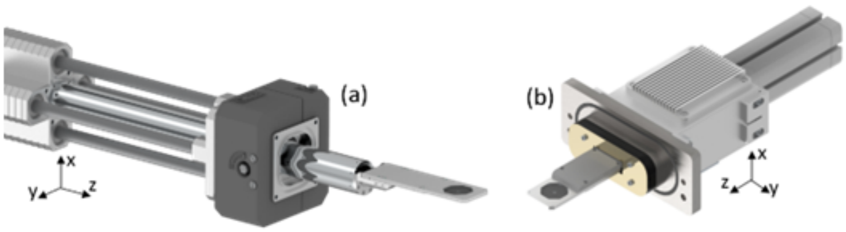

Keywords:

Scanning Transmission Electron Microscopy,Diode geometries

565

Multidimensional Electron Ptychography

Mr. Yu Lei[1], Biying Song[2], Zhiyuan Ding[2], Fucai Zhang[3], Xiaoqing Pan[4], Angus Kirkland[5], Dr Peng Wang[1]
[1]Department of Physics, University of Warwick, Coventry, United Kingdom, [2]College of Engineering and Applied Sciences, Nanjing University, Nanjing, China, [3]Department of Electrical and Electronic Engineering, Southern University of Science and Technology,, Shenzhen, China, [4]Department of Chemical Engineering and Materials Science, University of California, Irvine, United States of America, [5]The Rosalind Franklin Institute, Harwell Science and Innovation Campus, Didcot, United Kingdom

Poster Group 1

Background

Over recent decades, scanning transmission electron microscopy (STEM) has become widely used for matierals charaterizations, achieving atomic-level detail in structural analysis across various scientific disciplines, including physical, chemical, and biological studies. With the recent development of high-acquisition-speed pixelated detectors and advanced computational methodologies, 4D-STEM is progressively transforming into a standardized modality in high-resolution EM. This method integrates a range of applications, from orientation mapping and strain measurement to electric and magnetic field mapping. Furthermore, it transcends the boundaries of conventional STEM imaging to include super-resolution techniques and to provide phase-based imaging, such as ptychography.

Methods

Ptychography, a technique for phase retrieval that extends from the concept of scanning in-line holography introduced by Hoppe, involves shining a light source on a specimen. It captures a sequence of diffraction patterns based on the position of the light source and utilizes iterative algorithms to reconstruct the wavefunction of the sample's exit plane.. Ptychography has attracted considerable interest from both X-ray and electron communities for its potential applications in super-resolution imaging, reaching a resolution of 0.39 ångströms. Electron ptychography has proven to have high-contrast light-element detection detection, high dose-efficiency efficient and 3D imaging [1,2]. Recently we have shown its potential to yield high-contrast image and high sensitivity in capturing phase information from biological samples [3,4]. The significance of phase imaging extends beyond the ability to detect light elements at super-resolution and minimal dosage, as it also promises to provide unique information associated with local variations in magnetic and electrostatic fields.

Results

In this paper, we explore the established multidimensional applications of electron ptychography, such as 3D tilted tomography [2], and single-particle analysis [4], conducted under both room and cryogenic temperatures. Specifically, we introduce a new STEM configuration illustrated in Fig. 1. This setup features an advanced hollow detector that is adeptly coupled with an EELS spectrometer [1]. The design facilitate simulatious, complementary analysis, leveraging the capabilities of sensitive phase and Z-contrast detection alongside comprehensive chemical mapping.

Conclusions

In ptychography, the image-forming optics of traditional imaging modes are replaced by computational methods that utilize a series of electron diffractions collected by rapid detectors. This technique has exhibited great potential in various important applications, including the high-contrast detection of light elements and low-dose imaging. The concept of multidimensional ptychography expands upon this by recording data more than the two dimensions. This expansion may involve capturing changes in the third dimension, electron energy loss, or time.

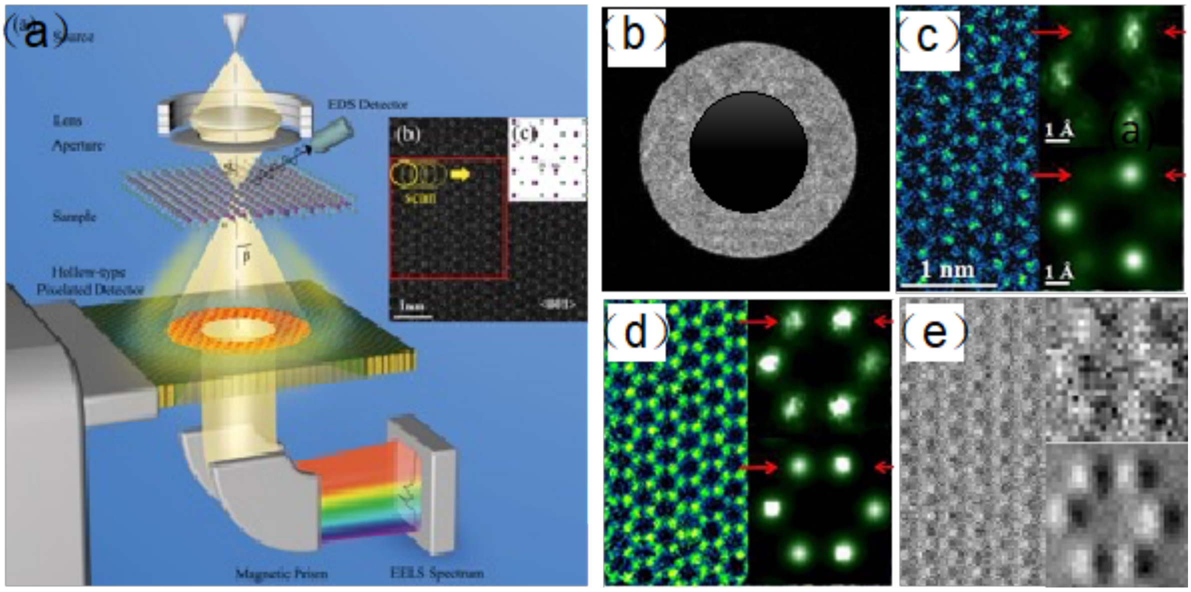

Keywords:

4D-STEM, Ptychography, Super-Resolution

Reference:

[1] Gao, S. et al. Electron ptychographic microscopy for three-dimensional imaging. Nature Communications 8, 163, doi:10.1038/s41467-017-00150-1 (2017).
[2] Ding, Z. et al. Three-dimensional electron ptychography of organic-inorganic hybrid nanostructures. Nature Communications 13, 4787, doi:10.1038/s41467-022-32548-x (2022).
[3] Zhou, L. et al. Low-dose phase retrieval of biological specimens using cryo-electron ptychography. Nat Commun 11, 2773, doi:10.1038/s41467-020-16391-6 (2020).
[4] Pei#, X. et al. Cryogenic electron ptychographic single particle analysis with wide bandwidth information transfer. Nature Communications 14, 3027, doi:10.1038/s41467-023-38268-0 (2023).
[5] Song, B. et al. Hollow Electron Ptychographic Diffractive Imaging. Physical Review Letters 121, 146101, doi:10.1103/PhysRevLett.121.146101 (2018).

593

Atomic-scale microscopy of different materials by ultrashort THz-driven Atom Probe Tomography

Dr. Matteo De Tullio[1], Michella Karam[4], Simona Moldovan[4], Mr. Ivan Blum[1], Mr. Emmanuel Cadel[1], M.me Laurence Chevalier[1], Mr. Martin Andersson[3], Mr. Gustav Eriksson[3], Mr. Jonathan Houard[1], Mr. Marc Ropitaux[2], M.me Angela Vella[1]
[1]Univ Rouen Normandie, INSA Rouen Normandie, CNRS, Normandie Univ, GPM UMR 6634 , Rouen, France, [2]Univ Rouen Normandie, GLYCOMEV UR4358, SFR Normandie Végétal FED 4277, Innovation Chimie Carnot, IRIB, Rouen, France, [3]Department of Chemistry and Chemical Engineering, Chalmers University of Technology, Gothenburg, Sweden, [4]GPM Laboratory, CNRS UMR 6634, Rouen University, Normandy, France

Poster Group 1

Background
Terahertz (THz) radiations with low energetic photons (meV) are used today in a wide range of applications such as imaging, sensing or spectroscopy. The low photon energy of THz radiation has the advantage of inducing low damages on fragile materials by reducing heating encountered when a visible wavelength is used.
Our research is based on the combination of a single-cycle THz source with atom probe tomography (APT) to study THz-assisted field evaporation on a wide range of materials, including metals, ceramics, semiconductors (crystalline silicon), and insulators (amorphous silica). Using our homemade THz-assisted APT setup - “TERA-SAT” - we aim to explore the new impacts of THz pulses on materials characterization at the atomic level.
Methods
Atom Probe Tomography (APT) is an imaging technique based on controlled field evaporation of atoms from a nanometric needle-shaped sample under a strong electric field. Evaporation of atoms is triggered by a laser pulse in the UV or THz domain. The ions are then directed onto a time- and position-sensitive detector. The 3D atomic positions are reconstructed through a back-projection algorithm and the chemical nature is determined by calculating the mass-to-charge ratio.
The experimental setup used (fig. 1(a)) in this study is composed of a pulsed THz source based on the two-color plasma generation process coupled with an APT chamber.
Results
THz radiation has been proven to be beneficial for the reduction of thermal effects in field evaporation of metals and low band-gap materials such as LaB6.
Further tests have also been performed on pure silicon nanotips, where the presence of thermal effect is strongly dependent on the spectrum of the THz radiation.
Finally, we analysed nanotips made of sol-gel amorphous silica, which is chosen as matrix for bio-molecules embedding for future studies. First, we demonstrated the possibility of field-evaporating such material in a well-controlled way using THz pulses. A more detailed comparison of the mass-to-charge ratio spectra obtained with THz-APT and UV-assisted APT (fig.1 (b)) reveals an increase of the signal to noise as well as an improvement in the mass resolving power which is inversely proportional to the full width of the peak at 1 and 10% of the maximum.
Conclusion
We have analyzed different materials using our TERA-SAT setup, demonstrating its ability to trigger field evaporation. The use of THz radiation is proven to reduce local heating phenomena, especially in the case of metals, allowing a-thermal field evaporation.
We have obtained encouraging results also for non-metallic samples, but further investigation will be necessary to find out the optimal parameters (THz amplitude, DC field) to improve the accuracy of

compositional analyses, thus to increase the signal to noise ratio and the mass resolution power of the mass spectra.

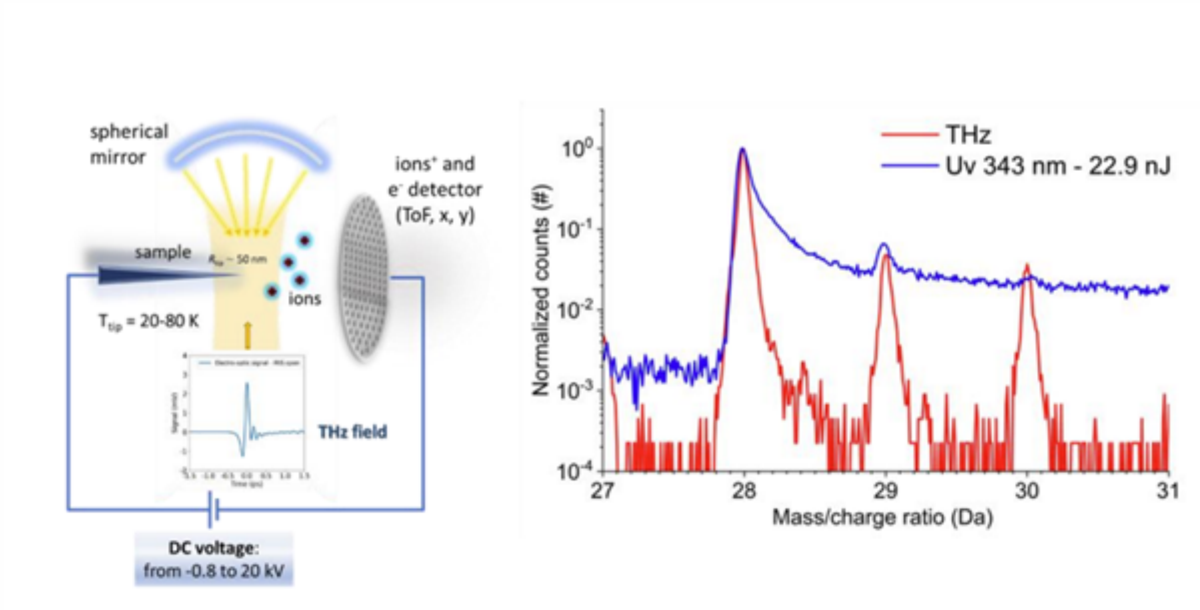

Keywords:

Atomic-scale-microscopy; Atom-Probe-Tomography; pulsed-THz; field-ion-emission

Reference:

[1] A. Vella et al., Sci. Adv., Volume 7, (2021).
[2] M. Karam, et al New Journal of Physics 25, 113017(2023).
[3] M. De Tullio, et al. arXiv preprint arXiv:2403.04470 (2024).
[4] T. Bartel, et al., Opt. Lett., Volume 30, (2005).
[5] G. Sundell, et al., Small, Volume 15, (2019).

613

Imaging Atomic Processes in Catalysts using a New High-Order Imaged-Corrected Environmental-TEM

Dr. Idan Biran[1], Mr. Ruben Bueno Villoro[1], Mr. Christian Kisielowski[2], Mr. Peter Christian Kjærgaard Vesborg[1,4], Mr. Maarten Wirix[3], Mr. Dennis Cats[3], Mr. Narasimha Shastri[3], Mr. Wessel Haasnoot[3], Mr. Jakob Kibsgaard[1,4], Mr. Thomas Bligaard[1,5], Mr. Christian Danvad Damsgaard[1,4,6], Mr. Joerg Jinschek[1,6], Mr. Stig Helveg[1]
[1]Center for Visualizing Catalytic Processes (VISION), Department of Physics, Technical University of Denmark, 2800 Kgs. Lyngby, Denmark, [2]The Molecular Foundry, Lawrence Berkeley National Laboratory, One Cyclotron Rd., Berkeley, USA, [3]Materials and Structural Analysis Division, Thermo Fisher Scientific, Eindhoven, Netherlands, [4]SURFCAT, Department of Physics, Technical University of Denmark, 2800 Kgs. Lyngby, Denmark, [5]Department of Energy Conversion and Storage, Technical University of Denmark, 2800 Kgs. Lyngby, Denmark, [6]National Centre for Nano Fabrication and Characterization (DTU Nanolab), Technical University of Denmark, 2800 Kgs. Lyngby, Denmark

Poster Group 1

Background incl. aims:
The current quest for sustainable energy and environmental technologies calls for a new view on catalysis. Today, catalysis of chemical reactions is commonly perceived as a complex surface phenomenon that inescapably links structural dynamics and functionality of the catalytic nanomaterials [1]. However, insight into this intricate relation between catalytic active surface sites and their mechanistic actions has remained limited due to the lack of suitable atomic-resolution imaging competences. The Center of Visualizing Catalytic Processes (VISION) addresses this core scientific challenge by introducing new electron microscopy technology and applications. In this contribution, we demonstrate a new-generation environmental transmission electron microscopy (ETEM) enabling three-dimensional atomic-resolution imaging of catalytic nanomaterials under exposure to reactive gas atmosphere in a chemical meaningful way.

Methods:
The VISION PRIME microscope is based on an ultra-stable Thermo Fisher Scientific SPECTRA ULTRA platform and designed for in-line holography to retrieve time-resolved exit-wave functions of catalyst nanomaterials during exposure to reactive gas environments at pressures of up to 10-20 mbar. The microscope is equipped with (i) a new 5th order aberration-corrector for the objective lens in broad-beam mode (CETCOR Prime), (ii) a four-stage differential pumping system for confining a reactive gas environment in the mbar range to the vicinity of the sample (ETEM), (iii) a monochromator setup to extend the information limit below 50 pm and (iv) direct electron detection acquisition (Falcon 4i) for low-dose-rate imaging to suppress electron-beam-induced sample alterations.

Results:
Here we present the design of this new-generation ETEM as well as selected performances and applications. Specifically, the ultra-stable electron optics allow the high-resolution transmission electron microscopy (HRTEM) mode to reach 60 pm resolutions routinely, and to further extend the resolution toward 50 pm, in both high vacuum and environmental modes. This is achieved by exploiting the high stability base and optics of the Spectra platform and integrating the ETEM module into it.
Using the flexible microscope illumination system enables to generate Nelsonian illumination with a rapid and flexible electron dose-rate control. This is key to suppress electron-beam-induced sample alterations [2,3]. Furthermore, direct electron detection capability in HRTEM mode helps to achieve the largest image signal for the fewest number electrons. In conjunction with the ultra-stable

electron optics direct detection enables the recovery of the electron exit-wave functions at the highest sensitivity from focal image series acquisitions. This uncovers the three-dimensional atomic structure of the catalyst nanomaterial [3,4].

Conclusions:
The VISION PRIME electron microscope offers a sample-limited rather than optical-limited resolution under high vacuum and environmental conditions. This atomic scale visualization capability offers new means to address the three-dimensional atomic structure and dynamic behavior of catalytic nanomaterials during exposure to relevant reaction conditions. The VISION PRIME is therefore key for uncovering the role of gas-surface interactions in complex catalytic nanomaterials at the atomic-scale and for advancing new catalyst design strategies.

Keywords:

Catalysis, high-resolution-transmission electron microscopy, ETEM

Reference:

1.S. Helveg, J. Catal. 328, 102 (2015)
2.C. Kisielowski, P. Specht, S.M. Gygax, B. Barton, H.A. Calderon, J.H. Kang, R. Cieslinski, Micron 68, 186 (2014)
3.S. Helveg, C.F. Kisielowski, J.R. Jinschek, P. Specht, G. Yuan, F. Frei, Micron 68, 176 (2014)
4.F.-R. Chen, D. Van Dyck, C. Kisielowski, L.P. Hansen, B. Barton, S. Helveg, Nat. Commun. 12, 5007 (2021).

* The Center for Visualizing Catalytic Processes is sponsored by the Danish National Research Foundation (DNRF146)

687

Mitigation of beam damage on MoS2 using electrostatic beam blanking in TEM

Mr Joakim Kryger-baggesen[1], Mrs. Noopur Jain[2], Mr. Mark van Rijt[2], Mr. Ruud Krijnen[2], Mr. Marteen Wirix[2], Mr. Pritam Banerjee[3], Mr. Joachim Dahl Thomsen[5], Mr. Jakob Kibsgaard[1,4], Mr. Christian Damsgaard[1,3], Mr. Joerg Jinschek[1,3], Mr. Stig Helveg[1]
[1]Center for Visualizing Catalytic Processes (VISION), Department of Physics, Technical University of Denmark, Kgs. Lyngby, Denmark, [2]Thermo Fisher Scientific, Achtseweg Noord 5, 5651 GG Eindhoven, Eindhoven, The Netherlands, [3]National Center for Nano Fabrication and Characterization, Technical University of Denmark, Kgs. Lyngby, Denmark, [4]Surface Physics and Catalysis, Department of Physics, Technical University of Denmark, Kgs. Lyngby, Denmark, [5]Ernst Ruska-Centre for Microscopy and Spectroscopy with Electrons, Forshungszentrum Jülich, 52428 Jülich, Jülich, Germany

Poster Group 1

Background

Transmission electron microscopy (TEM) has allowed for impressive opportunities to visualize matter at the atomic scale. In such experiments, the constituent atoms typically respond dynamically to the electron beam irradiation, alter the sample and, hence, modulate image contrast and intensities. While mitigation strategies have focused much on electron energy and dose variation, there is a growing emphasis on the role of the electron dose rate.

That is, for a broad class of materials, the electrons incident on the specimen is considered to cause phonon or electron excitations because the impingement rate is higher than the subsequent relaxation rate. Consequently, accumulation of energy and or charge leads to bond rupture and atom displacements. In this picture, pulsing the electron illumination seems beneficial as it enables a sharply defined maximum electron impingement rate to match the onset causing sample alterations. Here we show how a structured electron beam can suppress beam-induced alterations of a two-dimensional MoS2 by 50% compared to the continuous mode.

Method

The present experiments are conducted on a Thermo Fisher Scientific SPECTRA ULTRA microscope operated at 300 kV. An electrostatic beam blanker (ESBB) system developed by Thermo Fisher Scientific, is used to structure the electron beam with a 10 ns temporal electron delivery window with repetition rate of 1MHz. The microscope was operated in pulsed and continuous mode. In each mode, an electron diffractogram of the MoS2 was recorded at similar electron dose-rate and total dose. In pulsed mode the beam blanker was tuned to generate 1 electron per pulse. The area exposed was kept the same during acquisition to compare the behavior of the specimen in both modes.

Results

The electron diffractograms of MoS2 show for increasing electron dose and dose-rate had different evolution of the central diffraction peak intensities in pulsed and continuous modes. In continuous mode the diffraction peaks faded to ~60% of the original intensity due to loss of crystallinity caused by beam damage. In pulsed mode the diffraction peak intensities faded only by ~1%. A similar effect was observed by (1,2) delivering dose electron-by-electron and allowing relaxation time reduces beam damage. Further we found that the effect of pulsing decreased when increasing the number of electrons per packet. This is the first time that this effect is shown with only a beam blanker and on a nanosecond time scale.

Conclusion

Thus, the comparison of pulsed and continuous electron beams suggests that the electron-induced degradation of MoS2 is a multi-electron excitation rather than a single-electron scattering event, consistent with ref. (3,4) and that excitations on the microsecond timescale must be circumvented to maintain structural integrity of the MoS2 sample. We anticipate that beam blanker pulsed electron delivery may benefit the stability of other materials and enable novel experiments with beam sensitive materials in general.(5)

Keywords:

Beam damage, structured electron illumination

Reference:

1. C. Kisielowski, P. Specht, B. Freitag, E. R. Kieft, W. Verhoeven, J. F. M, van Rens, P. Mutsaers, L. Jom, S. Rozeveld, J. Kang, A. J. McKenna, P. Nickias, D. F. Yancey, Advanced Functional Materials, 29, 11 (2019)

2. E. Vandenbussche, D. Flannigan, Nano Letters 19(9) 6687-6694 (2019)

3 . T. Susi, J. C. Meyer, J. Kotakoski. Nat. Rev. Phys. 1, 405 (2019)

4 . F.-R. Chen, D. van Dyck, C. Kisielowski, L.P. Hansen, B. Barton, S. Helveg, Nat. Commun 12, 5007 (2021)

5. We thank Felix van Uden for preparing the microscope and Maarten Waaijer, Erik Kieft, Boy Markus, Bert Freitag and the rest of the Thermo Fisher Scientific team for participating in the initial discussions. Further we thank Tim Booth from the 2DTU group at DTU for assistance in providing MoS2 samples. The Center for Visualizing Catalytic Processes is sponsored by the Danish National Research Foundation (DNRF1462).

692

Recent developments and future trends in time-resolved cathodoluminescence: measuring dynamics at the nanoscale

Dr Herman Duim[1]
[1]Delmic, Delft, The Netherlands

Poster Group 1

Background
Cathodoluminescence spectroscopy is a well-established technique utilized to extract detailed information about the optical properties of materials [1, 2] at spatial resolutions surpassing the diffraction limit of light. By employing an electron beam as a broadband excitation source, materials can be brought into an excited state. The subsequent relaxation of these excited states typically follows intricate pathways involving both radiative and nonradiative recombination mechanisms. Gaining a comprehensive understanding of these dynamic processes is essential for the design and optimization of nanomaterials and devices.

Results
We will explore various experimental implementations of time-resolved cathodoluminescence (TRCL) that are applicable for lifetime mapping or g(2) imaging. In the former, a decay trace is measured following excitation with a pulsed electron beam, enabling the determination of the excited state's lifetime [3]. In the case of g(2) imaging, photon statistics are instead utilized to observe bunching and anti-bunching effects [4, 5]. By analyzing the bunching behavior in extended material systems, it becomes possible to extract valuable information about emission lifetime and excitation efficiency. An important advantage of this approach is its compatibility with a continuous electron beam, eliminating the need for modifications to the electron microscope.

Conclusions
Here we describe the latest advancements in time-resolved cathodoluminescence and future directions, drawing examples from semiconductor research to highlight the remarkable capabilities and value that TRCL brings as an advanced nanoscale characterization technique.

Keywords:

Time-resolved cathodoluminescence, spectroscopy, dynamics, ultrafast

Reference:

1. A Polman et al., Nat. Mater. 18, 1158 (2019)
2.M. Merano et al., Nature, 438, 479-482 (2005)
3. S Meuret et al., Phys. Rev. Lett. 114, 197401 (2015)
4. Robert J. Moerland, Optics Express, 24, 24760-24772 (2016)
5. S. Meuret et al. Ultramicroscopy, 197, 28-38 (2019)

720

Evaluation of SXES on different kind of materials : successes and failures

Jean-Louis Longuet[1]
[1]CEA Le Ripault, Monts, France

Poster Group 1

First, a brief reminder of the main aspects of wavelength dispersion spectrometry (WDS) will be given, with examples illustrating the contribution of WDS analysis compared to EDS analysis. Then, we will introduce the problem of detecting low energy X-ray photons (less than 1 keV) and the useful information on the sample that can be derived from it.
Among others, the “SXES” type detector (Soft X-ray Emission Spectroscopy) is one of the technical solutions developed by manufacturers to enable the detection and analysis of X-ray photons in this energy range. Their principle is based on the use of a variable pitch array (VLS) and a CCD camera instead of the analyzer crystals and proportional counters of traditional WDS spectrometers. The lithium detection capacity, getting information on the chemical environment at the local scale or even the very good detection sensitivity for light elements are the main advantages of this device. Examples, successful (or not!) will be presented and compared to data accessible by WDS crystal spectrometry.
To conclude, other technological solutions (already marketed or in development) will be presented such as new EDS spectrometers or new WDS analytical crystals for the detection of Li, as well as RZP (Reflective Zone Plate) type grating spectrometers for example.

Keywords:

EPMA SXES WDS EDS

749

Microchannel Plate-based Detector with High Pressure Operation up to 1 Pa for Scanning Electron Microscopy

Mr Masahiro Hayashi[1], Mr. Yuya Washiyama[1], Dr. Matthias Sachsenhauser[2]
[1]Hamamatsu Photonics K.K., Hamamatsu , Japan, [2]Hamamatsu Photonics Deutschland GmbH, Herrsching, Germany

Poster Group 1

Background incl. aims

Microchannel Plates (MCP) are electron multipliers with a secondary electron amplifier mechanism. MCP detectors have many advantages such as small size, high temporal resolution, high gain, and very high detection efficiency for electron energies of the order of tens to hundreds of electron volts in scanning electron microscopy (SEM). Recently, almost all commercially available SEMs are operated in low vacuum conditions caused by flowing neutralization gas into the specimen chamber to suppress charging on the sample surface. However, MCPs cannot be utilized in low vacuum conditions because of ion feedback.

Ion feedback, a peculiar phenomenon of secondary electron multipliers, can cause discharges and degradation of signal-to-noise ratio. Ions generated by electron ionization are converted into electrons and multiplied by the secondary multiplier. The generation of ion feedback cannot be suppressed under low vacuum due to the presence of neutralization gas in SEM.

MCPs are powerful to detect secondary and backscattered electrons in SEM, but the challenge is stable operation under low vacuum conditions. Therefore, we have developed a novel detector structure that maintains the advantages of MCPs even under low vacuum conditions. In particular, its specific structure has proven to reduce ion feedback . Instead of using a bi-planar structure, as is the case in conventional MCP detectors, a triode structure is adopted. When a novel electric field configuration is applied to the electrodes, the triode structure can effectively suppress ion feedback even under low vacuum conditions.

Methods

The mechanism of ion feedback was investigated, when residual gas ions are generated by reactions between the residual gas and secondary electrons from the MCP channels. The ions (ionized residual gases) are accelerated by the electric field towards the MCP. If they can gain enough energy to release secondary electrons as they impinge on the channel walls, a second electron avalanche will be initiated. These “false” after-pulses would not only disturb the measurement, but could also ultimately lead to a permanent glow discharge. After-pulses appear several tens of nanoseconds after the "original" output signal, occur repeatedly and sometimes become even larger compared to the original signal. Considering the collision probability of electrons and gas molecules, ion feedback is likely to disturb the output signal, when MCPs are operated at a higher gain, or when increasing the input signal to the MCP.

It is found that residual gas ions causing ion feedback occur between MCP and anode, rather than inside the MCP channels. We concluded that controlling ions is more important than suppressing ion generation. Therefore, a triode-type detector structure was developed, in which a mesh anode was placed between MCPs and a dynode. It is confirmed that the dynode prevents ion feedback by capturing residual gas ions.

Results

First, we examined the effect of the triode structure for operation under low vacuum conditions by using a first prototype detector, which was composed of chevron stack MCPs (dimeter of 14.5 mm), a mesh anode and a metal dynode, in a vacuum chamber. While adjusting the degree of vacuum in the chamber, the detector was operated in two voltage modes: standard potential mode, i.e., MCP-in < MCP-out < anode = dynode, and novel potential mode, i.e., MCP- in < dynode < MCP-out < anode. As a result, when the gain of detector is low, there is no difference between the two potential modes in high pressure operation up to 1 Pa with or without input signals. When the gain becomes higher (105), ion feedback occurs at 10-3 Pa in standard potential mode, even without input signals, but does not occur in novel potential mode up to 1 Pa. Hence, it is confirmed that MCP detectors are capable of high-pressure operation by adapting the triode structure with novel potential mode. The second prototype detector is under development with a very compact size to optimize it for SEM. The detector can be simplified by setting MCP-in and dynode at the same potential, and it fits into confined space by having an outer diameter of 35 mm, a height of 3 mm and a center hole diameter of 6mm. Our target specification of the detector is to maintain a gain of 5×106 up to 1 Pa without generating ion feedback signal.

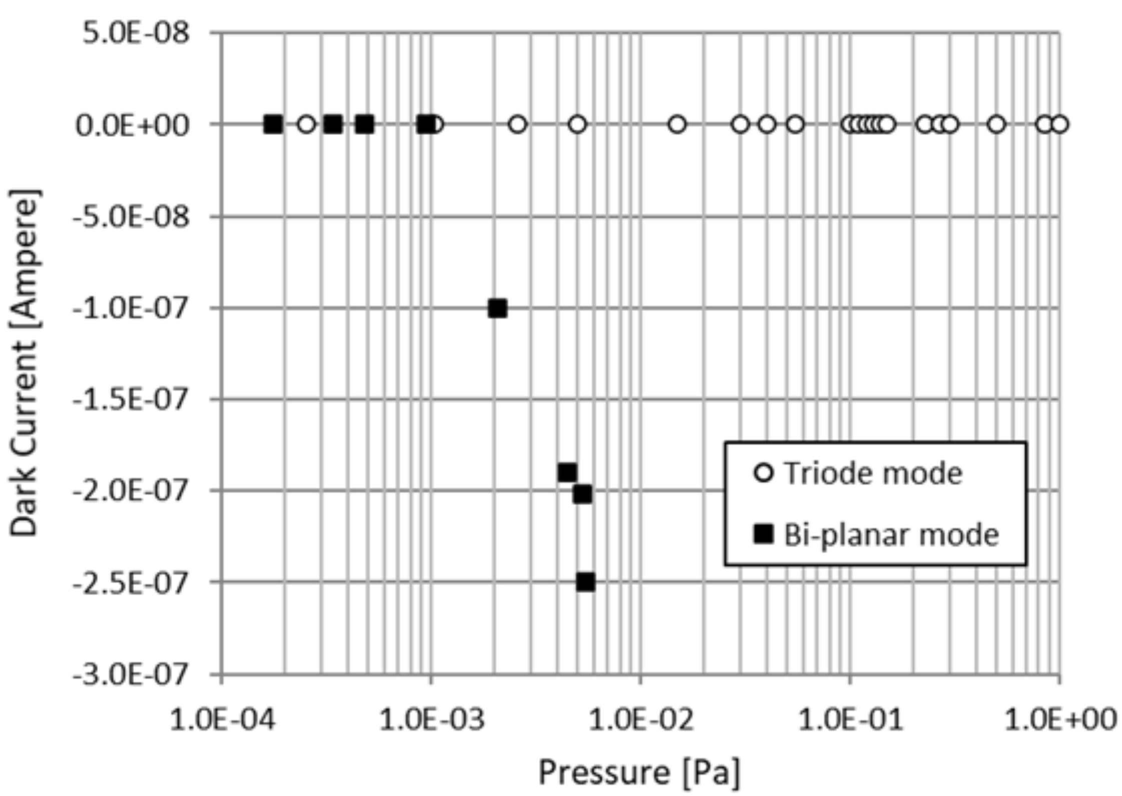

Keywords:

MCP, triode detector, low vacuum

758

An analytical ion microscope for high-resolution imaging, nanoscale analytics and nanofabrication

Peter Gnauck[1], Torsten Richter[1], Alexander Ost[1]
[1]Raith GmbH, Dortmund, Germany

Poster Group 1

The Liquid Metal Alloy Ion Source (LMAIS) has been described as a high-impact technology offering new insights into the structure and function of nanomaterials [1]. Combining the high brightness of a Liquid Metal Ion Source (LMIS) with the capability of emitting light and heavy ions such as Silicon and Gold or Lithium and Bismuth simultaneously makes the LMAIS the ideal ion source for high-resolution imaging, nanofabrication, and nano-analytics (Fig. 1) [2]. The ion species are emitted simultaneously from a single source and separated in a downstream Wien filter. This mature source technology allows for high-resolution Secondary Electron (SE) imaging with exceptional surface details by using light primary ions as well as adjusting the required sputter yield and resolution for nanofabrication and sample modification by selecting the most suitable ion species from the LMAIS.
With a top-down FIB geometry and capability of fast ion toggling a novel workflow for 3D sample reconstruction with sample tilt becomes possible: heavy ions have an excellent depth resolution for sample delayering. The selection of various beam paths or looping strategies as known from many applications in nanofabrication minimize selective sputtering and redeposition while digging into the sample.
Intermittent imaging with light ions prevents further sputtering and allows 2D sample imaging for mapping the region of interest layer by layer. Obtained ion images are then stacked for 3D sample reconstruction [2].

By adding a specifically designed compact magnetic sector mass spectrometer, the ion microscope becomes a high-resolution analytical instrument [3].
Secondary Ion Mass Spectrometry (SIMS) is a robust and highly sensitive surface analysis method capable of detecting all elements ranging from hydrogen to uranium. It offers trace element identification, differentiation of isotopes, elemental imaging at the nanoscale, shallow depth profiling, and three-dimensional analysis.
By selecting the most suitable ion species from the LMAIS the SIMS system takes advantage of the LMAIS technology by selecting the most suitable primary ion species for the analysis.
The SIMS system is based on:
(i) specifically designed secondary ion extraction and transfer optics for highest extraction efficiency and transmission, resulting in excellent sensitivity.
(ii) a compact floating double focusing magnetic sector mass spectrometer allowing operation in the DC mode at high transmission and hence avoiding secondary ion losses due to duty cycles like in TOF systems.
(iii) a focal plane detection system allowing the detection of all masses in parallel (up to 400 m/z).

This contribution outlines the working principles and features of the focal plane magnetic SIMS detector combined with a LMAIS. By combining LMAIS technology with a stable stage and sensitive SIMS unit, this system offers a pathway for advanced nano-analytics, surpassing conventional methodologies for sample analysis.

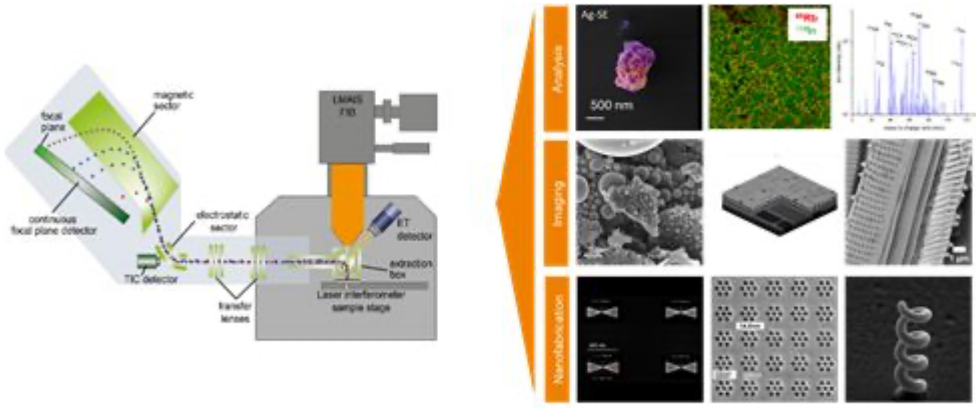

Keywords:

FIB, SIMS, LMAIS, Microscopy, Ion

Reference:

[1] L. Bischoff et al., Applied Physics Reviews 3, 021101 (2016)
[2] A. Nadzeyka et al., J. Vac. Sci. Technol. B 41(6) (2023)
[3] J-N. Audinot et al., Rep. Prog. Phys. 84 (2021)

768

Crystalline analysis by W-SEM using a newly developed EBSD detector

Dr. Yohei Kojima[1], Yuta Matsumoto[1], Daniel Goran[2], John Gilbert[2], Naoki Kikuchi[1]
[1]JEOL, Ltd., 3-1-2, Musashino, Akishima, Japan, [2]Bruker Nano GmbH, Am Studio 2D, Germany

Poster Group 1

Background incl. aims

Understanding crystalline properties of material is essential for controlling its physical characteristics. EBSD method in SEM (SEM-EBSD) is a well-established technique for investigating the phase orientation and identification of single or polycrystalline materials. It is commonly used to determine crystalline properties in micro and nanotextures [1]. The development of SEM-EBSD significantly contributes to the analysis of microstructure, crystallography and physical properties in various fields, including materials science and mineralogy, such as metals, ceramics, and minerals. Thus, the SEM-EBSD method is widely recognized as a requisite tool in these fields now.

To obtain high-quality EBSD measurement results, large probe currents ranging from several 10 to 100 nA are generally required. Therefore, the SEM equipped with a Schottky-type field emission gun (FE-SEM) has been basically employed for EBSD measurements due to its ability to maintain high resolution even when large probe currents are applied. On the other hand, the crystal grains to be measured by EBSD are usually a few to several 10 of micrometers in size, which falls within the measurable range of the SEM with Tungsten thermal filament (W-SEM). However, there are few cases where W-SEM is installed together with the EBSD detector in laboratory, because the spatial resolution of Tungsten filament gun when using a large probe current is significantly inferior to that of field-emission guns [2].

Recently, CMOS has increasingly replaced CCD as the image sensor in EBSD detectors. This shift has made it possible to obtain fast and clear EBSD patterns with less probe current, resulting in more practical EBSD measurement by W-SEM. Here, we present a new EBSD detector from Bruker (e-Flash XS) in combination with JEOL's entry-level W-SEM. Although the body of e-Flash XS is significantly smaller than the conventional EBSD detectors, its CMOS image sensor provides high-definition EBSD patterns even at a small beam current, enabling fast analysis. The EDS detector is also included in this system, called ED-XS, which allows an elemental analysis during the EBSD measurement simultaneously. This report presents an overview of the e-Flash XS with ED-XS system and one of its applications.

Methods

The ED-XS system including an EDS (XFlash 630; Bruker Nano GmbH) and an EBSD detector (e-Flash XS; Bruker Nano GmbH) is installed on the entry model W-SEM, JSM-IT200 (JEOL, Ltd.). Details are described in the following "Results" section. Cross section of zirconia ceramic made with Cross Section Polisher (IP-19520CCP; JEOL, Ltd.) was used as a specimen. The crystal structure of cubic zirconia (ZrO2, Fm-3m, No. 225) was used for EBSD pattern analysis. The acquisition parameters were an acceleration voltage of 20 kV, a probe current of 15 nA, a working distance (WD) of 7 mm, and a chamber vacuum of 10 Pa.

Results

Graphic (a) displays an external view of the complete ED-XS system with JSM-IT200. Simultaneous acquisition of EDS and EBSD is possible because the detectors are located in the same direction. The phosphor screen inside the sample chamber can be manually attached and detached. A specimen to be measured is mounted on a pin-type stub and placed in a designated holder with the specimen surface tilted at 70 degrees. This holder allows high-resolution EBSD measurements with a short WD of less than 15 mm (minimum 6 mm) without tilting the stage.

The pattern quality map of the zirconia ceramic obtained by e-Flash XS is shown in graphic (b) at a magnification of 5,000. Although this ceramic is the non-conductive material, EBSD measurements can still be performed without a conductive coating using the low-vacuum feature. The pattern quality map reflects the shape of the grains and their boundaries based on the clarity value of the Kikuchi pattern image. Then, the crystal grain size of the zirconia ceramic measured in this study was found to be approximately 2-3 µm for the largest ones and several 100 nms for the smallest ones. Additionally, inverse pole figure (IPF) map indicates that the orientation of the individual grains are random, while kernel average misorientation (KAM) map demonstrates that there is little local plastic deformation in the ceramic. Moreover, simultaneous EDS elemental map revealed that Zr and O were mainly present thoughout the measurement area, with small amounts of Y and Hf also detected. No segregation of other elements was observed, indicating the absence of foreign materials.

Conclusion

In this report, we present a new EBSD detector e-Flash XS and ED-XS integrated system designed for the compact model of W-SEM. As described, this small detector can measure the properties of crystal grains as small as several 100 nm, even under low-vacuum conditions using W-SEM. Electron channeling contrast images are generally used for measuring crystal grains. However, it is important to note that the contrast of these images can be affected by changes in the acceleration voltage or angle of incidence of the electron beam. On the other hand, crystal grain measurement via EBSD can be performed independently for acceleration voltage and angle of incidence. In addition, it is possible to analyze distortion and deformation resulting from differences in crystallographic orientation. This system is optimal for all SEM users, especially W-SEM users, to enhance their crystallographic analysis.

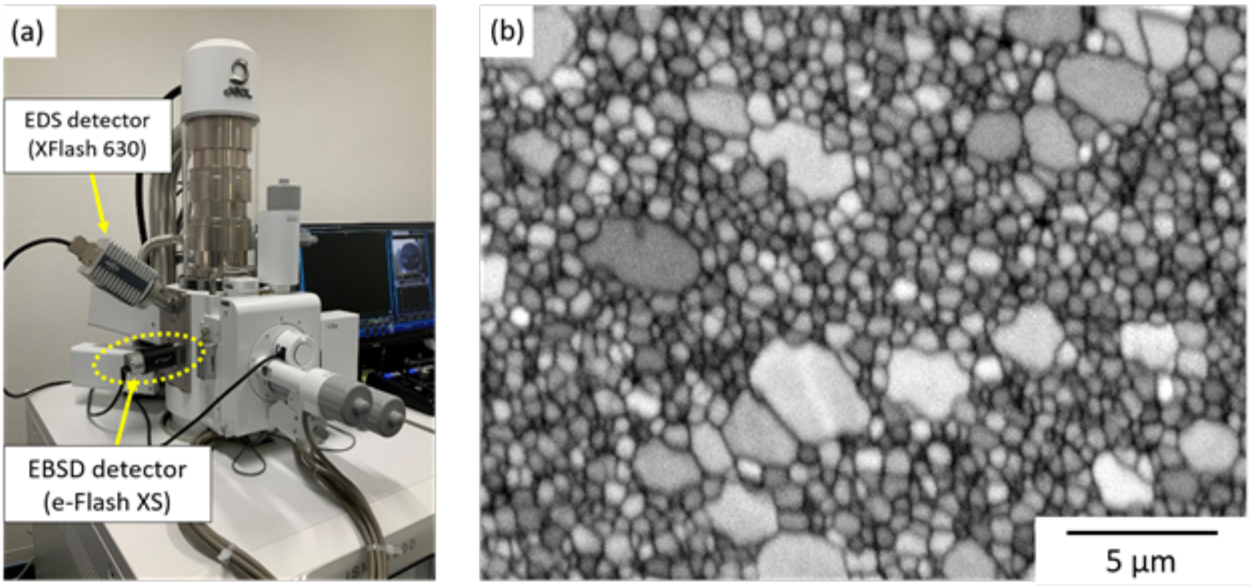

Keywords:

EBSD
W-SEM
Crystal analysis

Reference:

[1] J. I. Goldstein, D. E. Newbury, J. R. Michael, N. W. M. Ritchie, J. H. J. Scott, D. C. Joy, New York: Springer Nature, (2018).
[2] P. McSwiggen, IOP Conf. Ser.: Mater. Sci. Eng., 55 (2014) 012009.

775

Novel, low-cost hardware for ‘STEM in SEM’ imaging

Mr Andrew Sturt[1], Dr Gareth Hughes[1], Dr Ian Griffiths[2], Dr Phani Karamched[1], Dr Neil Young[1]
[1]Department of Materials, University of Oxford, , United Kingdom, [2]JEOL (UK) Ltd, Welwyn Garden City, United Kingdom

Poster Group 1

Background
Scanning transmission mode imaging can offer better contrast and resolution than secondary electron imaging in nano, soft and biological materials[1]. The concept of ‘STEM in SEM’ is to replicate the improved image quality of scanning transmission electron microscopy (STEM) in lower-cost scanning electron microscopes (SEM). In the hardware discussed in this work, a conversion plate allows the transmitted electrons to produce a signal using the Everhart-Thornley Detector (ETD). This enables bright field STEM imaging to be added to most SEMs through using only an additional sample holder.

Although this is not a new concept [2], little work has been published on the optimisation of the design and operational parameters. A higher efficiency allows a lower probe current to be used. In the SEM, the spot size is limited by the probe current and the brightness of the source. Due to this the improved efficiency in ‘STEM in SEM’ results in improved resolution.

The schematic (a) shows the basic concept of the ‘STEM in SEM’ holder. A standard TEM grid is clamped between plates at the top of the holder. The electron beam passes through the sample and reaches a conversion plate. Here transmitted electrons generate secondary electrons within the plate which may be detected by the ETD. Furthermore, an aperture may be inserted between the sample and the conversion plate to control the acceptance angle of the detector.

Methods
The optimisation process consisted of a series of experiments analysing the effect of each parameter in isolation.

The efficiency of the conversion of transmitted electrons to secondary electrons was simulated using CASINO, a Monte Carlo method simulation program [3] . The modelling indicated an improved conversion yield when an oxide forming metal coats the surface. The model was validated by comparing the ETD signal produced when a range of coated glass substrates were scanned with a focussed electron beam. The increase in secondary electron yield due to a sputtered aluminium surface coating was verified experimentally. As secondary electrons only escape from within a few nanometres of the surface, only a coating of high-yield material is needed. This was implemented at a low cost by sputtering a gold-aluminium bilayer coating onto glass substrate.

Significant geometrical optimisations in both the angle of the conversion plate and the working distance were found. The image brightness was measured whilst varying the conversion plate angle. It was found that the efficiency of the plate has a significant peak at the optimised angle. It is thought that this is for two reasons. Firstly, as the angle increases, the transmitted electrons travel a greater distance within the material at a depth at which secondary electrons can escape. Secondly, the alignment of the emitted electrons to the ETD improves the detection efficiency.

One of the challenges with ‘STEM in SEM’ is the convolution of the desired transmitted signal with undesirable secondary electrons from the sample. The difference in detection efficiency of the ETD at different working distances was used to combat this. The ETD has poor detection efficiencies close to the polepiece. When using a sample working distance of 3mm and a converter plate working distance of 18mm, the signal was dominated by the transmission mode. The noise was further reduced by a reduction of the ETD cage bias from the 250-400V typically used to 50V. This limited the detected electrons to those emitted aligned closely to the detector.

The overall performance of the 'STEM in SEM 'converter was evaluated by imaging drop cast 40nm and 20nm nominal size silver nanoparticles on a holey carbon TEM grid. Ostwald ripening of the nanoparticles produced a broad distribution of particle sizes for resolution testing. The samples were imaged at 30kV using a tungsten filament SEM. The other microscope parameters were adjusted to suit the two imaging methods.

Results

The figure shows silver nanoparticles on a holey carbon film observed whilst using a tungsten filament SEM in (b) secondary electron mode at 30kX magnification and (c) using the STEM converter at 75kX magnification. The contrast was improved using the optimised 'STEM in SEM' converter when compared to secondary electron imaging. An improvement in contrast to noise ratio was seen in the STEM images. The improved contrast enables faster and easier imaging of the nanoparticles in the STEM mode. The smallest particles seen in secondary electron mode were 75nm in diameter. With the STEM converter, this was improved to 25nm.

Conclusion

The optimised 'STEM in SEM' converter presented here is a low-cost method to enable transmission mode imaging in the SEM. It has been shown this can be utilised to improve the image quality when imaging nanoparticles. Although, this does not represent new functionality compared to dedicated silicon STEM detectors, it is a much more accessible method of adding STEM capabilities to an SEM.

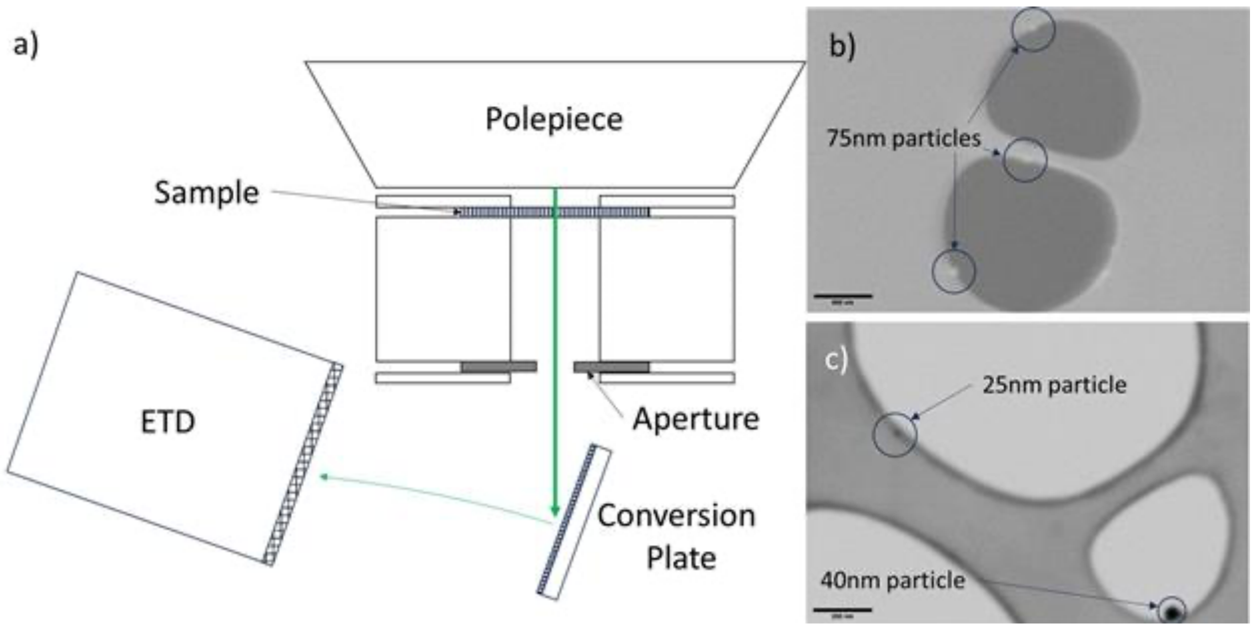

Keywords:

STEM, SEM, nanoparticles, low-voltage STEM

Reference:

[1] U. Golla-Schindler, B. Schindler, G. Schneider, Contrast and spatial resolution enhancement with the transmission mode in SEM, Microscopy and Microanalysis 27 (2021) 1820–1822. https://doi.org/10.1017/s1431927621006668.

[2] U. GOLLA, B. SCHINDLER, L. REIMER, Contrast in the transmission mode of a low-voltage scanning electron microscope, J Microsc 173 (1994) 219–225. https://doi.org/10.1111/J.1365-2818.1994.TB03444.X.
[3] H. Demers, N. Poirier-Demers, A.R. Couture, D. AJoly, M. Guilmain, N. de Jonge, D. Drouin, Three-dimensional electron microscopy simulation with the CASINO Monte Carlo software, Scanning 33 (2011) 135–146. https://doi.org/https://doi.org/10.1002/sca.20262.

831

3D calibration for SEM and optical microscopy - First results with next generation 3D standards

Dr.-Ing. Matthias Hemmleb[1], Celina Hellmich[2], Lena Heinrich[2], Sebastian Buetefisch[2]
[1]point electronic GmbH, Halle (Saale), Germany, [2]PTB Physikalisch-Technische Bundesanstalt, Braunschweig, Germany

Poster Group 1

Marker based 3D standards, in the form of cascading step-slope pyramids, enable the calibration of all three scaling factors and all three coupling factors of measurement instruments using only a single sample and a single measurement [1]. They are suitable for automated calibration and therefore offer better convenience than conventional methods and are therefore increasingly applied [2]. With the introduction of a new scalable wafer-based manufacturing technology, the current application range for calibration of atomic force microscopy (AFM) and SEM can be expanded to optical 3D measurement instruments. First prototypes of these next generation 3D standards are applied for example calibrations of topographic 3D-SEM and confocal laser scanning microscopy (CLSM). The results show the easy and smooth application of the new standards as well as the high conformity of the calculated calibration parameter with conventional methods.
Currently used 3D standards are produced with FIB. Each standard is therefore a cost-intensive custom-made product that also requires time-consuming calibration. The maximum size of these standards is 80 µm with a marker diameter below 1 µm, which cannot be sufficiently resolved with optical 3D microscopes. Therefore, a wafer-based mask process for the fabrication of 3D standards was developed, allowing many structures to be fabricated reproducibly and the geometric dimensions to be adapted to the respective device to be calibrated. First results are prototypes with sizes of 400 µm and 1200 µm for use with optical microscopes, as well as standards with 80 µm size as replacement for AFM and SEM calibration [3]. Figure 1 (SEM and CLSM image with field of view about 400 µm) shows a first prototype, which was successfully used for the calibration of a CLSM (Olympus Lext OLS 4100). The calibration results were compared to the results from a conventional calibration which was carried out as a combination of a step height and a grid standard.
Compared to currently established traceability of FIB standards, which finally based on a reference measurement with a metrological large-range AFM (Met. LR-AFM), providing the required reference data for the wafer-based manufactured standards is easier and more efficient due to their better conformity. Therefore, a combination of traceable calibrated SEM and stylus profilometry was used for the measurement of the reference data [3].
For the coordinate measurement of the reference marks with subpixel methods, as well for the calibration parameter estimation with statistical methods, the dedicated software microCal was applied, which was already validated for this purpose [4].
The prototypes of the next level 3D standards can be used with the applied CLSM and the calibration software microCal without any problems and due to automatization very effective. All markers were measured with the required accuracy. In comparison with the more complex conventional CLSM calibration, the difference between lateral and height scale is below 4x10-4 and difference in lateral shearing is 1x10-4. In addition, a significant vertical shearing was determined, which is hardly possible to identify with conventional methods.
Ongoing work is on further accuracy aspects of the new calibration samples and the specification of the uncertainty budget for providing traceable reference data. Due to the promising results, it is planned to make the new generation of 3D calibration samples commercially available in the near future.

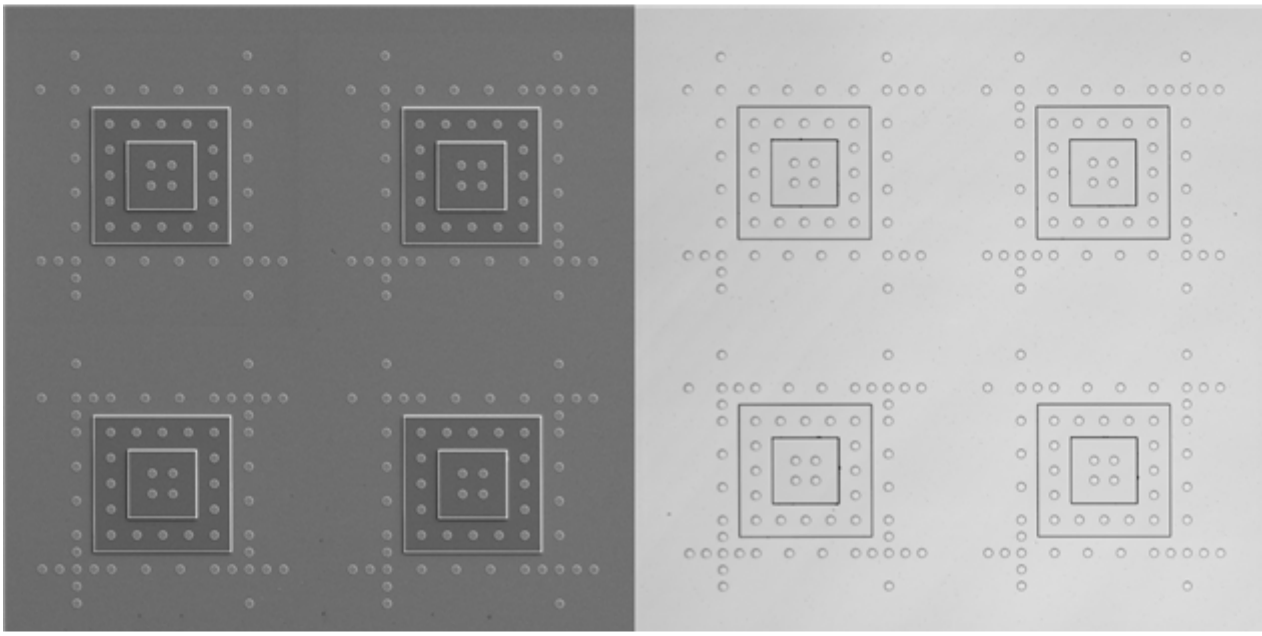

Keywords:

3d metrology standards calibration

Reference:

[1] Ritter, M., Dziomba, T., Kranzmann, A., Koenders, L., A landmark-based 3D calibration strategy for SPM, Meas. Sci. Technol. 18 (2), 404-414 (2007), DOI: 10.1088/0957-0233/18/2/S12
[2] Hemmleb, M., Berger, D., Ritter, M., Automated geometric SEM calibration, Imaging & Microscopy 17 (1), 42-44 (2015), DOI: 10.1002/imaging.4807
[3] Hellmich, C., Heinrich, L., Hemmleb, M., Buetefisch, S., Weimann, T., Kroker, S., Process development and validation of next-generation 3D calibration standards for application in optical microscopy, Meas. Sci. Technol., submitted for publication
[4] Xu, M., Hemmleb, M., Dai, G., Validation of evaluation algorithm for 3D calibration, Meas. Sci. Technol., submitted for publication

910

Electron beam manipulation with auto-ponderomotive potentials for interaction-free measurements

Msc. Franz Schmidt-Kaler[1], Mr. Michael Seidling[1], Mr. Robert Zimmermann[1], Mr. Nils Bode[1], Mr. Fabian Bammes[1], Mr. Lars Radtke[1], Mr. Peter Hommelhoff[1]
[1]AG Laserphysik, Friedrich-Alexander Universität Erlangen-Nürnberg, Germany

Poster Group 1

Background incl. aims
In many electron microscopy applications, beam damage is a serious issue, often preventing true single particle imaging with atomic resolution to date. When one and the same electron interacts with the sample multiple times, the extracted information can be increased for the same amount of damage [1, 2, 3]. This is at the core of what is known in quantum mechanics as interaction-lean or also interaction-free or measurement (IFM). This concept has been demonstrated to work well with light [6]. We aim at realizing this approach with electrons.

The IFM concept was introduced by Elitzur and Vaidman [1]. Recently, a first demonstration experiment with electrons in an interferometer scheme but without multipassing was reported [4]. To increase the scheme's efficiency substantially, a resonator structure is needed to enable repeated electron-sample interrogation [5]. A quantum electron microscope can be set up in different ways [5], all of which are technically highly demanding. We focus on auto-ponderomotive structures acting as electron guide, beam splitter and resonator. We demonstrated electron beam guiding and splitting [6, 7], as well as 7 round trips in an auto-ponderomotive electron resonator [8]. The current state of the experiment will be reported.

Methods
Auto-ponderomotive structures rely on electrodes applied with alternating DC voltages. In the frame of the swift electrons, an oscillatory potential results forming transverse guiding and beam splitting potentials. We experimentally demonstrated electron beam guiding as well as electron beam splitting in a conventional Philips XL30 SEM at energies up to 9.5 keV and 1.7 eV respectively. Our auto-ponderomotive structures were aligned towards the electron beam with a 5D stage. The electron distribution after the auto-ponderomotive structures (guiding and splitting) was imaged with a micro-channel plate detector via fluorescence detected by a camera (Fig. 1).

Furthermore, we designed a 87.95 mm long resonator, consisting of a central auto-ponderomotive guiding structure [6] and two switchable electron mirrors acting as “barn doors” at the entrance and exit of the resonator. We laser-triggered electron bunches of a nanometric tungsten tip and used deflectors and electron optical elements to steer them into our resonator. The electron barn doors could be opened and closed within nanoseconds at a variable delay towards the laser triggering event. Varying the delay of the outcoupling mirror towards the delay-line detector resulted in detection of up to 7 round trips (Fig.2).

Results
We show successful electron beam guiding as well as electron beam splitting of up to 1.7 keV. In a separate setup, we could demonstrate up to 7 round trips in our auto-ponderomotive resonator. All three modalities create new possibilities for enhanced electron beam control needed for an interaction-free measurement with electrons in a future quantum electron microscope.

Conclusion

We demonstrated controlled electron beam guiding and resonated 50 eV electrons for up to 7 round trips. In addition, we show an electron beam splitting auto-ponderomotive layout for 1.7 keV electrons and electron guiding up to 9.5 keV.

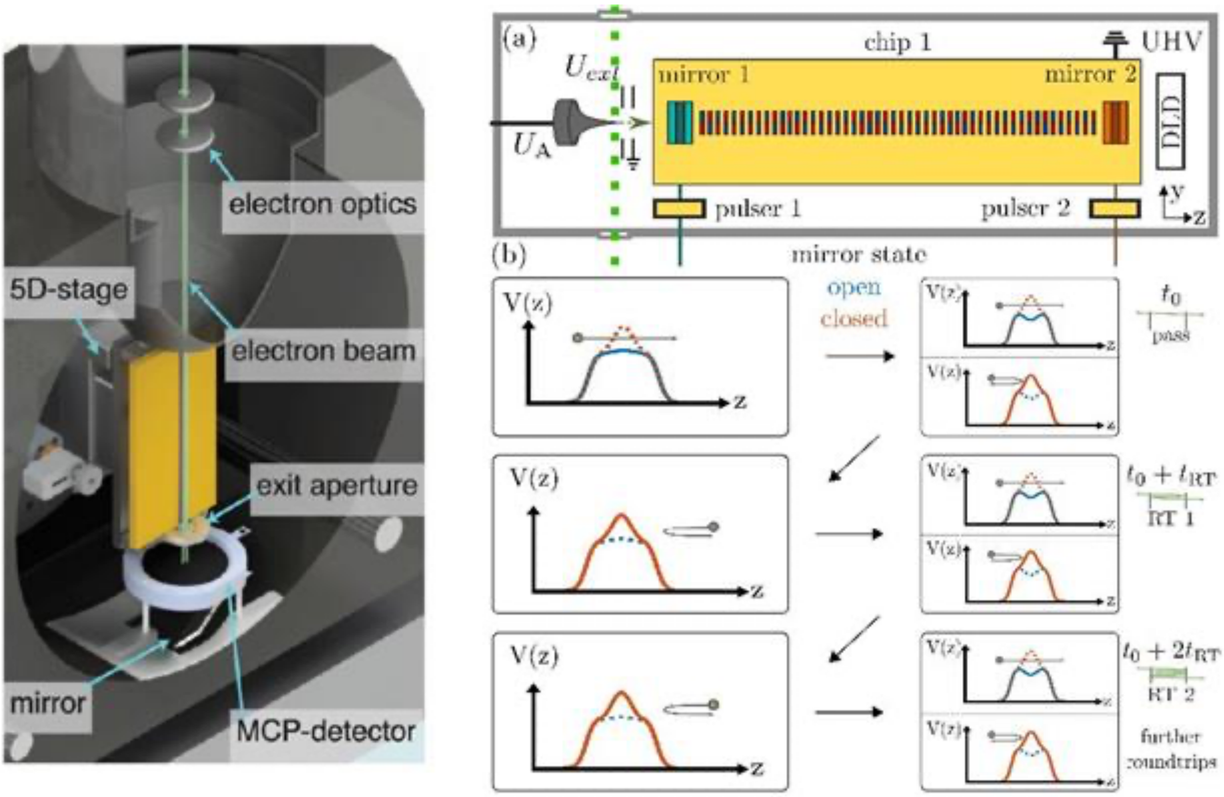

Keywords:

Interaction-free-measurement, quantum-electron-microscope, electron-beam-splitter, electron-resonator, auto-ponderomotive-potentials

Reference:

[1] Elitzur and Vaidman. Quantum mechanical interaction-free measurements. Foundations of Physics, 1993, 23: 987-997
[2] Thomas, Kohstall, Kruit and Hommelhoff. Semitransparency in interaction-free measurements. Physical Review A, 2014, 90: 053840
[3] Stewart Koppell and Mark Kasevich. Information transfer as a framework for optimized phase imaging. Optica, 2021, 8: 493-501[4] Turner et al. Interaction-free measurement with electrons. Physics Review Letters, 2021, 127: 110401
[5] Kruit et al. Designs for a quantum electron microscope. Ultramicroscopy, 2016, 164: 31-45
[6] Kwiat, Weinfurter, Herzog, Zeilinger and Kasevich. Interaction-free measurement. PRL, 1995, 74: 4763-4766
[6] R. Zimmermann, M. Seidling and P. Hommelhoff, Nature Communications, 2021, 390: 12
[7] M. Seidling, R. Zimmermann and P.Hommelhoff, Applied Physics Letters, 2021, 118: 034101[8] Seidling, Schmidt-Kaler et al. Resonating electrostatically-guided electrons. Under review, 2024

954

New strategies of TEM sample preparation for the mitigation of carbon contamination

Dr. Julia Menten[1], Dr. Daniela Ramermann[1], Prof. Dr. Robert Schlögl[1,2], Dr. Walid Hetaba[1]
[1]Max Planck Institute for Chemical Energy Conversion, Mülheim an der Ruhr, Germany, [2]Fritz Haber Institute of the Max Planck Society, Berlin, Germany

Poster Group 1

Transmission electron microscopy (TEM) measurements can be impaired by carbon contamination, which is caused by volatile organic components that get reduced by the electron probe and form a layer of amorphous carbon on the sample's surface. These contaminants often originate from the sample itself or are introduced during the TEM sample preparation process, e.g., when a sample is dispersed in a solvent for applying it to a TEM grid. In our work, we quantify the amount of accumulated contamination depending on the electron beam exposure time by electron energy loss spectroscopy (EELS) thickness measurements with a focus on different sample preparation parameters and mitigation strategies. A better understanding of the impact of these factors helps us to develop new sample pre-treatment strategies and thus drastically reduce carbon contamination in order to acquire clean TEM data.
TEM analysis was performed with a Thermo Scientific Talos F200X transmission electron microscope and a Gatan Continuum S spectrometer. Accumulated contamination was quantified by EELS thickness measurements by applying the log-ratio method [1]. The approach of contaminant removal in a self-built heatable vacuum sample cleaning station was compared regarding its efficiency to other established cleaning procedures.
Our experiments show that the amount of accumulated carbon contamination strongly depends on many factors that were investigated in our work: We have compared the amount of contamination caused by different solvents that are commonly used during the sample preparation or during the synthesis of a sample (fig. 1). Also, the impact of sample preparation parameters, i.e. the drying time of the sample, the duration a specimen remains in the microscope and the impact of the solvent's purity, was studied. In addition, we have investigated the efficiency of different established procedures for mitigating the formation of contamination. These strategies include established cleaning methods, that are compared to our novel approach of a designated sample cleaning station. Our results show in depth how the sample cleaning station performs compared to other mitigation strategies and can be integrated in the sample preparation process in order to achieve clean TEM measurements. The different methods were compared regarding their impact on the accumulated contamination (fig. 2), but also on their abrasiveness and influence on a sample's properties.
Carbon contamination can be reduced by careful consideration of the sample preparation parameters. Our results give insight in how to mitigate the deposition of contamination using established and new strategies, and can be extended to other challenging specimens, allowing to obtain high-quality, clean TEM measurements of samples that are prone to contamination.

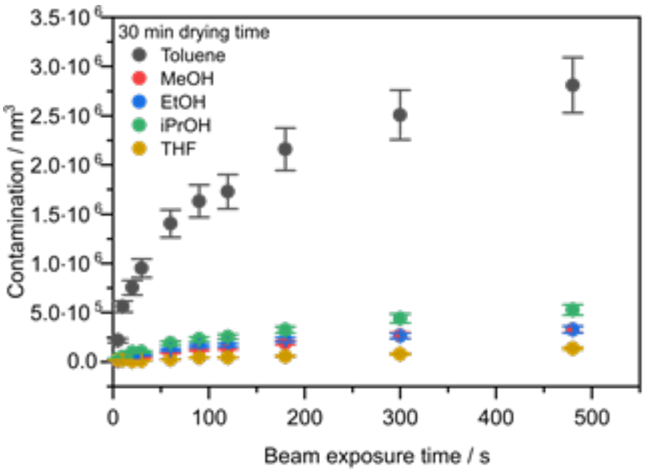

Fig. 1: Accumulated carbon contamination dependin on the beam exposure time for different solvents used during the sample preparation or chemical synthesis.

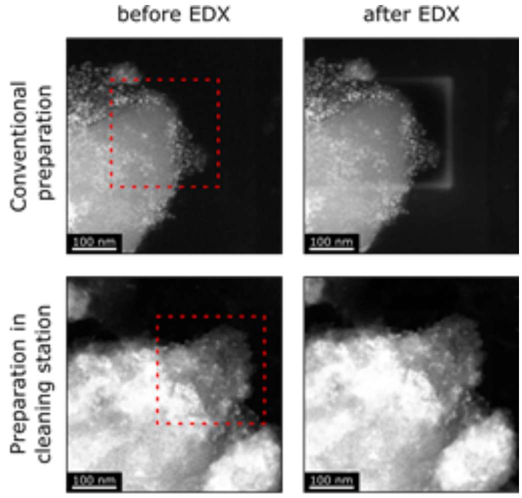

Fig. 2: Comparison of metal phosphide nanoparticles in SILP dispersed in THF prepared in a conventional way (top) or with our designated cleaning station (bottom). While the conventional preparation results in contamination after EDX analysis, the sample prepared in our cleaning station is not contaminated.

Keywords:

Sample preparation; carbon contamination

Reference:

T. Malis, S. C. Cheng, and R. F. Egerton. EELS log-ratio technique for specimen-thickness measurement in the TEM. Journal of Electron Microscopy Technique, 8(2):193–200, 1988

983

Establishment of 30mm diameter milling and curtaining effect reduction by large area planar surface milling

Mr. Yuji Hasebe[1], Munehiro Kozuka[1], Takashi Sueyoshi[1], Akihiro Tanaka[1], Tatsuhito Kimura[1], Tamae Omoto[1], Yasuaki Yamamoto[1], Koji Todoroki[1], Hiroshi Onodera[1]
[1]JEOL Ltd, Akishima city/ Musahino3-1-2, Japan

Poster Group 1

Background incl. aims
The planar surface milling method is effective for sputtering a specimen surface by irradiating an Ar ion beam at an adjusted irradiation angle while the specimen is continuously rotated. This method is used for final finishing of mirror polished specimens by mechanical polishing for SEM observation and EBSD analysis. And the sputtering area is about 5 mm in diameter using the conventional planer surface milling method. However, there is an increasing demand for final finishing by planer surface milling over a larger area, such as a diameter of over 10 mm, where mechanical polishing is generally used. The followings are some of the issues with conventional planar surface milling.
Problem 1: Ion irradiation is performed from one direction at the periphery of the ion irradiation area. This causes a curtaining effect, making it difficult to obtain a flat surface over a large area.
Problem 2: Differences in etching rates are caused by differences in specimen material and crystal orientation, resulting in unevenness on the ion-irradiated surface1).
In this study, we examined methods to resolve these issues.
Methods
Specimen for this test is rolled aluminum foil (100 µm thickness) without mirror polishing or other pretreatments. This is because this specimen has uniform scratches in one direction generated during rolling process, and these scratches were evaluated as polishing scratches.
The Ar ion beam processing system IB-19530CP/IB-10500HMS (JEOL Ltd.), and IB-11550LSRH (JEOL Ltd.) as holders for planer surface milling were used for this study. By combining these units, the stage rotating and stage swinging during planer surface milling can be executed simultaneously. This enables milling over a large area. We named this method to large area planar surface milling. In this method, the center of rotation and the ion beam center are eccentrically aligned during the swing of the specimen stage, allowing ion beam irradiation of the outer periphery from various directions. Therefore, it can reduce the curtaining effect at the outer area of the ion irradiation area. In addition, the tilt angle of the planar surface milling holder is adjusted to make the ion beam irradiation angle lower to 10° or less, which can suppress the unevenness of the ion irradiated surface2).
Experiment 1: Verification of reducing the curtaining effect
Specimens were prepared by the planar milling method using a specimen rotation motion and by the large area planar milling method which combines the specimen rotation with the stage swing motion. Subsequently, the quality of surface was compared. Specimens were processed under the following conditions: an acceleration voltage of 10 kV, a processing time of 1 hour, and an ion beam irradiation angle of 5°. In the large area plane milling method, the stage swing angle was set to ±30°.
Experiment 2: Verification of unevenness reduction
Specimens were prepared using the large area planar surface milling method at ion irradiation angles of 5° and 2°, and the quality of surface was compared. Specimens were processed under the following conditions: an acceleration voltage of 10 kV, a stage swing angle of ±30°, and a processing time depended on irradiation angle of ion beam : 12 hours at an ion beam irradiation angle of 5° and 24 hours at an ion beam irradiation angle of 2°.
An FE-SEM (JSM-IT800 (JEOL Ltd.)) and an AFM (JSPM-5200 (JEOL Ltd.)) were used to observe each processed surface.
Results

1. comparison of the conventional method and large area planar surface milling method
The conventional method produces a flat surface in the vicinity of the milling center. However, striped structures can be seen on the surface about 5 mm away from the milling center due to the curtaining effect caused by the limited direction of ion beam irradiation. On the other hand, the large area planar surface milling method reduced the curtaining effect even at a distance of about 5 mm away from the milling center. (Fig. 1 A).
2. effect of irradiation angle on large area planar surface milling:
Unevenness due to differences in etching rate, such as crystal orientation, could be reduced by changing the ion beam incidence angle from 5° to 2°. In addition, the average surface roughness of the center of the processed area was measured using AFM. The average surface roughness was Ra: 86.7 nm at an ion beam irradiation angle of 5°, and Ra: 24.1 nm at an ion beam irradiation angle of 2°. This indicates that unevenness reduction was achieved even in the center of the processed area. The processing at an ion beam incidence angle of 2° extends the ion irradiation range, and thus reduces the curtaining effect over a wide area of 30 mm diameter (Fig. 1 B).
Conclusions
We examined the reduction of unevenness and increase of the milling area by the planar surface milling. Using a new method that combines a large area planar surface milling method with an extremely low-irradiation angle ion beam, the unevenness caused by etching rate differences in materials or crystal orientation was reduced and a large range of specimen processing could be performed. This method is expected to be applied to specimens that are not easy to mechanically polish or as an alternative technique to buff polishing, because it can produce a fine surface with reduced unevenness over a wide area exceeding 20 mm in diameter.
In this presentation, application examples will be presented in addition to the above results.

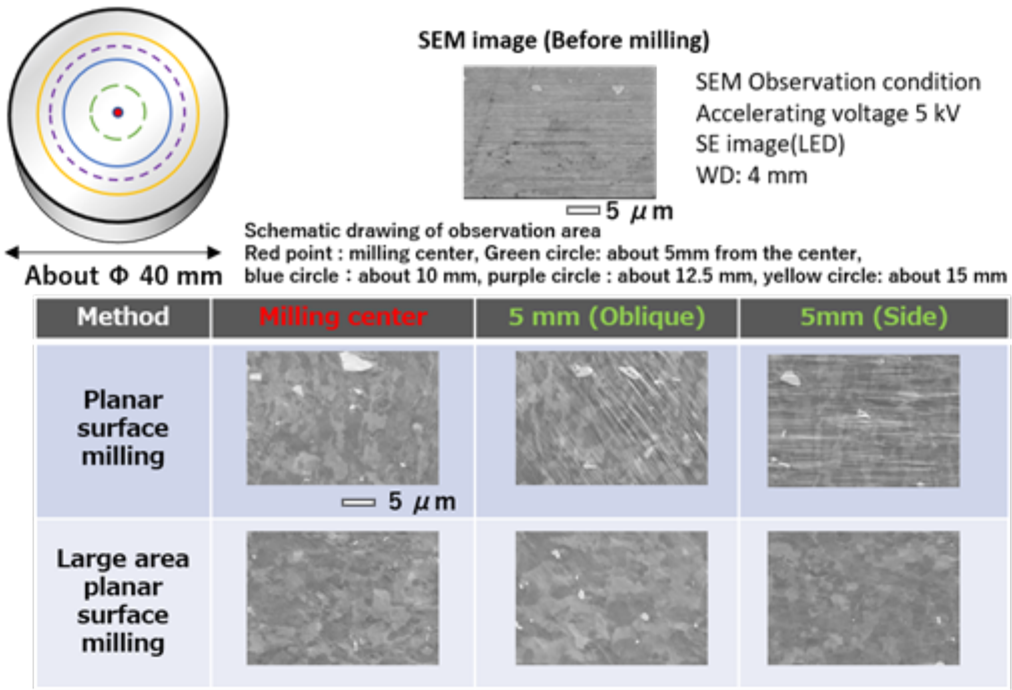

Fig 1A: Comparison of planar surface milling and large area planar surface milling

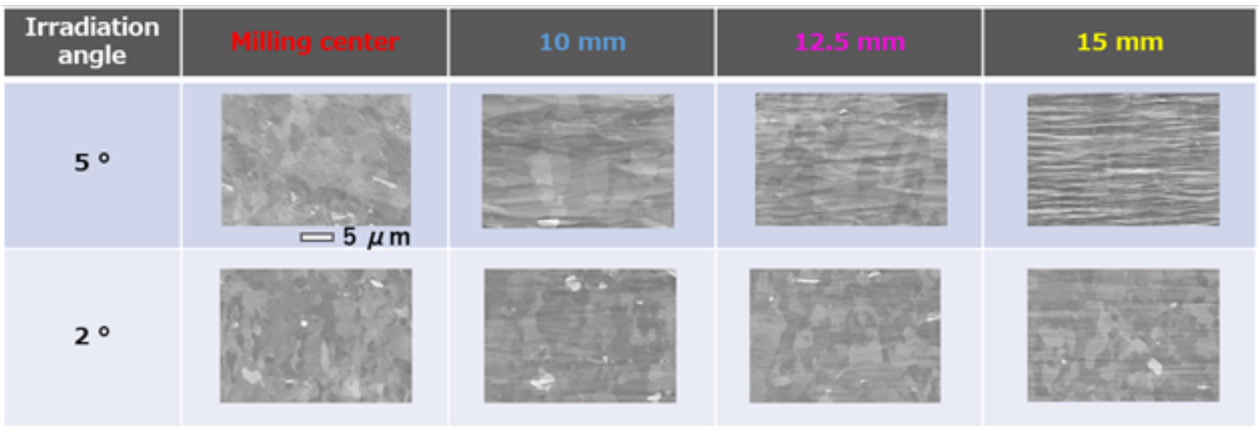

Fig 1B: Comparison of irradiation angle 5° and 2° by large area planar surface milling

Keywords:

Ion etching, Specimen preparation method

Reference:

1 R. Gago, et al., Applied Physics Letter, 78, 3316-3318(2001).
2 A.W. Barnard, et al, Microscopy and microanalysis, 12, 1318-1319 (2006).

992

Optimizing optical STEM detection for faster acquisition speeds in scanning electron microscopy

Arent J. Kievits[1], Monika Molnar[1], Jacob P. Hoogenboom[1]
[1]Department of Imaging Physics, Delft University of Technology, Delft, The Netherlands

Poster Group 1

Background
Optimization of acquisition speed is important for large-scale and volume electron microscopy (EM) experiments of tissues and cells, as these are characterized by long acquisition times due to the low inherent throughput of electron microscopes. Developments in scanning electron microscopy (SEM) techniques have increased acquisition speed by orders of magnitude through the use of more sensitive detectors, electrostatic and magnetic immersion fields, and multibeam scanning electron microscopes (mSEM), in which the sample is scanned in parallel with an array of beams (1,2). Optical scanning transmission electron microscopy (OSTEM) offers a way to discriminate the signals from the individual beamlets in mSEM (3). In OSTEM, ultrathin biological sections are placed on a thin film-coated scintillator substrate, which converts transmitted electrons into photons. These photons are collected by a high NA optical objective and projected onto a multipixel photon counter (Figure 1A).

We have recently shown that OSTEM performs similar to backscatter electron detection (BSD) and SE detection on ultrathin biological samples (3), in terms of contrast, image resolution and signal-to-noise ratio (SNR). At short dwell times, OSTEM outperforms BSD and SE detection in SNR. However, BSD in combination with electrostatic immersion still outperforms OSTEM. Moreover, the SNR of OSTEM stagnates for moderate to high beam currents, suggesting a potential saturation point in the detection scheme. In general, signal generation and collection in OSTEM has not been thoroughly investigated and as a result, optimization of the OSTEM detector layout has not yet been performed.

To better understand signal generation and collection in OSTEM, a physics model is required that describes electron scattering in the substrate, its conversion to light, and the subsequent collection of this light signal. This model then must be verified with experimental results to be used to optimize the substrate design. We aim to develop this OSTEM signal generation model and use it to obtain a rational substrate design optimized for detection efficiency and acquisition speed.

Methods
In OSTEM, ultrathin biological sections are placed on a cerium-doped single-crystal yttrium aluminum garnet (ce:YAG) scintillator, coated with a thin (~30 nm) conductive Molybdenum coating. OSTEM is implemented in a Verios 460 (FEI Company) equipped with a SECOM integrated fluorescence microscope (Delmic) without the emission filters (Figure 1A). In an alternative setup, photons are directly detected by a multipixel photon counter array placed underneath the scintillator (Figure 1B). The photon output and SNR are evaluated by focusing the electron beam on the empty substrate surface or a biological sample respectively, and recording the photon intensity with the MPPC or a CCD camera, for a given beam current, dwell time and landing energy. The SNR is computed by averaging the spectral SNR over the full frequency space of every electron micrograph.

Electron scattering is modeled with Monte-Carlo simulations in CASINO (4) and NEBULA (5), by computing the electron energy loss per voxel. The material properties of ce:YAG and molybdenum are taken from literature. We assume that energy conversion to photons fully relies on low energy loss events (<50eV). Different possible saturation mechanisms are modeled by limiting the photon output as a function of the input energy per voxel. Additionally, the loss of photons in the detection is taken into account by a transmission coefficient that depends on the thin-film coating composition.

Results

The photon output of the empty substrate demonstrated a sublinear relationship with the beam current (Figure 1C), suggesting a partial saturation effect. MPPC saturation was excluded as the main cause, since validation experiments with a neutral density filter and a CMOS camera showed similar sublinear relationships. The photon output does increase linearly at higher beam energies (Figure 1D), indicating the partial saturation is prevented in a larger electron interaction volume. Initial modelling with CASINO software showed proportionally more scattering events in the thin-film coating than in the scintillator (Figure 1E), although the majority of secondary electron generation takes place in the scintillator. However, CASINO does not accurately model low-energy secondary electrons. To better understand the signal generation and simulate the energy deposition at low energy (0-50eV), for which most of the energy transfer to the active scintillator dopant is expected, we intend to use NEBULA to calculate the energy loss per voxel as a function of the electron beam energy and current. NEBULA has been developed to provide fast and accurate simulations of low energy electron-matter interactions with first-principle physical models (5).

Conclusion

Optical scanning transmission electron microscopy (OSTEM) is an alternative SEM detection technique for imaging thin biological samples, and can be used for electron detection in multibeam scanning electron microscopy. Partial saturation of the scintillator and energy loss in the thin-film coating of the scintillator are hypothesized to limit the signal generation in OSTEM. In this work, a first attempt is made to model energy conversion from a focused electron beam to a photon signal. With a physically valid model, different substrate combinations can be tested. Subsequent optimization of the OSTEM substrate may increase acquisition speeds in single-beam and multi-beam scanning electron microscopes.

Caption

Figure 1: Optimization of optical STEM detection. A: Optical STEM detection with optical detection path. B: Optical STEM detection with direction detection of photons. C: Photon intensity on detector as a function of beam current, demonstrating a sublinear relationship. D: Photon intensity as a function of beam energy, demonstrating a linear relationship for higher energies. E: CASINO simulation of interaction volume of a 4keV beam in ce:YAG (>0z) with 30nm molybdenum (-30z to 0z). Blue: primary electrons, red: backscattered electrons, green: secondary electrons.

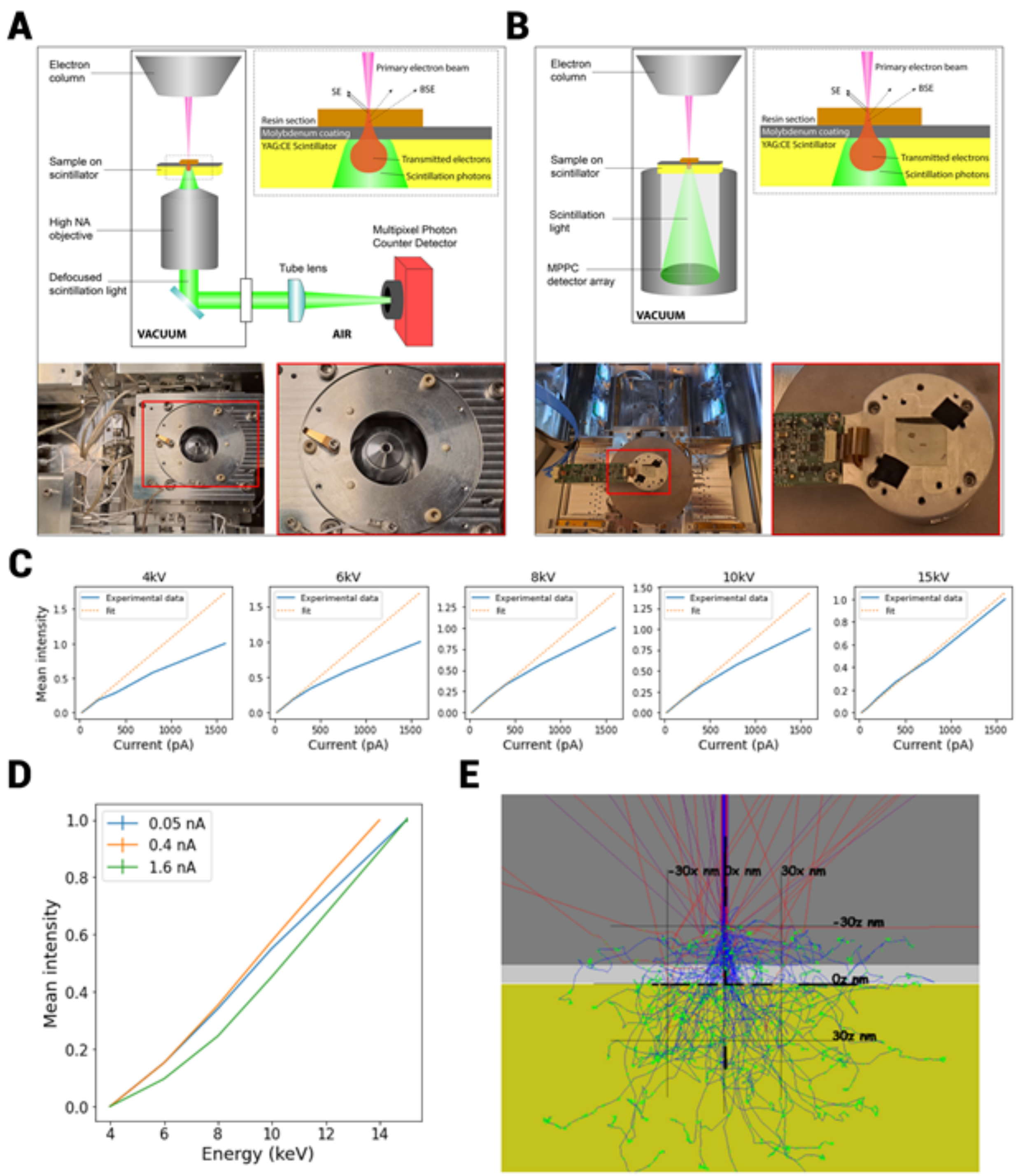

Keywords:

SEM, OSTEM, Scintillation, Simulations

Reference:

1. A. L. Eberle, S. Mikula, R. Schalek, J. Lichtman, M. L. K. Tate, D. Zeidler, High-resolution, high-throughput imaging with a multibeam scanning electron microscope. J. Microsc. 259, 114-120-114–120 (2015).

2. Y. Ren, P. Kruit, Transmission electron imaging in the Delft multibeam scanning electron microscope 1. J. Vac. Sci. Technol. B Nanotechnol. Microelectron. Mater. Process. Meas. Phenom. 34, 06KF02-06KF02 (2016).

3. A. J. Kievits, B. P. Duinkerken, J. Fermie, R. Lane, B. N. Giepmans, J. P. Hoogenboom, Optical STEM detection for scanning electron microscopy. Ultramicroscopy 256, 113877 (2024).

4. H. Demers, N. Poirier-Demers, A. R. Couture, D. Joly, M. Guilmain, N. de Jonge, D. Drouin, Three-dimensional electron microscopy simulation with the CASINO Monte Carlo software. Scanning 33.3, 135-146 (2011)).

5. L. van Kessel, C. Hagen, Nebula: Monte Carlo simulator of electron–matter interaction. SoftwareX 12, 100605 (2020).

1007

The importance of an open camera system demonstrated with wide-ranging applications of MerlinEM detector

Dr Matus Krajnak[1], Dr Gearoid Mangan[1]
[1]Quantum Detectors Ltd, Harwell Oxford, United Kingdom

Poster Group 1

Background inc. aims
The MerlinEM detector has gained widespread acceptance in the transmission electron microscopy (TEM) community due to its versatility and adaptable integration with various systems. The detector provides hybrid pixel electron counting based on Medipix3 technology, bringing in high detective quantum efficiency, rapid readout speed, high dynamic range, and radiation hardness.
Methods
Enabling direct access to data and camera operation is essential in exploring new applications and improving established techniques. The MerlinEM system provides this, together with live 4D scanning transmission electron microscopy (4D-STEM) capabilities (Fig. 1). Additionally, Quantum Detectors recently redesigned the retractable version of the MerlinEM platform, MerlinEM RDP, which now fits more microscopes and will support future generations of hybrid pixel detectors (Fig. 2).
Results
Open data formats and remote operation capabilities were essential in exploring new applications and improving established techniques, such as imaging electromagnetic fields [1] and ptychographic imaging [2]. Rapid data streaming to third-party software has been utilised for live ptychography [2] and integrated centre of mass imaging [3], while collaborations with commercial partners like NanoMegas (scanning precession electron diffraction toolkit), CEOS and Université Paris-Saclay (spectrometer systems) enhanced the capabilities of TEM instrumentation.
Conclusions
The openness of the detectors has fostered community collaboration, exemplified by projects like LiberTEM [4], pyXem [5] and others. These initiatives facilitate sharing data processing routines, accelerating the development of innovative methods for extracting sample information and addressing a wider range of specimens more efficiently.

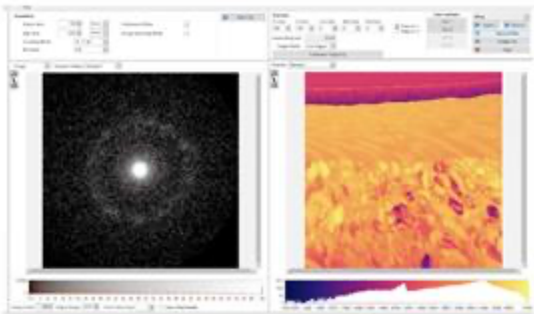

Fig. 1: 4D-STEM interface for MerlinEM

Fig. 2: The new MerlinEM RDP

Keywords:

4D-STEM, electron counting, direct detection

Reference:

[1] T Lorenzen et al. 2024 Scientific Reports 14.1:1320.
[2] A Bangun et al. 2023 Microscopy and microanalysis 29.3: 994-1008.
[3] CP Yu et al. 2022 Microscopy and Microanalysis 1526-37.
[4] https://libertem.github.io/LiberTEM/applications.html (accessed Jan 2024)
[5] https://pyxem.readthedocs.io/en/stable/ (accessed May 2024)

1050

Fast mass spectrometry imaging for immunohistochemistry

Dr. Mariya Shamraeva[1], Dr. Edith Sandström[1], Kimberly G. Garcia[1], Distinguished Professor Ron M. A. Heeren[1], Dr. Ian G. M. Anthony[1], Dr. Sebastiaan van Nuffel[1]
[1]Maastricht MultiModal Molecular Imaging Institute (M4i), Maastricht, Netherlands

Poster Group 1

Immunofluorescence microscopy (IFM) is the current "golden standard" in histopathology and biomedical research. IFM enables simultaneous imaging of multiple fluorescently tagged antibodies, but multiplexing beyond seven different fluorophores is impractical without photobleaching and re-staining, which it may cause sample degradation and difficulties with registering the separately-taken images. Other disadvantages are autofluorescence which can hinder detection of low-abundance proteins and signal bleeding. These disadvantages are absent in mass spectrometry-based approaches. Most mass spectrometry imaging (MSI) immunohistochemistry (IHC) is performed in “microprobe mode” which images pixel-by-pixel [1] and is limited to approximately 1,000 pixels per second, limiting the field of view. To overcome this limitation of typical MSI, fast mass microscopy (FMM) has been developed to acquire pixels, and collect many spectra, in parallel with a continuously moving stage, enabling orders of magnitude faster imaging [2]. Here we describe advancements in FMM for biomedical applications for the detection of multiple isotopically enriched metal tags that enable multiplex antibody panels, thus facilitating studies of multiple proteins in one imaging experiment.

Methods

MIBI staining with metal-conjugated antibodies (CD11b 155Gd, CD3 159Tb, Keratin 165Ho, α-SMA 164Dy) is performed similarly to traditional IFM. Flash-frozen tissue blocks were sectioned with a thickness of 12 µm using a Leica cryostat microtome. Serial sections from the same tissue block were obtained and collected on clean indium tin oxide coated glass slides. The stained human intestinal tissue and mouse tissue sections were analyzed with time-of-flight secondary ion mass spectrometry (ToF-SIMS) imaging using a PHI nanoTOF instrument II (Physical Electronics, Chanhassen, MN, USA) with tandem MS capability equipped with a liquid metal ion gun, C60 ion gun, and Ar cluster ion gun. FMM-IHC was done using an instrument based on the TRIFT II mass microscope (Physical Electronics, Inc. (PHI) Chanhassen, MN, USA) and equipped with a C60 ion beam (IOG C60-20S, Ionoptika, Chandler’s Ford, UK), with a Timepix3 ASIC-based camera (TPX3CAM, Amsterdam Scientific Instruments, Amsterdam, NL).

Results

The acquired ToF-SIMS and FMM mass spectral images of biological tissue show promise for antibody detection comparable to those observed using standard microscope-based workflows. Using IMS-IHC, it was possible to visualize elemental ions in fresh-frozen tissue sections with a high spatial resolution. The results were correlated with adjacent serial sections using optical microscopy and standard histological staining (H&E staining). A proof-of-concept study demonstrated the use of FMM as a tool for imaging by measuring the unfrosted part of a microscopy slide (23.5 x 40 mm) in under 4.5 minutes, at a pixel size of 900 nm.

Conclusion

The first steps of implementing FMM as a technique for MSI-IHC experiments instrumentation are presented. The elemental-mass-based multiplexed analysis, used to visualize protein expression on fresh frozen tissue, bypasses the limitation of both the traditional staining techniques relying on optical absorbance or fluorescence signals and mass spectrometry imaging performed in “microprobe mode”.

Keywords:

mass spectrometry imaging, mass microscopy

Reference:

1. McDonnell, L. A., Heeren, R. M. A., 2007 Mass Spect. Rev. 26, 4, 606-43
2. Körber, A., Keelor, J. D., Claes, B. S. R., et al. 2022 Anal. Chem. 94, 14652–58.

1086

Interference based optical instrument for high-throughput characterization of nanoparticles in complex biofluids

M.Sc.(Eng.) Carl Emil Schøier Kovsted[1], M.Sc. Yingchao Li[1], M.Sc.(Eng.) Lasse Pærgård Kristiansen[1], Ph.D. Jeppe Revall Frisvad[2], Ph.D. Jaco Botha[1], Ph.D. Emil Boye Kromann[1]
[1]Department of Health Technology, Technical University of Denmark, Kgs. Lyngby, Denmark, [2]Department of Applied Mathematics and Computer Science, Technical University of Denmark, Kgs. Lyngby, Denmark

Poster Group 1

Background incl. aims

Extracellular vesicles (EVs) are biological nanoparticles found in biofluids such as blood. EVs have been suggested to play an important physiological role, and potentially serve as markers for various diseases. However, EVs are often confounded with other bio-nanoparticles, such as lipoproteins and protein complexes. Currently no method can detect and characterize EVs in a high-throughput manner. We present an optical instrument with spatial resolution to detect and characterize EVs based on light scattering measurements. The underlying technology relies on creating a standing wave of two interfering lasers, of which one is variably phase modulated to displace the interference pattern within the intersection of the two laser beams (Fig. 1A).

Methods

The core concept is inspired by amplitude modulation radio. Specifically, this optical instrument encodes spatial information in the illumination source, manifested as an interference pattern that can variably sweep in the interrogation zone. By phase delaying one of the laser beams, we can produce a sweeping interference pattern with a known scrolling frequency (Fig. 1A-B). As nanoparticles traverse the sweeping interference pattern, the light scattered by these particles oscillate with the scrolling frequency. This enables “locking-in” on the narrow bandwidth of the oscillating signal and exclusion of the majority of broadband noise (Fig. 1C). Hereby we can increase the signal-to-noise ratio (SNR) of these already dim scattered light intensities from nanoparticles, and thus improve the lower detection limit. Furthermore, it is possible to determine size of nanoparticles and extrapolate the refractive index from the measured signal. Thus, the inherent nature of this optical instrument allows us to distinguish between different classes of bio-nanoparticles in a label-free manner (Fig. 1D). To validate the presented optical instrument, a range of nanostructures with known sizes and refractive indices were fabricated and used to probe produced light field. This was done to characterize (1) the actual wavelength of the standing wave, and (2) the extent of the interrogation zone. We are further validating that scattered light from bio-nanoparticles can be expressed with Lorenz-Mie theory to develop an accurate model for extrapolation of particle refractive index.

Results

Currently, we have constructed a prototype of the optical instrument. This serves to prove the core concepts and demonstrate the feasibility of this instrument to (1) improve the SNR for dim light scatter signals, (2) distinguish between nanoparticles based on size and refractive index. To assess these features, we are fabricating a range of nanostructures with differing shape, size, and material properties, which we can use to characterize the performance of the optical instrument.

Conclusion

The complex bio-nanoparticle landscape is yet to be explored, and no methods have been demonstrated to have adequate sensitivity for high-throughput characterization and distinction between different classes of bio-nanoparticles. In this poster abstract we present an optical instrument that addresses these short-comings by utilizing a scrolling interference pattern to characterize bio-nanoparticles capable of measuring size and modelling refractive index. The project is still in an early stage, and the technology is yet to be fully demonstrated.

Concept for proposed instrument

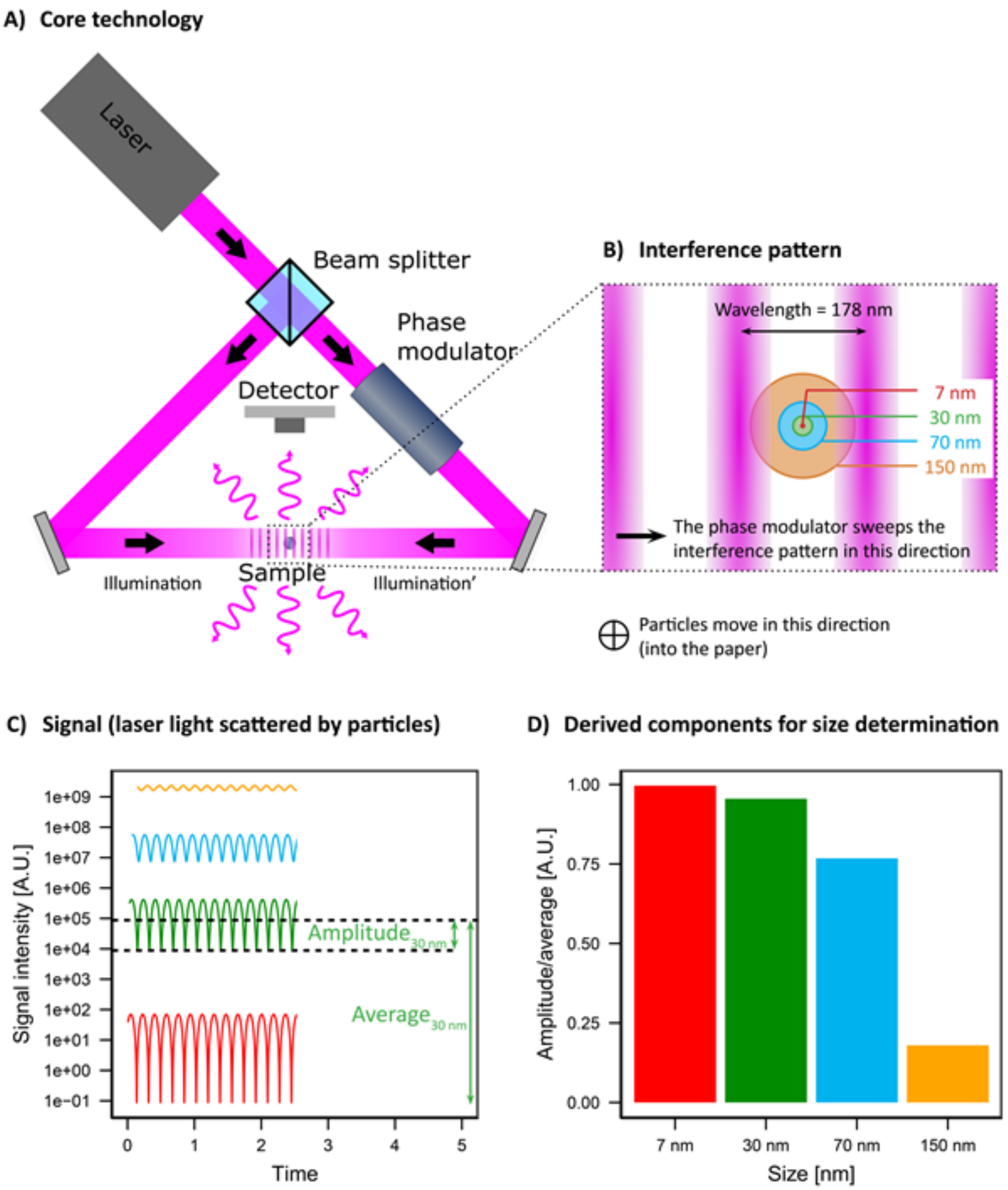

Figure 2: Core technology - Principle of my new illumination strategy. (A) Using a passive beam splitter crystal, we will divide a single laser beam into two laser 'arms', which will interfere at the laser-interrogation zone inside the flow cell, forming a standing wave with a very short wavelength (λ = 178 nm). **(B)** A phase modulator contains a crystal with a tunable refractive index. Using a phase modulator, we can introduce an arbitrary phase delay in one of the laser-arms, thus shifting the standing wave left/right across particles in the laser-interrogation zone (inset, note that particles travel in the direction perpendicular to the depicted plane). Detectors outside the flow-cell will detect laser-light scattered from particles as they transit the laser-interrogation zone. **(C)** Using the phase modulator, we can quickly sweep the standing wave across particles, as they transit the laser-interrogation zone. Thus, we will record an oscillating signal of scattered laser-light with a temporal frequency proportional to the well-defined sweep-speed of the interference pattern. **(C)** Notably, the ratio between the average signal and the amplitude of signal oscillations will be proportional to particle size and independent of refractive index. Having derived particle size in this manner, we can proceed to compute refractive index based on the average light scatter intensity. Together, particle size and refractive index unambiguously distinguish between particle types and enable high-throughput mapping of the bio-nanoparticle landscape.

Keywords:

Extracellular vesicles, Light scattering, Label-free

Reference:

van der Pol, E. et al. Particle size distribution of exosomes and microvesicles determined by transmission electron microscopy, flow cytometry, nanoparticle tracking analysis, and resistive pulse sensing. Journal of Thrombosis and Haemostasis 12, 1182–1192 (2014).

Théry, C. et al. Minimal information for studies of extracellular vesicles 2018 (MISEV2018): a position statement of the International Society for Extracellular Vesicles and update of the MISEV2014 guidelines. J Extracell Vesicles 7, (2018).

Yuana, Y., Sturk, A. & Nieuwland, R. Extracellular vesicles in physiological and pathological conditions. Blood Rev 27, 31–39 (2013).

Bohren, C. F. Absorption and scattering of light by small particles. Absorption and scattering of light by small particles (1983) doi:10.1088/0031-9112/35/3/025.

1113

MEMS Monochromator

Martijn Adriaans[1], Dr. Jacob Hoogenboom[1], Dr. Ali Mohammadi-Gheidari[1]
[1]Delft University of Technology, Delft, The Netherlands

Poster Group 1

Background and Aims
Present ultra-high-resolution SEM and S(T)EM commonly use high brightness electron source such as Schottky source (SFE) or cold field emitter (CFE) with a relatively high reduced brightness of about 1x108 and 2x108 [A/Sr.m.V] respectively. A typical energy spread of these electron sources are 1eV and 0.4eV respectively. For most applications requiring narrower energy spread, these are too large. Two examples of these applications could be: 1]- Extremely low voltage imaging with electrons known as LVSEM with a typical landing energy (LE) of only a few tens of electron-volts where chromatic aberration limits the resolution, 2]- Energy resolved applications such as high-resolution electron energy-loss spectroscopy (HREELS) where an extremely lower energy spread of only a few meV is required. A lower energy spread could only be obtained when a monochromator is used.
In the current monochromators, the increased demand on performance has increased the complexity of the monochromator designs, decreasing their user friendliness: to reach a few meV energy resolution, multiple power supplies have to be tuned to reach an optimal performance. The complexity in terms of large number of power supplies with extremely accurate temporal stability can partly be attributed to the form factor of the design. For instance, the main feature of a monochromator is a large deflection angle, with an associated three dimensionally shaped macroscopic geometry with inherently large aberrations, while also being very sensitive to small mechanical misalignments . These geometric and parasitic aberrations require compensation using extra multipole correctors. Moreover, adding extra multipoles in the design, extends the geometry of the monochromator, and consequently requires a reduced probe current for suppressing the energy broadening due to the Boersch effect. The increasing complexity demands a new design capable of achieving similar output in terms of energy resolution and current while reducing the number of required voltage supplies and their combined stability.
Methods
We present a new fully electrostatic monochromator based on Micro-Electro-Mechanical-Systems (MEMS). This manufacturing approach allows fabrication of monochromator parts with an unprecedentedly accuracy. While conventional monochromator deflectors can be approximated using 2D methods with multipole approximation, this approach is inadequate when the aperture sizes are large compared to the curvature of an electron beam's path. A 3D approach is required in the case of free form MEMS-based electron optics. To do so, a BEM method, is used for design and optimization of a new, fully electrostatic design. The optimization is partially automated by tuning the voltages in the design based on fitted optical aberrations.
Results
The new monochromator consists of 8 power supplies (including ground), and has a 1-to-1 ratio between voltage supply and beam energy drift. The new 5 mm long monochromator images / disperses the input plane to a selection slit plane with a unit magnification and a dispersion of 6 µm/eV at a beam energy of 500 eV. At the slit plane, an energy resolution better than 20 meV with a probe current of 5nA can be selected. The dispersion is a result of a (large) deflection angle using Fring Field deflectors. These fringe fields are created by extremely low aspect ratio MEMS multipoles. Accurate fabrication and lower aspect ratio arrangement of main deflection fields eliminates the need for additional multipoles to compensate for geometric and parasitic mechanical misalignments.
Conclusions

In conclusion, monochromators represent a field of technology where the integration of MEMS techniques has shown novel promise in reducing complexity while maintaining crucial parameters. In addition to energy filtering, the newly found configuration could be used for other related applications such as energy analysis. The next step in the project will thus be to manufacture the new design for integration and testing in an electron microscope.

Figure:

Cross-section of monochromator layout, with an exaggerated initial energy distribution (+/- 5 V). The electrodes in the design are a series of stacked electrodes, with differing shapes of apertures created in each layer. The colours of the elements depict the surface charge densities resulting from the application of optimal voltages in the geometry. The dispersed beam enters in the left of the image, and is deflected and imaged towards the output plane on the right. The field free energy selection slit has been left out to favour simulation and make show the dispersed spot in the image plane.

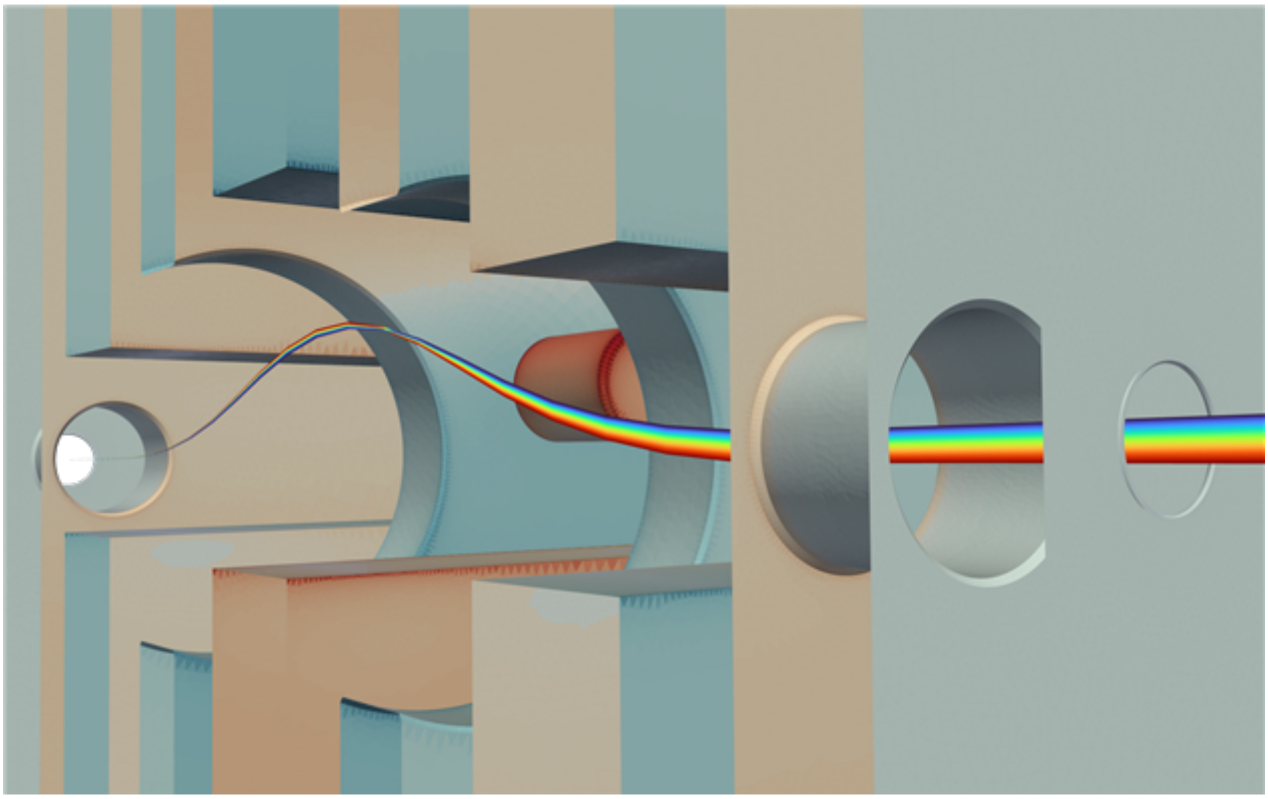

Keywords:

Monochromator Spectrometer MEMS LVSEM stability

Reference:

Lopatin, Sergei, et al. "Optimization of monochromated TEM for ultimate resolution imaging and ultrahigh resolution electron energy loss spectroscopy." Ultramicroscopy 184 (2018): 109-115.
Börrnert, Felix, et al. "A novel ground-potential monochromator design." Ultramicroscopy 253 (2023): 113805.
De Loos, M. J., and S. B. Van der Geer. "General Particle Tracer: A new 3D code for accelerator and beamline design." 5th European Particle Accelerator Conference. Vol. 1241. 1996.

1161

Novel scan coil design for high spatiotemporal-resolution imaging in the scanning transmission electron microscope

Mr Adam Phipps[1,2], Dr. Lewys Jones[1,2], Dr. Jonathan Peters[1,2]
[1]Advanced Microscopy Laboratory, CRANN, Dublin, Ireland, [2]School of Physics, Trinity College Dublin, Dublin, Ireland

Poster Group 1

The Scanning Transmission Electron Microscope (STEM) is a highly versatile tool that is used to study a wide range of materials, from semiconductors to biological cells. It operates by scanning a beam across a specimen and then recording the beam that has been transmitted through the specimen at these points. STEM is a powerful technique for probing specimens down to the atomic scale, but the slow imaging speeds can result in excessive beam exposure, and therefore damage, and the inability to capture dynamic in-situ events. Increasing the scanning speed is therefore an attractive proposition for better control of the dose-rate on the sample as well as improved temporal resolution

Currently, the main limitations to the scanning time in a STEM are imposed by the response time of the scanning coils, determined largely by their inductance. For this reason conventional imaging requires a flyback wait time between scan lines to reduce inductive hysteresis. Flyback time may be eliminated using novel scan paths, though at fast scan speeds the inductive effects are still problematic. Similarly, techniques such as compressed sensing can increase frame-rates but retains issues regarding the hysteresis of the scanning coils. Previous work by Ishikawa et al. shows scan coils with an inductance ~240 times less than the conventional scan coils, though with a limited scan area.

In this work we present a scan coil system to greatly improve the response time of the scanning system. Alongside the existing, main scan coils, we add additional deflectors with lower inductance to work simultaneously with the main scan coils. By using the second coils to counteract the effects of hysteresis in the main scanning coils, imaging at lower dwell and flyback times without image distortion or compromising scan area. The additional coils themselves are not perfect and further sets of coils could be used to compensate remaining hysteresis. Equally, the use of electrostatics due to the rapid response time and lack of hysteresis could be deployed in tandem. With our design, we hope to make fast scanning in STEM practicable and enable high-resolution imaging to improve dose-control and in-situ measurements.

Keywords:

Coils, Hysteresis, Induction, Flyback

Reference:

A.P. is supported by SFI award number URF/RI/191637. J.J.P.P. and L.J. acknowledge SFI grant 19/FFP/6813,

Using your beam efficiently: Reducing Electron-dose in the STEM via Flyback Compenstion, Microscopy and Microanalysis, 1-9, Mullarkey T., Peters J. J. P., Jones L. (2022)
How Low Can You Go: Pushing the Limits of Dose and Frame-time in the STEM, Microscopy and Microanalysis 28, Mullarkey T., Peters J.J.P., Geever M., Jones L., (2022)
high spatiotemporal-resolution in the scanning transmission electron microscope, Microscopy (Oxf.), 240-247, Ishikawa R. et. al., Jul 2020

1182

Scanning patterns evaluations towards FIB-SEM/SIMS low-dose high-speed acquisition

Dr Andrés Miranda Martínez[1], Dr. Tom Wirtz[1], Dr. Santhana Eswara[1]
[1]Luxembourg Institute of Science and Technology (LIST), , Luxembourg

Poster Group 1

Two fundamental artifacts that affect resolution in Focused Ion Beam - Scanning Electron Microscopy (FIB-SEM) and Secondary Ion Mass Spectrometry (SIMS) are beam damage and shot noise. Beam damage is a well-known factor that causes structural modifications and impacts the image quality of sensitive samples. On the other hand, shot noise limits the signal-to-noise ratio (SNR) of the image, increasing distortion. These limitations affect the mentioned techniques and reduce their capabilities to analyse beam sensitive materials properly [1].
For image acquisition, the scanning process involves focusing the ion (or electron) beam to scan the sample row by row. At the end of each line, the beam is returned to the start of the next line, a movement known as “flyback”. This conventional raster is the most used due to its simple application and ease of reconstruction. However, for fast scan, it suffers from deformations due to flyback, thus requiring a delay time to avoid distortion. Also, an extra dose is injected into the sample during the flyback, which may further alter sensitive samples [2].
Reducing the dose rate can be achieved by accelerating the scan. This can be done by decreasing the dwell time, but this reduction will lead to a low SNR. Other solution is to implement a continuous scanning method to eliminate the need for flyback. A moderate number of studies have focused on the development of alternative scanning patterns to reduce beam damage or increase image acquisition speed in FIB-SEM/SIMS. Patterns like bi-directional, spiral, Hilbert, and Z-order are pointed out for this application. These different patterns move the ion or electron beam continuously along the raster, aiming to improve acquisition time and reduce beam damage [1].
The bidirectional (serpentine) scan pattern, also simple to implement, improves scanning by avoiding flyback but encounters distinct distortions for leftwards and rightwards trajectories, necessitating post-processing for image improvement. The spiral scan pattern also avoids flyback delay and benefits from smooth movements that reduces distortions, yet it produces non-uniform image quality and requires post-processing. The Hilbert pattern is a space-filling curve that changes the scanning direction by no more than two steps, resulting in small changes in both axes during the scan. This method avoids flyback delay, follows an isotropic path, and reduces acquisition time but experiences distortions when using small dwell times. Similarly, the Z-order scan pattern provides an isotropic path and reduces acquisition time, with the drawback of potential distortions due to short flyback times in small dwell times [2, 3].
Lastly, the sparse scan pattern reduces acquisition time by scanning only a portion of the total pixels and minimizes distortions caused by the finite response time while maintaining an isotropic path. However, it is sensitive to drift and necessitates a reconstruction procedure. Its implementation requires a higher level of complexity [4].
Each pattern offers unique benefits and challenges, influencing their suitability for different microscopy applications.
As an aid to implementing the scanning methods previously discussed, the application of deep learning algorithms contributes to the smart low-dose high-speed acquisition and reconstruction. However, their implementation involves increasing the complexity of the system and requires more computational resources [4].
Our objective is the implementation of new scanning methods that allow for low-dose high-speed acquisition in a high-vacuum FIB-SEM platform (Scios) from Thermo Fisher Scientific equipped with a

SEM column, a Ga liquid metal ion source (LMIS)-based FIB column (Ga-FIB), and a magnetic sector SIMS system [5].
To achieve this goal, we have successfully implemented and tested the different patterns mentioned before to control the raster of ion and electron beams to form secondary electrons images in the Scios instrument.
To control the deflection system and collect data from the Everhart Thornley Detector (ETD), we employed a custom-built acquisition system that uses a USB-6351 acquisition card from National Instruments. The system is divided into two parts: i) scan control and ii) data acquisition. The scan control was managed using the two analog outputs of the acquisition card, with each signal controlling one coordinate position of the beam (X, Y). The data acquisition involved receiving secondary electron signals from the ETD via the digital input. A LabVIEW program was developed to manage the system.
To test the functionalities of the system, we used a non-sensitive solid sample (FeTi). The system can set the image size in pixels, dwell time, and scan pattern. Other parameters, such as accelerating voltage, field of view (FOV), or beam current, must be defined using the microscope's internal system.
The novel raster schemes being explored for low-dose high-speed ion or electron beam imaging are expected to accelerate materials research by enabling high-resolution imaging of transient processes and/or radiation sensitive samples.

The authors acknowledge funding from Opincharge and Battery 2030+ projects, and Tim Dahmen of DFKI (Deutsches Forschungszentrum für Künstliche Intelligenz) for his support.

Keywords:

FIB/SEM, High-speed low-dose acquisition, scan-patterns

Reference:

[1] D Nicholls et al., Ultramicroscopy 233, 113451 (2022)
[2] A Velazco et al., Ultramicroscopy 215, 113021 (2020)
[3] X Sang et al., Advanced Structural and Chemical Imaging 2, 1-8 (2016)
[4] P Trampert et al., Microscopy and Microanalysis 25.S2, 158-159 (2019)
[5] O. De Castro, et al. Analytical Chemistry, 94, 10754−10763 (2022)

1320

In-Situ Microstructure-Mechanical Property Mapping of Multi-Component Materials Using PI 89 Auto SEM PicoIndenter

Sanjit Bhowmick[1], Kevin Schmalbach[1], Justin Cheng[2], Eric Hintsala[1], Douglas Stauffer[1], Nathan Mara[2]
[1]Bruker, Minneapolis, United States, [2]Department of Chemical Engineering and Materials Science, University of Minnesota, Minneapolis, United States

Poster Group 1

Background
Next-generation structural materials are designed to achieve superior performance by combining different elements and phases, each contributing distinct properties such as strength, toughness, or corrosion resistance. However, the often complex distribution of these multiple phases leads to challenges in characterizing the variations in mechanical properties across different regions of the material. Understanding these spatial variations is crucial for further refinement and optimization of the chemistry and microstructure of these complex alloys. Precise knowledge of how each phase and its distribution affect the overall mechanical behavior allows researchers and engineers to fine-tune the material for specific applications, ensuring optimal performance and reliability.

Methods
One major challenge for the characterization of these materials is the alignment of separately measured mechanical property and microstructure maps. Bruker's PI 89 Auto introduces advanced automation to the Hysitron PI 89 SEM PicoIndenter to address this challenge. This tool automates the positioning of the Rotation and Tilt Stage (R/T stage) for indentation after SEM imaging and EBSD/EDS mapping. The integration of TriboScan Auto software allows high-throughput testing with precision and control, seamlessly transitioniong between nanoindentation, SEM imaging, and EBSD/EDS analysis. From an EDS/EBSD map, the PI89 auto enables the co-localized acquisition of quantitative in-situ mechanical data at user-defined regions of interest. This significantly enhances the efficiency and accuracy of correlative structure-property analysis, facilitating advancements in material science and engineering. In this study, two heterogeneous alloys, a two-component steel and an accumulative roll bonded copper-niobium (ARB Cu/Nb) nanolaminate, are selected. The steel sample demonstrates significant variations in properties resulting from differences in chemistry and microstructure introduced during the synthesis process. This steel is fabricated by laser cladding 410 stainless steel onto a 4140 steel substrate, a technique that produces distinct microstructural zones identifiable through chemistry maps from Energy Dispersive Spectroscopy (EDS) and grain orientation maps from Electron Backscatter Diffraction (EBSD). These zones include: (1) the base 4140 steel substrate; (2) the heat-affected zone; and (3) the high chromium (Cr) 410 steel cladding.

Results
Figure 1 illustrates the three microstructural zones and their mechanical properties, which are assessed through a lateral nanoindentation hardness profile. Notably, the heat-affected zone is considerably harder than both the base substrate and the cladding. This increased hardness is attributed to the microstructural alterations induced by the laser cladding process, which include grain refinement and potential phase transformations due to the severe local heating. Elevated hardness in heat affected zones is commonly observed in many structural metals, but the facilitated correlation of chemistry and structural data makes it quick to identify these regions and measured their local properties with high spatial resolution.

The accumulative roll bonded copper-niobium (ARB Cu/Nb) alloy exhibits differences in mechanical properties across its component phases. This alloy is synthesized through a process involving repeated stacking, roll-bonding, and cutting of pure copper and niobium sheets. This method results in a lamellar microstructure characterized by alternating layers of copper and niobium. An array of Berkovich nanoindentations placed across several layers of the ARB Cu/Nb material allows for precise mapping of the mechanical properties of individual phases, as illustrated in Figure 2. By aligning a chemical map from Energy Dispersive Spectroscopy (EDS) with a nanoindentation hardness map, the mechanical heterogeneity of the respective component phases is correlated. This analysis reveals that the niobium phase is stiffer than the copper phase as expected. The increased hardness of the copper relative to the niobium phase is not necessarily intuitive, and can be attributed to the distinct grain sizes within each phase. Specifically, the copper phase exhibits a smaller grain size compared to the niobium phase. This disparity arises from the greater propensity for dynamic recrystallization in copper during the accumulative roll bonding process. Dynamic recrystallization, which involves the formation of new, strain-free grains during deformation, is more pronounced in copper due to its lower melting point and higher diffusivity compared to niobium.

Conclusions

This work highlights the utility of the PI 89 Auto in correlating local mechanical behavior with differences in grain structure and chemistry. By providing seamless integration of nanoindentation with SEM imaging and EBSD/EDS analysis, the PI 89 Auto enables high-resolution, high-throughput characterization of complex materials like ARB Cu/Nb and laser-clad steel. This capability is crucial for advancing our understanding of the relationships between microstructure and mechanical properties, thereby facilitating the development and optimization of advanced structural materials.

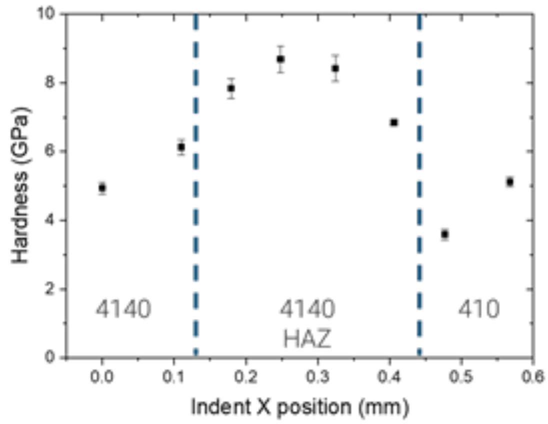

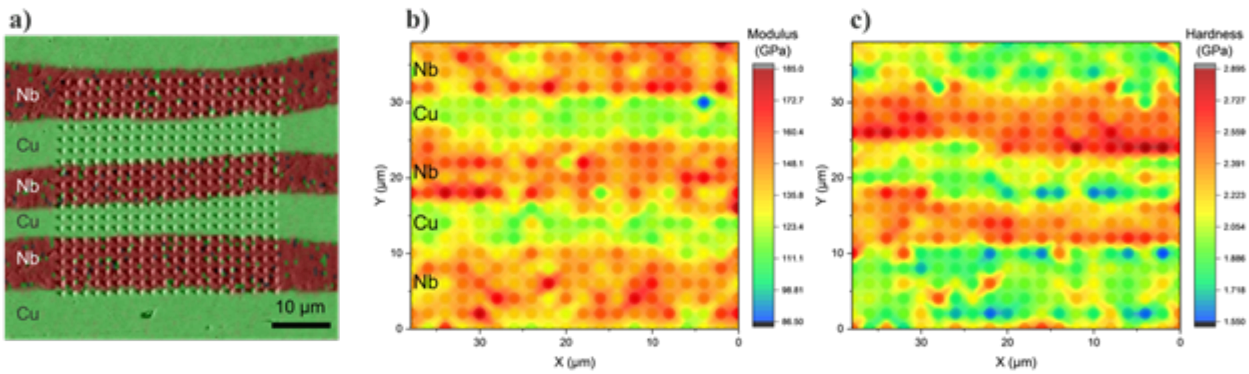

Keywords:

SEM PicoIndenter, Mechanical Property Mapping